

**Towards a new assay to investigate
electron transfer in DNA**

Inauguraldissertation

zur

Erlangung der Würde eines
Doktors der Philosophie

vorgelegt der

Philosophisch-Naturwissenschaftlichen Fakultät
der Universität Basel

von

Stéphanie Saigne

aus Colmar

France

Basel 2005

Genehmigt von der Philosophisch-Naturwissenschaftlichen Fakultät der Universität Basel
auf Antrag der Herren Professoren

Prof. Dr. Bernd Giese

Prof. Dr. Andreas Pfaltz

Basel, den 7. Juni 2005

Prof. Dr. Hans-Jakob Wirz
(Dekan)

The work presented herein was initiated and guided by Prof. Dr. B. Giese at the Institute of Organic Chemistry of the Philosophic-Scientific Faculty of the University of Basel, during the period from January 2000 to December 2004.

Excerpts from this work have been presented in the following meetings:

“ Electron transfer through DNA: Phenol as charge acceptor”, S. Saigne, N. Amiot, B. Giese, 23rd *International Symposium on Organic Synthesis and Catalysis*, Falkau (Germany), September **2003**.

“ Towards a new assay to investigate electron-transfer in DNA”, N. Amiot, S. Saigne, B. Giese, *Fall Assembly of the New Swiss Chemical Society*, Lausanne (Switzerland) October **2003**.

I wish to thank:

Prof. Dr. B. Giese for the challenging problems, the many inspiring discussions and for his continuous support during the realization of this work.

Dr. Nicolas Amiot for his intensive help and for the many stimulating discussions during his postdoctoral time in Basel. Sandra Thöni for her continuous availability and for her help to resolve many technical problems.

Dr. Nicolas Amiot and Sandra Thöni for correcting this thesis.

All members of the Giese group for their help, the nice atmosphere and for the fun during work.

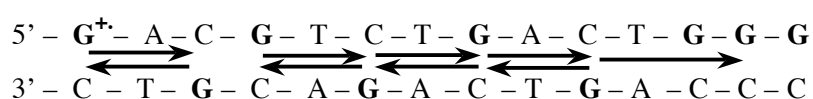
Dr. Klaus Kulicke, Dr. Heinz Nadig and Dr. Werner Kirsch for their analytical measurements.

My family for his invaluable support during the writing of my thesis.

*For my parents,
Arnaud and Emilie.*

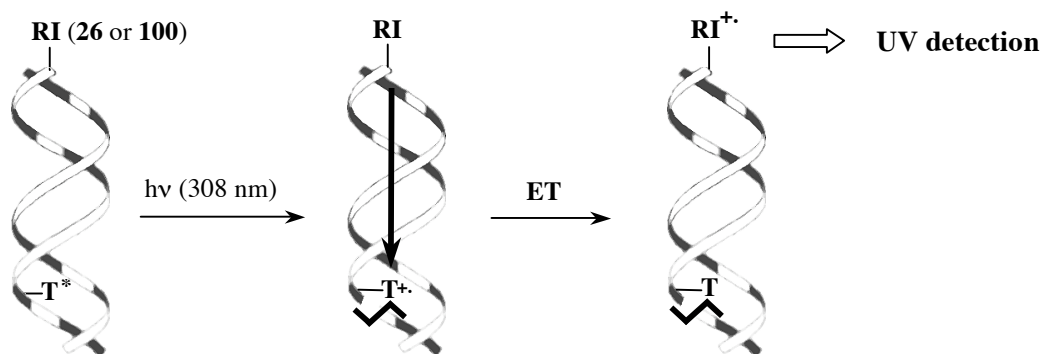
Summary

The aim of this work was to develop a new system to investigate electron transfer in DNA using UV active entities acting as charge acceptor in DNA. The long-range charge transfer in DNA can be viewed as a series of short range hops between the energetically appropriate guanine bases, which have the lowest oxidations potential of all the nucleobases. The total charge transport is considered to be a sequence of single, reversible transfer steps between guanines bases, and these steps are highly distance dependent since the charge is tunnelling between donor and acceptor. It is characterized as a super exchange mechanism (Scheme A).



Scheme A hopping mechanism and super exchange mechanism

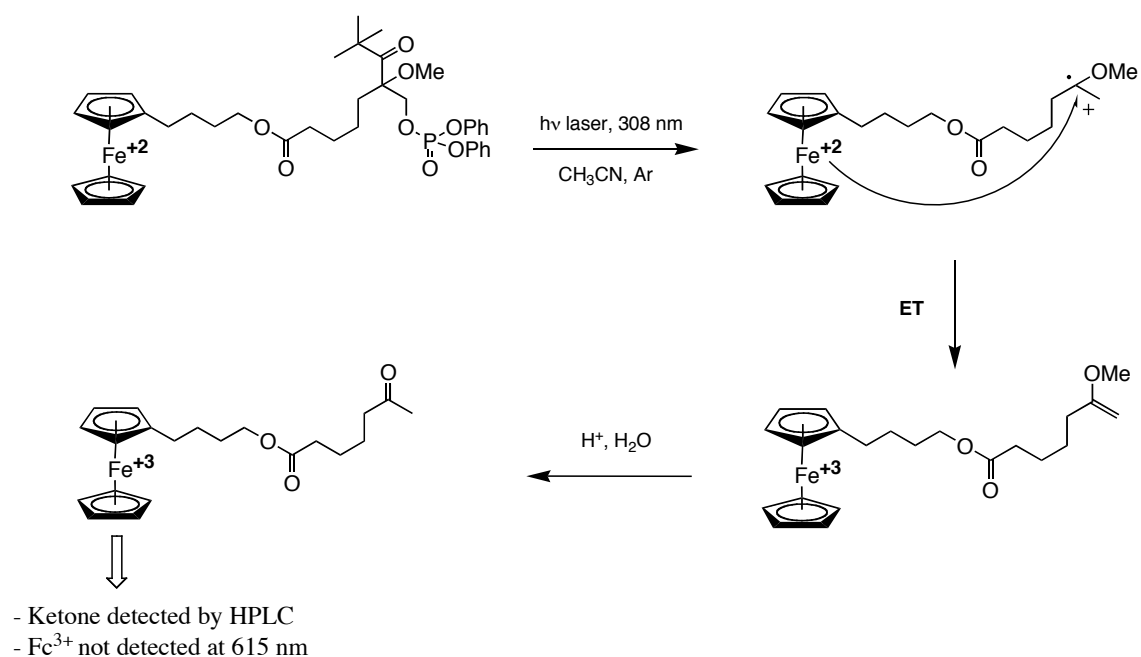
Our project is based on the use of redox-indicators (RI) like ferrocene or phenol as charge acceptor/detector in DNA (Scheme B). The UV transient absorption spectroscopy is used to measure the oxidation of the charge acceptor during electron-transfer. Both compounds ferrocene and phenol have lower oxidation potentials than the guanine ($E_{\text{ox}}^{\circ} = 1.29 \text{ V vs NHE}$) and possess distinct UV-absorption spectras which should allows us to measure the electron transfer using UV transient absorption spectroscopy. Ferrocenium, the oxidized form of ferrocene, has a characteristic absorption at $\lambda_{\text{max}} = 615 \text{ nm}$ such as the phenoxyl radical which absorbs at $\lambda_{\text{max}} = 410 \text{ nm}$.^{59,100}



Scheme B Novel assay to investigate ET in DNA using a redox-indicator covalently linked to the DNA as charge acceptor.

Nanosecond flash-photolysis has been employed to induce the electron transfer in DNA, using the 4'- pivaloyl modified thymidine T* developed in the Giese group as charge injector. This charge injector has the advantage to initiate a localized charge transport from a fixed starting point within the DNA backbone.

Ferrocene was first investigated in a simple D-A system (Scheme C) in order to show that ferrocene can be used as a charge acceptor in electron transfer processes. The first results based on a RP-HPLC analysis of the irradiated products were very promising. They proved that electron transfer occurs from the ferrocene to the radical cation because the ketone, the product of electron transfer was clearly identified on the HPLC chromatogram. However, despite our first hopes, the second series of experiment based on laser flash photolysis and transient absorption spectroscopy measurement shows that ferrocenium could not be detected by UV because of its too low extinction coefficient. The spectroscopic properties of ferrocene can not be used to measure electron transfer using laser flash photolysis and transient absorption spectroscopy in such systems.



Scheme C

Ferrocene as charge acceptor in a simple D-A system

Electron transfer was then investigated in DNA using phenol as charge acceptor. A phenol modified nucleoside was synthesized and incorporated into DNA using fully automated solid-phase synthesis (Figure A).

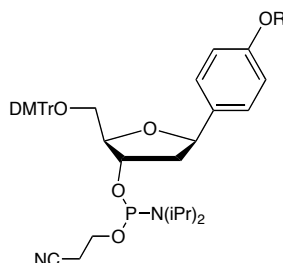
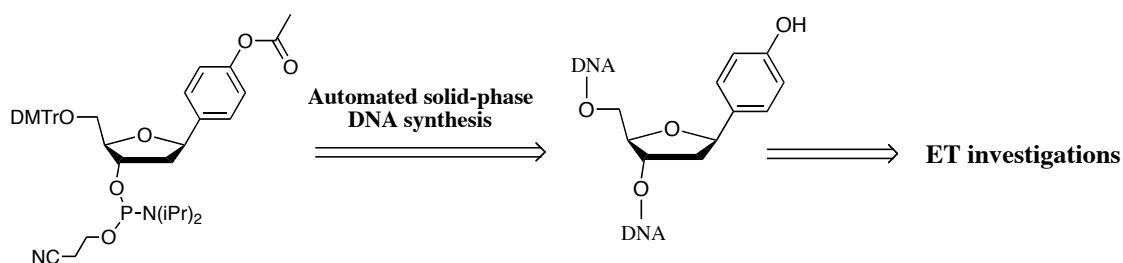


Figure A Phenol modified nucleoside ($R = \text{Me, All, AOC or Ac}$)

The choice of the phenol protecting group was a key point of the synthesis of the phenol modified nucleoside. The acetyl protecting group appeared to be ideal because it withstood the nucleoside synthesis conditions, it was compatible with the standard procedures for DNA synthesis and finally it was easily removed during ammonia treatment used to cleave the DNA strand from the solid support (Scheme D). The synthesis of the acetyl protected building block was achieved successfully in 10% yield over 10 steps and its incorporation within oligonucleotides was performed with efficient coupling using standard automated DNA synthesis.



Scheme D The acetyl protecting group strategy for incorporation of the phenol nucleoside into DNA using automated solid-phase DNA synthesis and further ET investigations

Photolysis of single and double strand phenol-labeled oligonucleotides followed by HPLC analysis of the irradiated products demonstrated that phenol is an excellent electron donor. The electron-transfer rates measured in single and double strand experiments are in agreement with the low oxidation potential of the phenol.

Theoretical Part

1	Introduction	1
1.1	The structure of Deoxyribose Nucleic Acid (DNA).....	1
1.2	DNA: the storage of the genetic code.....	3
1.3	Oxidative damage to DNA	4
1.3.1	The oxidative stress and its consequences	4
1.3.2	Electron transfer as cathodic protection against oxidative stress	6
2	Charge transport in DNA	7
2.1	Background	7
2.2	Charge injection in DNA.....	10
2.3	Charge migration in DNA.....	12
2.4	Charge transfer detection	13
2.4.1	By competition between charge transfer and water trapping reaction.....	13
2.4.1.1	Gel electrophoresis and phosphorimagery detection	13
2.4.1.2	HPLC detection.....	14
2.4.2	Detection by photochemical methods	16
3	Proposal.....	17
4	Ferrocene as charge acceptor in a simple D-A system.....	19
4.1	Introduction.....	19
4.1.1	The use of ferrocene and its derivatives in chemical and biological systems	19
4.1.2	Incorporation of ferrocene into DNA.....	19
4.1.3	Why ferrocene?.....	21
4.2	Our project.....	22
4.3	Synthesis of the ferrocenyl precursor	23
4.4	Photolysis experiments.....	26
4.4.1	HPLC analysis	26
4.4.1.1	Synthesis of the electron transfer product as reference.....	27
4.4.1.2	Blind test.....	28
4.4.2	Laser experiment.....	31
4.5	Conclusion	33

5	Phenol as charge acceptor	35
5.1	Introduction.....	35
5.2	Our project.....	36
5.3	Synthesis of the phenol modified nucleoside	37
5.3.1	Synthesis background.....	37
5.3.2	Synthesis strategy.....	40
5.3.3	Synthesis of the anisole nucleoside.....	41
5.3.4	Synthesis of the phenol protected nucleoside.....	44
5.3.4.1	The anisole approach: cleavage of the methyl ether	44
5.3.4.2	A new approach: the benzyl approach	46
5.3.5	Summary.....	49
5.4	Incorporation of the building blocks into DNA	50
5.4.1	Usuel procedures for oligonucleotides synthesis.....	50
5.4.2	Characterization of the mofified oligonucleotides.....	52
5.4.2.1	The anisole nucleotides	52
5.4.2.2	Deprotection of the phenol nucleotides in DNA	53
5.4.3	Summary.....	56
5.5	Investigation of electron transfer using HPLC analysis	57
5.5.1	Single strand experiments.....	57
5.5.1.1	Estimation of the $k_{ET,rel}$	57
5.5.1.2	Anisole as electron donor	60
5.5.2	Double strands experiments.....	62
5.5.2.1	Estimation of the $k_{ET,rel}$	62
5.5.2.2	Comparison with other electron donors	65
5.5.2.3	Further experiments	71
5.6	Investigation of electron transfer using UV detection of the phenoxyl radical	73
5.7	Conclusion	75
5.8	Further work and outlook	76

Experimental Part

6	Instruments and materials.....	79
6.1	Physical Data	79
6.1.1	NMR spectroscopy.....	79
6.1.2	Mass spectroscopy	80
6.1.3	UV-Vis spectroscopy	81
6.1.4	Elemental analysis	81
6.2	Chromatographic Methods.....	82
6.2.1	Thin Layer Chromatography	82
6.2.2	Flash Column Chromatography.....	82
6.2.3	High Pressure Liquid Chromatography.....	82
6.3	Irradiation instruments	83
6.4	DNA instruments.....	84
6.5	Chemicals and Solvents.....	84
7	General methods	85
7.1	Synthesis	85
7.2	General oligonucleotide procedures	85
7.2.1	Synthesis.....	85
7.2.2	Purification	86
7.2.3	Unmodified strands	86
7.2.4	Mass analysis	87
7.2.5	Quantification by UV-absorption	87
7.2.6	Hybridization	88
7.2.7	Melting point determination by UV-vis spectroscopy	88
7.2.8	Photolysis	88
7.3	Quantification of the photolysis products by RP-HPLC	89
7.3.1	Ferrocene derivatives photolysis	89
7.3.2	Phenol oligonucleotides photolysis.....	89

8	Synthesis of the ferrocenyl derivatives.....	90
8.1	Synthesis of the ferrocenyl linker, the 4- Ferrocenylbutanol (49).....	90
8.2	Synthesis of the radical injector (53)	94
8.3	Synthesis of the ferrocenyl precursor (42)	97
8.4	Synthesis of the ketone reference (58)	101
8.5	Synthesis of the phenyl derivatives for the blind test.....	102
9	Synthesis of the phenol nucleoside	107
9.1	The benzyl approach.....	107
9.2	The methoxy approach	124
10	Deprotection of the allyloxycarbonate protected oligonucleotide	135
11	Oligonucleotide sequences	136
12	Literature	137
13	Abbrevitions and Acronyms.....	145

Theoretical Part

1. Introduction

1.1 The structure of Deoxyribose Nucleic Acid (DNA)

DNA is a biopolymer with a pivotal role in biology as the carrier of genetic information in all living species.^{1,2} "This molecule of life" possesses a highly ordered structure which have been originally postulated in 1953 by the pioneers James Watson and Francis Crick.³

DNA is composed of repeating subunits (deoxyrinucleotides) and each nucleotide is further composed of a phosphate group, a sugar the 2'-deoxyribose, and a heterocyclic base. Four different bases are found in natural DNA: the pyrimidine bases cytosine (C) and thymine (T) and the purine bases adenine (A) and guanine (G). The linkage of the sugar-phosphate backbone of a single DNA strand is such that there is a directionality. That is, the phosphate on the 5' carbon of deoxyribose is covalently linked to the 3' carbon of the next deoxyribose. This lends a 5'-3' directionality to a DNA strand (Figure 1.1).

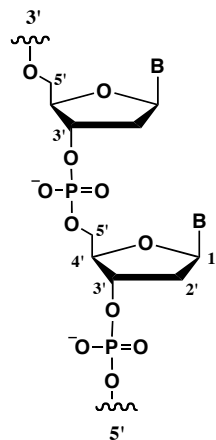


Figure 1.1 Primary structure of a DNA oligonucleotide

Under physiological conditions DNA exists predominantly as a double helix where the two oligonucleotide strands are coiled around each other around a common axis. The strands are arranged in opposite directions, the strands are thus anti-parallel. The two chains are held together by hydrogen bonds formed between pairs of bases. Pairing is highly specific: Adenine pairs with thymine, while guanine always pairs with cytosine (Figure 1.2). This satisfies Chargoff's rule that the amount of adenine is equal to the amount of thymine ($A = T$) and the amount of guanine equal

to the amount of cytosine ($G = C$). Adenine and thymine are connected by two hydrogen bonds while guanine and cytosine are connected by three hydrogen bonds.

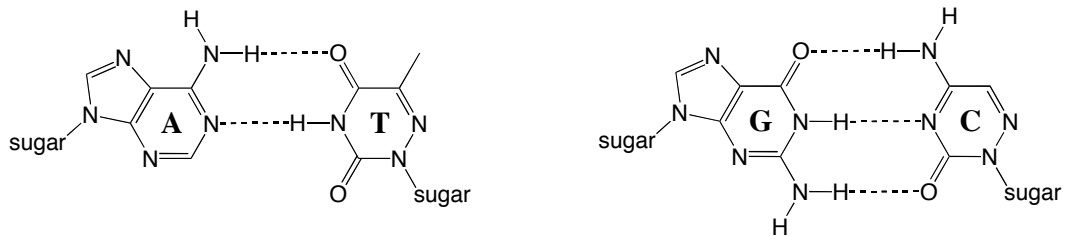


Figure 1.2 Watson-Crick hydrogen bonding

Duplex DNA can adopt several secondary structures; the most common is the B-form (Figure 1.3). B-DNA features a right-handed double helix in which the hydrophobic base pairs are on the inside of the helix and form a π -stacked core whereas the phosphate and the deoxyribose units are situated on the outside. The planes of the base residues are perpendicular to the helix axis. While the planes of the sugar residues are almost at right angles to those of the bases. The diameter of the helix is 20 Å. Adjacent bases are separated by a stacking distance of 3.4 Å along the helix axis. Hence the helix repeats itself every 10 residues on each chain at intervals of 34 Å.⁴

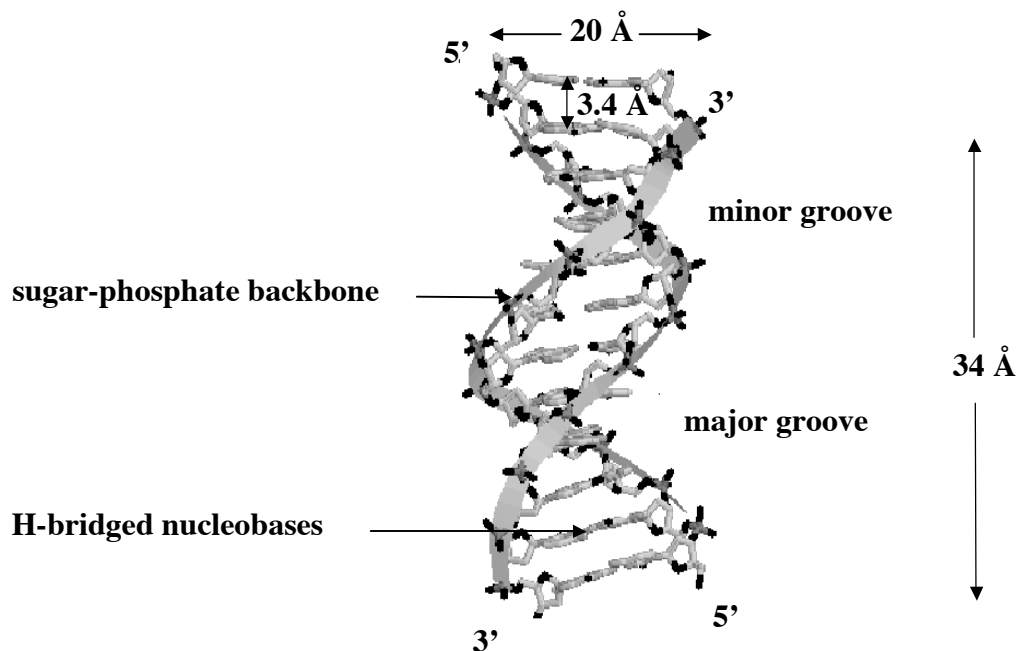


Figure 1.3 The structure of a B-DNA duplex

In addition to hydrogen bridging, the helical structure is substantially stabilized by π -stacking interactions between neighbouring nucleobases. Since the phosphate on the backbone is negatively charged, the DNA is surrounded by positive “counterions”.

Other secondary structures of DNA are the A- and the Z-form. For example, in a solution with higher salt concentrations or with alcohol added some specific sequences such as poly-G : poly-C favor the A-form, which is still right-handed, but makes a turn every 23 Å and there are 11 base pairs per turn.^{5,6} Another DNA structure is called the Z form, because its bases seem to zigzag. Z DNA is left-handed. One turn spans 46 Å, comprising 12 base pairs. The poly-GC : poly-CG DNA sequences in alcohol or high salt solution (> 4M NaCl) tends to have such structure.^{7,8}

Under the experimental conditions of this work we can assume that duplex DNA possesses a B-form structure. The B-form DNA structure is ideal for electron transfer because some of the electron orbitals belonging to the bases overlap quite well with each other along the long axis of the DNA.²⁷

1.2 DNA: the storage of the genetic code

Within a gene, the sequence of nucleotides along a DNA strand defines a protein, which an organism is liable to express at one or several points in its life using the information of the sequence.⁹ The relationship between the nucleotide sequence and the amino-acid sequence of the protein is determined by simple cellular rules of translation: the genetic code. Reading along the protein-coding sequence of a gene, each successive sequence of three nucleotides (called a codon) specifies or “encodes” one amino acid. Any changes to those instructions can alter the gene's meaning and therefore change the protein that is made (or how or when a cell makes that protein). In the living cell, DNA undergoes frequent chemical changes, especially during replication. Most of these damages are quickly repaired. Those that are not result in a mutation, increasing the risk of cancer.¹⁰ Numerous damages to DNA are also caused by oxygen radicals.

1.3 Oxidative damage to DNA

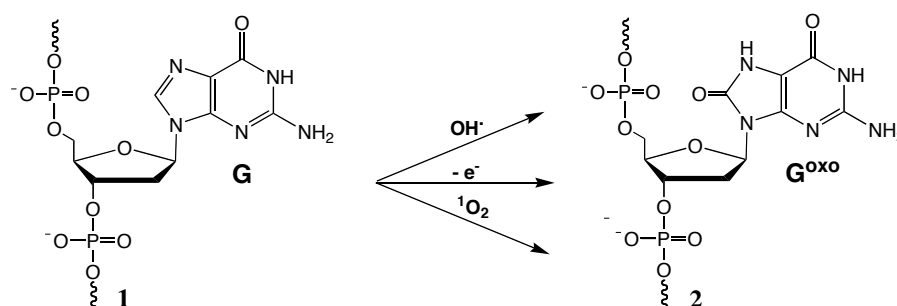
1.3.1 The oxidative stress and its consequences

Reactive oxygen species (ROS) are activated oxygen reagents such as hydroxyl radical OH[•], superoxide radical O₂^{•-}, hydroperoxide H₂O₂ or singlet oxygen ¹O₂. ROS induce numerous lesions in essential biomolecules, such as lipids, proteins and particularly DNA.^{10,11}

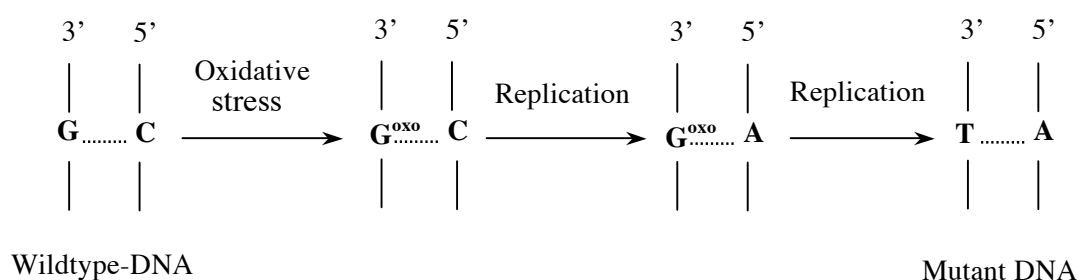
ROS are products of the oxygen metabolism in all aerobic organisms. ROS are principally generated as a result of energy production from the mitochondria (from the electron transport chain). Environmental agents such as ultraviolet light, ionizing radiation, redox chemicals and cigarette smoke also readily generate ROS.¹² The antioxidant defense system in most cells is composed of two components, the antioxidant enzymes (superoxide dismutase, catalase, glutathion peroxidase) and the low molecular weight antioxidants (vitamins A,C and E, glutathion and thioredoxin). These substances are the body's natural defense against endogenous generated ROS and other free radicals, as well as ROS generated by external environmental factors. Oxidative stress occurs when the production of ROS exceeds the body's natural antioxidant defense mechanisms, causing damage in cells notably to DNA. It has been estimated that endogenous ROS can result in about 200 000 base lesions per cell per day.^{13,14}

Oxidative stress to DNA causes deletions, mutations and other lethal genetic effects.^{11,15} Characterization of this damage to DNA has indicated that both the sugar and the base moieties are susceptible to oxidation, causing base degradation, single strand breakage, and cross-linking to protein.¹⁶ The biological consequences of many of the oxidative products are known. For example, unrepaired thymine glycol, an oxidative product of pyrimidine damage, is a block to DNA replication and is thus potentially lethal to cells.

The guanine base is particularly sensitive to oxidative stress because it has the lowest oxidation potential (1.29 vs NHE) of all the natural nucleobases.¹⁷ Guanine **1** can be oxidized by OH[•] attack, by ¹O₂ addition or by electron transfer, which generates for example 8-oxo-7,8-dihydro-2'-deoxyguanosine (G^{oxo}) **2** (Scheme 1.1). G^{oxo} **2** is readily bypassed by the DNA polymerase and is highly mutagenic because unrepaired G^{oxo} will mispair with A, leading to an increase in G to T transition mutations (Scheme 1.2).¹⁸



Scheme 1.1 Formation of oxoG by oxidative stress



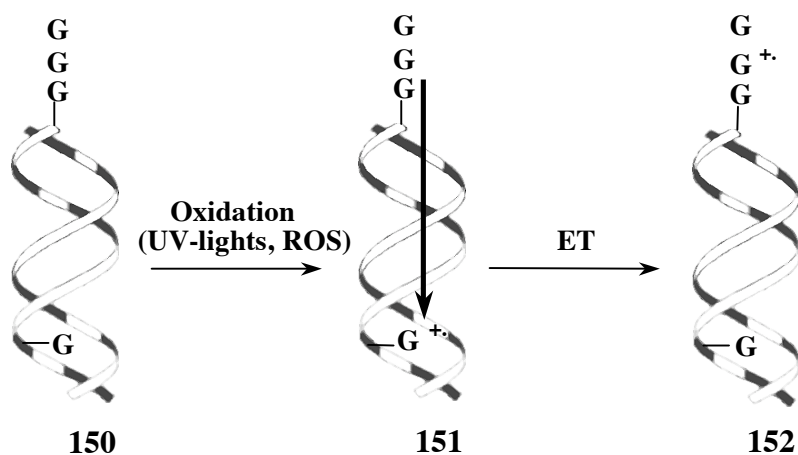
Scheme 1.2 Mutation generated into DNA by unrepaired G^{oxo}

An other consequence of oxidative stress is the DNA strandbreak. The principal cause of single strand break is oxidation of the sugar moiety by the hydroxyl radical OH[•]. Oxidative attack by OH[•] on the deoxyribose moiety will lead for example to the release of free bases from DNA, generating strand breaks with various sugar modifications and simple abasic sites.¹⁹

1.3.2 Electron transfer as cathodic protection against oxidative stress

In order to maintain the fidelity of the genetic material, all organisms have evolved many different biological pathways to repair or remove various types of DNA damage, resulting from either endogenous or external DNA reactive agents.^{20, 21} The migration of electron holes in DNA has been proposed among these pathways to serve as a protection of the genetic information against oxidative stress.²²

Oxidation of a guanine leads to the intermediate guanine radical cation $G^{\cdot+}$ (**150**→**151**) (Scheme 1.3). This $G^{\cdot+}$ can initiate a hole migration through the DNA towards a GG-doublet or GGG-triplet (**151**→**152**), which is more easily oxidized due to the GG stacks and therefore acts as a thermodynamic sink for the positive charge.²³



Scheme 1.3 DNA repair through electron transfer

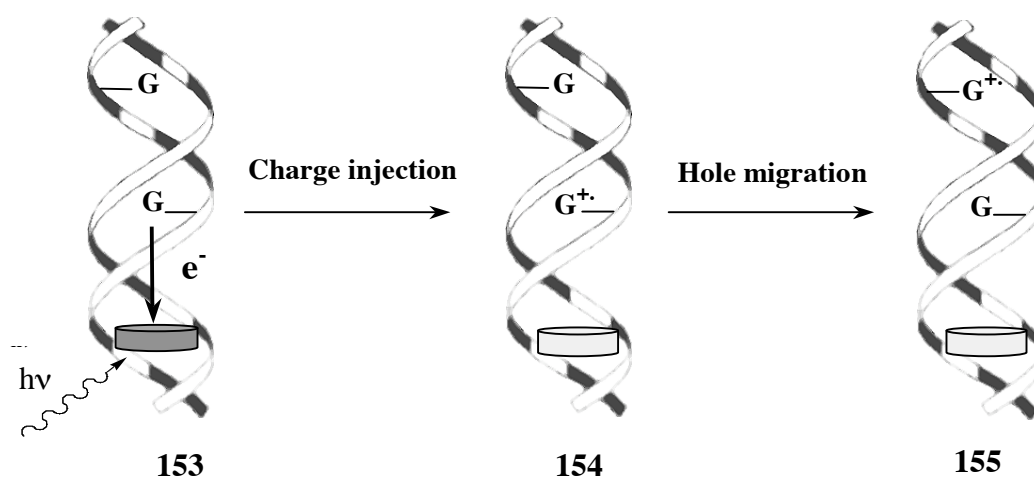
In some organisms sacrificial G-rich DNA sequences presumably protect genes and other essential chromosomal domains against oxidative damage. When an essential element of the genome is attacked by an oxidizing agent, a less essential element of their genome is sacrificed and oxidized through electron transfer. Protection can be provided by an insulating, but very short G-rich single strand (~10-18 base long) such as the telomeric 3'-overhang located at the termini of chromosomes or by a highly conductive long double strand (>103 base pair long) such as the long CpG islands found at the 5'-ends of genes in animal chromosomes. These islands consist mostly, or exclusively, as their name indicates, of CG base pairs.^{24,25,26} Neither the CpG islands nor the telomeric overhangs are transcribed. The sacrificially oxidized domain may have only a protective function.

2. Charge transport in DNA

2.1 Background

The structure and properties of duplex DNA have a special fascination for chemists, materials scientists, and life scientists. The possibility that the one-dimensional array of π -stacked base pairs in B-DNA might serve as a pathway for charge migration was suggested over 40 years ago by Daniel Eley and D.I.Spivey,²⁷ soon after Watson and Crick discovered the double-helix structure.³ Interest in DNA electron transfer has been spurred by its relevance to oxidative damage and repair mechanisms in DNA as shown before (Chapter 1.3) and by its potential applications in molecular electronics.

During the last decade hole transport in DNA has been extensively investigated by several different photochemical methods.^{28,29,30} The principle behind these experiments is straightforward (Scheme 2.1). A photoactivated oxidant, covalently linked or intercalated to the DNA, captures an electron from a neighboring nucleobase, with preference from a guanine because guanine has the lowest oxidation potential of the four DNA bases (1.29 V vs NHE)¹⁷ (**153**→**154**) and a guanine radical cation G^+ is generated in the core of the DNA. This electron-loss center ultimately ends up at G residues via hole migration through the DNA duplex (**154**→**155**).^{31,32,33}



Scheme 2.1 General method for charge transport in DNA

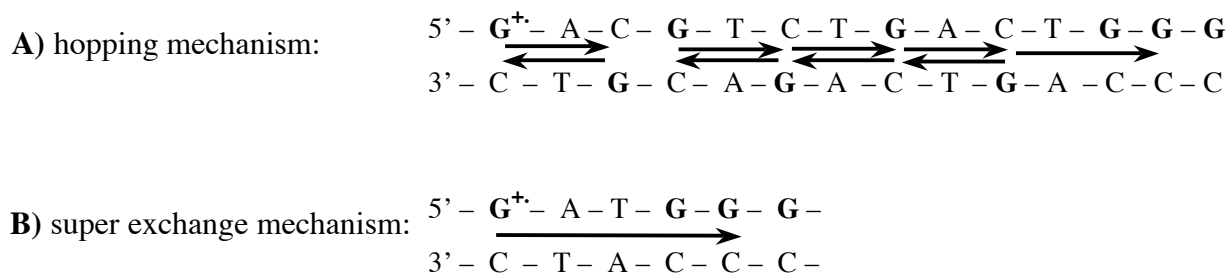
Initial studies on electron transfer through DNA employed randomly intercalated metal complexes (ruthenium) as excited acceptors and either a second intercalator, nucleobase, or modified nucleobase as the donor.³⁴ Uncertainty concerning the donor-acceptor separation has made the interpretation of these studies problematic. Then, several different chromophores were developed which are tethered to the end of an oligonucleotide and are proposed to intercalate between base pairs near the end of the duplex.³⁵ Fukui and Tanaka³⁶ employed DNA-acridine conjugates in which the acridine is proposed to substitute for a base pair upon hybridization with a complementary oligonucleotide. Both end-tethered and mid-strand-tethered anthraquinone chromophores have been employed by Schuster and coworkers.³⁷ More recently, Kelly and Barton³⁸ have investigated the interaction of fluorescent nucleobase analogues of adenine with donor nucleobases. Our approach in the Giese group is fundamentally different since we employ a photocleavage reaction to irreversibly generate a guanine radical cation which can undergo hole transfer to a trap site consisting of three guanines in the same strand (a GGG unit).³⁹

The intense discussion of results obtained is centered around the β -value of the Marcus-Levich-Jortner correlation (Eq. 2.1) that describes the exponential influence of the donor-acceptor distance (Δr) on the electron transfer rate (k_{ET}) in a single-step process.¹³⁰⁻¹³²

$$k_{ET} \propto e^{-\beta \cdot \Delta r} \quad (\text{Eq. 2.1})$$

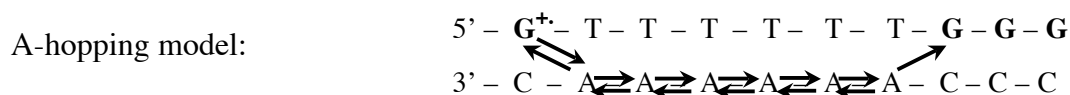
The β -value characterizes the extent of the distance dependence and varies with the nature of the donor-bridge-acceptor (D-B-A) system. Depending on the experiment, β -values between 0.1 and 1.4 \AA^{-1} have been reported for DNA double strands.³⁸⁻⁴⁰ These differences in β -values demonstrate dramatic divergent effects of the distance on the electron-transfer rate. It was possible to explain the contradictory results regarding the range and rate of the electron transfer by a new model: the hopping model. In this model, the long-range charge transfer in DNA can be viewed as a series of short range hops between energetically appropriate guanine bases (Scheme 2.2 A)^{31,32,41} The total charge transport is considered to be a sequence of single, reversible transfer steps between guanines bases, and these steps are highly distance dependent since the charge is tunnelling between donor and acceptor.

The bridge (AT base pairs <4) is not oxidized or reduced during this process. It is characterized as a super exchange mechanism (Scheme 2.2 B) The hopping mechanism has been intensively studied in the Giese group using the Giese charge injection system.^{42,43,44}



Scheme 2.2 A) The ET hopping mechanism. B) The ET super exchange mechanism

Recently a new model was developed in the Giese group to explain the electron transfer over long (A-T)_n sequences: the A-hopping model (Scheme 2.3). This new model takes into consideration the oxidation of adenine and involves adenine as charge carriers.^{146,147}



Scheme 2.3 The A-hopping model

2.2 Charge injection in DNA

Different radical injectors were developed in the Giese group in order to investigate charge transport through DNA (Fig. 2.1).^{42,43,44} These radical injectors are photolabile modified nucleosides which are incorporated into DNA and which generate a C4'-deoxyribose radical cation upon irradiation. This method has the advantage to offer a unique opportunity to induce a localized charge transport from a fixed starting point within the DNA backbone and with little disruption of the DNA shape.⁴⁵

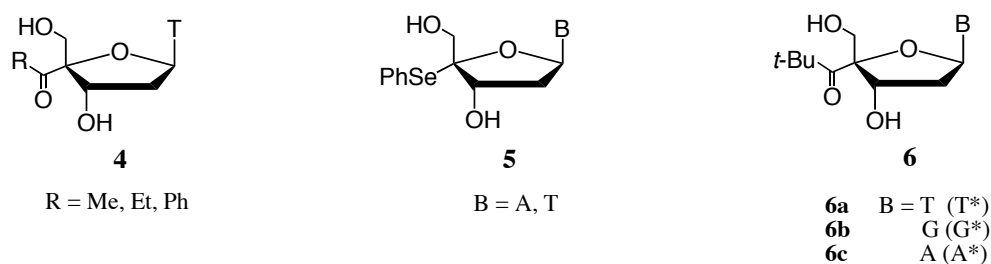


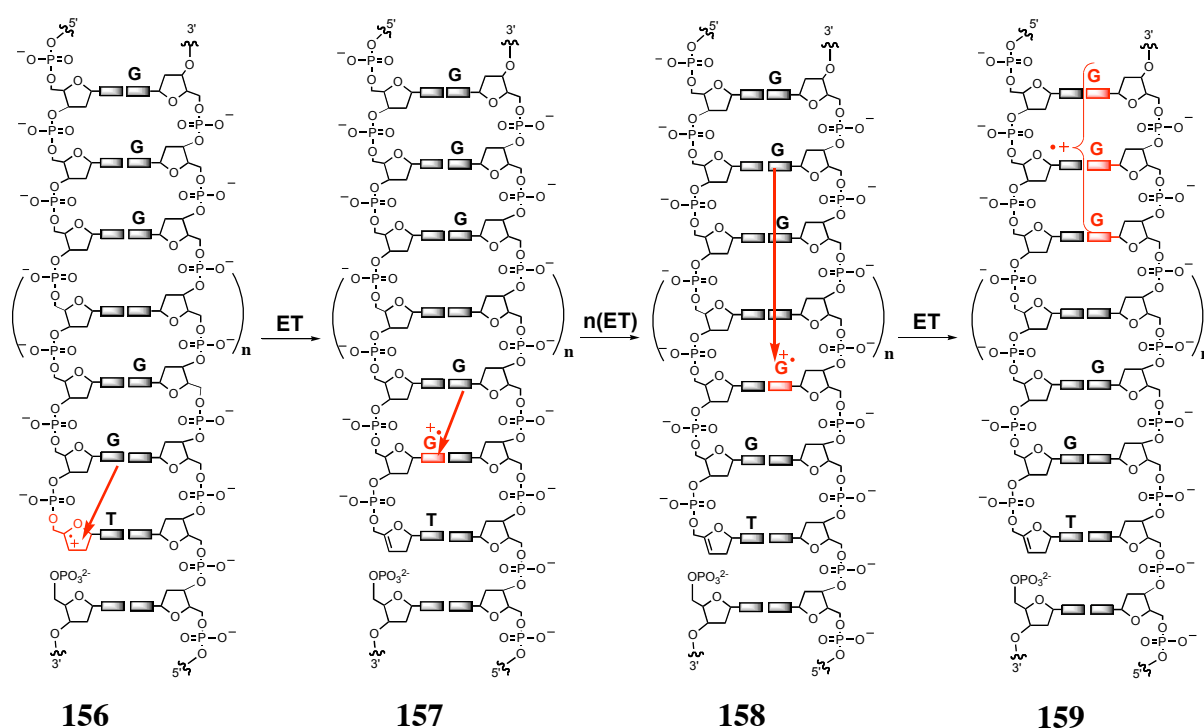
Figure 2.1 Radical injectors of the Giese group that can generate C4'-ribose radicalcations

The pivaloyl modified injector **6** is the most efficient one upon irradiation with a 320 nm cut-off filter. At this wavelength the homolytic cleavage of the C4' bond occurs with high yield and the nucleobases of the DNA are not damaged. In this work, we will use the C4'-pivaloyl substituted thymidine nucleotide T* **6a** as charge injector.

Photolysis of a DNA strand **7** containing T* (**6a**) leads via Norrish Type I cleavage to the C4'-riboradical **8** (Scheme 2.4).⁴² Norrish Type I cleavage of ketones or aldehydes is an homolytic cleavage originating from their excited $n\pi^*$ state. Cleavage of the excited carbonyl compound leads to an acyl-alkyl radical pair which generates another alkyl radical and carbon monoxide through decarbonylation. The more stabilized the generated radical the easier is the α -cleavage. Therefore *tert*-butylketone does lend itself for Norrish Type I reactions.⁴⁶ The semi occupied orbital of **8** destabilizes the adjoining 3'-C-O bond which undergoes rapid heterolytic 3' β -elimination forming selectively the strand break product C4'-radical cation **9** and 5' phosphate **10**. This mechanism has been confirmed by numerous experimental and theoretical studies.^{47,48}

2.3 Charge migration in DNA

As stated before, a guanine base within the DNA strand preferentially acts as an electron donor and reduces the radical cation **9** to the enol ether **11** (**156**→**157**) (Scheme 2.6). The initial charge transfer from guanine to the sugar radical cation **9** is due to the low oxidation potential of this base ($E^{\circ}_{\text{ox}} = 1.29 \text{ V vs NHE}$)¹⁷. The efficiency of this charge transfer depends on the distance between the radical cation **9** and the guanine base. The resulting guanine radical cation $\text{G}^{\bullet+}$ can then initiate electron transfer through DNA mediated by guanine bases (**157**→**158**). A triple GGG unit was used as a thermodynamic sink for the positive charge (**158**→**159**).²³



Scheme 2.6 Charge migration in DNA through the guanine bases

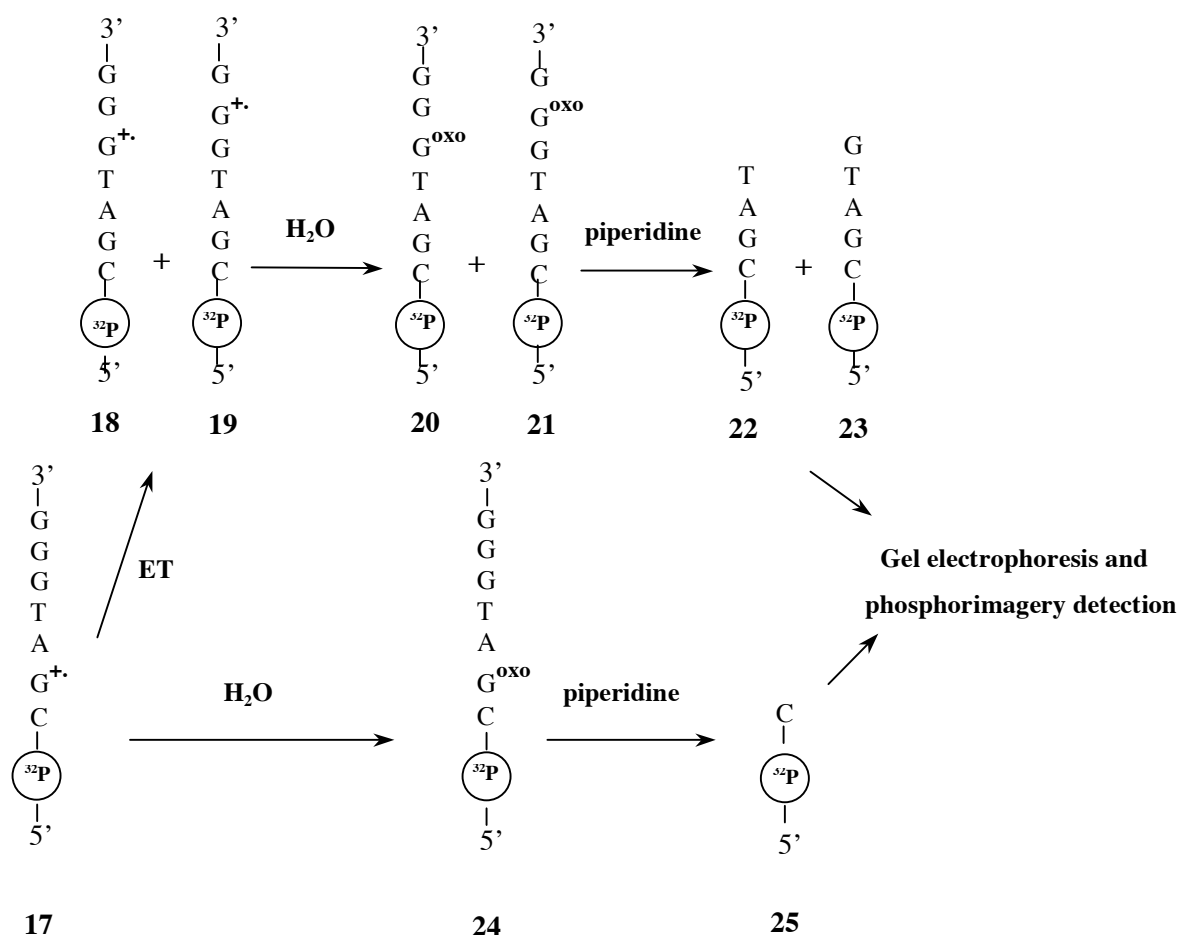
One of the side reactions that occurs during charge transfer is the addition of water to the sugar radical cation⁴⁹ (Scheme 2.5) or to the guanine radical cation.⁵⁰ This leads to oxidatively modified nucleotide fragments. This competition reaction between charge transfer and water addition has been used for the detection of the electron transfer and for the measurement of its efficiency in DNA.

2.4 Charge transfer detection

2.4.1 By competition between charge transfer and water trapping reaction

2.4.1.1 Gel electrophoresis and phosphorimagery detection

For analytical reasons the positive charge of the first formed G^+ is transferred to an adjacent G of the complementary strand **17** which is ^{32}P radiolabeled at its 5'-end (Scheme 2.7). Water addition on G^+ leads to an oxidatively modified guanine, the oxoguanine that can be cleaved off selectively by base treatment.⁵⁰⁻⁵² Once the charge arrives on the triple GGG it is trapped by nucleophilic addition of water.³¹ Hot piperidine is used to cleave the DNA strand at the oxoguanine site. This cleavage yields the corresponding ^{32}P -labeled fragments that can be analyzed and quantified by gel electrophoresis and phosphorimagery.



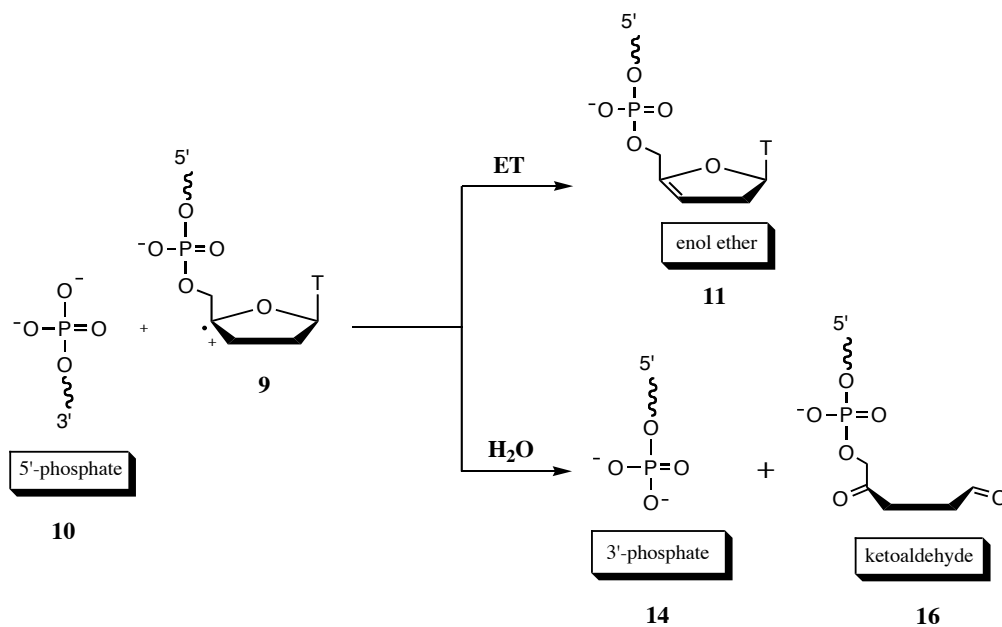
Scheme 2.7 Charge detection by water addition and piperidine treatment followed by gel electrophoresis and phosphorimagery

The relative electron transfer rate ($k_{ET,rel}$) is given by the ratio (Eq. 2.2) between the rates of the electron transfer reaction (k_{ET}) and water addition (k_{H_2O}) because of first-order or pseudo first-order conditions (excess of H_2O):

$$k_{ET,rel} = \frac{k_{ET}}{k_{H_2O}} \propto \frac{22 + 23}{25} \quad \text{Eq. 2.2}$$

2.4.1.2 HPLC detection

We have seen that charge transfer (**9**→**11**) competes with water reaction that leads to 3'-phosphate **14** and ketoaldehyde **16** (Scheme 2.8). This competition between water addition (**9**→**14**+**16**) and electron transfer (**9**→**11**) can be used to determine relative rates for the electron transfer from an electron donor (e.g. guanine) to the sugar radical cation **9** by means of the competitive reaction kinetic procedure. The yields of the different fragments **10**, **11**, **14** and **16** were obtained by RP-HPLC analysis of the irradiated solution (Figure 2.2).



Scheme 2.8 Competition between ET and H₂O addition to radical cation **9**

A typical RP-HPLC chromatogram of the irradiated solution containing both electron transfer and water addition products is shown below (Figure 2.2). Once isolated, all the products were characterized by mass spectroscopy (MALDI-ToF-MS).

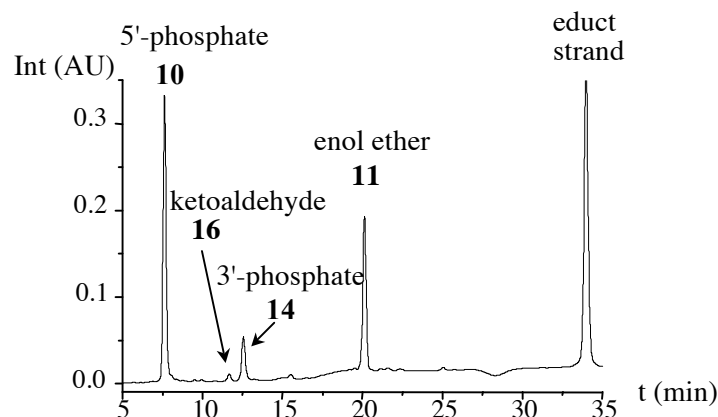


Figure 2.2 Typical HPLC chromatogram of the irradiated solution containing both electron transfer and water addition products

During a complete conversion of the radical cation **9** to enol ether **11** and water addition products **14** and **16** the relative electron transfer rate could be given by the ratio :

$$k_{ET,rel} = \frac{k_{ET}}{k_{H_2O}} \propto \frac{[\text{enol ether } \mathbf{11}]}{[3' \text{- phosphate } \mathbf{14}] + [\text{keto-aldehyde } \mathbf{16}]} \quad \text{Eq. 2.3}$$

However, because of first-order or pseudo first-order conditions (excess of H_2O) the ratio between the rates of the electron transfer reaction (k_{ET}) and all other trapping reaction like the water addition (k_{H_2O}) is also given by the concentration ratio :

$$k_{ET,rel} = \frac{k_{ET}}{k_{H_2O}} \propto \frac{[\text{enol ether } \mathbf{11}]}{[5' \text{- phosphate } \mathbf{10}] - [\text{enol ether } \mathbf{11}]} \quad \text{Eq. 2.4}$$

Under the assumption that the competing reactions are not dependant upon the nucleotide sequence, we used the ratio k_{ET}/k_{H_2O} as the relative rate $k_{ET,rel}$ of the electron transfer step.⁴⁸ It is important to note that in contrast to photoinduced electron transfer studies, in our ground state experiments the electron transfer is irreversible, there is no back electron transfer.

Both methods based on competitive kinetic reaction between electron transfer and water addition have the advantage to mimics the natural conditions of DNA reactions in a living cell.

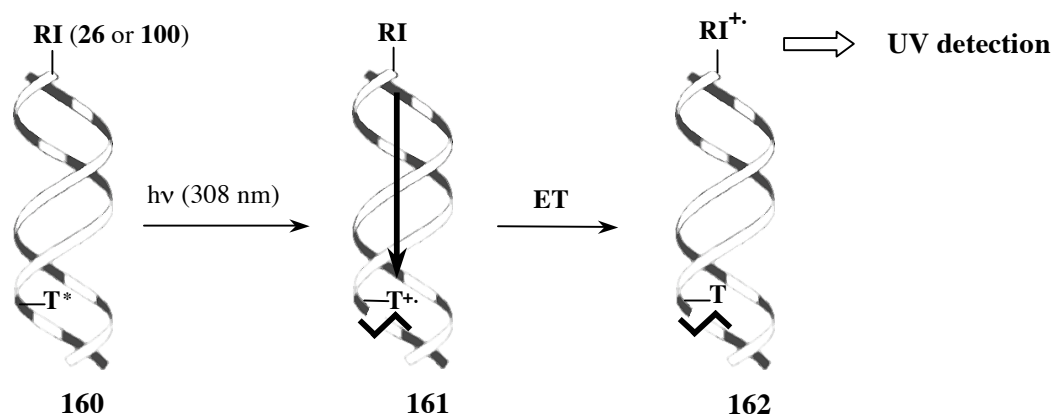
2.4.2 Detection by photochemicals methods

Other methods also exist for the study of charge transport in DNA. In most of these studies the rates were determined by fluorescence quenching of photoactivated metal complexes or aromatic compounds intercalated into DNA.^{29a,53} Measurements of electron transfer-rate by fluorescence quenching often yield more than one rate for the electron transfer through DNA. This is interpreted as a result of the reactions of different conformations or, alternatively, as competing side reactions that have nothing to do with the electron transfer through DNA. EPR and transient absorption spectroscopy were also employed to detect radical intermediates in flash-quench studies of charge transfer through DNA.¹⁴⁴ The flash-quench technique was originally developed to explore charge transport in proteins.⁵⁶ but has been applied effectively to DNA systems. However the DNA systems used in these studies present the disadvantage that either the electron donor or the electron acceptor were intercalated complexes, which might perturb the DNA

3. Proposal

In order to decipher the elementary steps and the mechanism of electron transfer, one has to directly measure the dynamics in real time and in suitably designed, structurally well characterized DNA assemblies. As stated before, transient absorption spectroscopy can be used to directly observe the formation and decay of the radical ion intermediates in photoinduced electron transfer processes. Such measurements have been routinely employed to determine the kinetics of charge separation and charge recombination in synthetic D-B-A systems and in proteins, they also aid in the assignment of multiple decay components to specific species.^{54,55}

Our approach to the kinetic investigation of electron transfer through DNA is based on the use of an unnatural redox-active nucleotide **26** or **100** (Figure 3.1) acting as charge detector when incorporated into DNA. Both artificial building blocks **26** and **100** have lower oxidation potentials than the guanine¹⁷ and would therefore also be oxidized during the electron transfer process (scheme 3.1). We plan to use transient absorption spectroscopy in order to monitor the formation of the oxidized redox-indicators (RI) **26** or **100** in DNA because both compounds possess also distinct UV-absorption spectras. The long-range charge transport through DNA would also be measured more precisely using optical methods. Nanosecond flash-photolysis shall be employed to induce the electron transfer in DNA, using the 4'- pivaloyl modified thymidine T* as charge injector. This charge injector has the advantage to initiate a localized charge transport from a fixed starting point within the DNA backbone.⁴⁵



Scheme 3.1 Novel assay in kinetic investigation of ET through DNA using a redox-indicator covalently linked to the DNA, which can be detectable by transient UV-spectroscopy

We chose to carry out our experiments with ferrocene and phenol as redox-indicators since both have lower oxidation potential than the guanine ($E^{\circ}_{\text{ox}} = 1.29 \text{ V vs NHE}$).¹⁷ The oxidation potential of ferrocene was found to be $E^{\circ}_{\text{ox}}(\text{Fc}^{2+}/\text{Fc}^{3+}) = 0.40 \text{ V vs NHE}$ in acetonitrile⁵⁷ and that one of phenol $E^{\circ}_{\text{ox}}(\text{PhOH} / \text{PhOH}^{\cdot}) = 0.86 \text{ V vs NHE}$.¹⁴¹ Moreover ferrocenium, the oxidized form of ferrocene, has a characteristic absorption at $\lambda_{\text{max}} = 615 \text{ nm}$ ⁵⁸ such as the phenoxyl radical which absorbs at $\lambda_{\text{max}} = 410 \text{ nm}$.^{59,100}

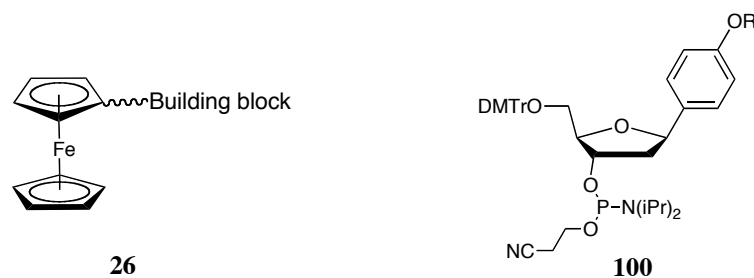


Figure 3.1 Building blocks containing the redox-indicators ferrocene (**26**) or phenol (**100**). *R* is a protecting group which has to be removed once building block **100** is incorporated into DNA

We thus intended to synthesize modified nucleotides containing ferrocene **26** or phenol **100** and to examine, first in simple D-A systems, if these redox indicators can act as charge traps. If this proved successful we will incorporate the modified nucleotides into DNA and examine the subsequent charge transport. The following work consists of two parts, a first part about ferrocene as charge acceptor in a simple D-A system, and a second about phenol as charge acceptor in DNA.

4. Ferrocene as charge acceptor in a simple D-A system

4.1 Introduction

4.1.1 The use of ferrocene and its derivatives in chemical and biological systems

Investigations of photoinduced electron transfer processes in biological systems such as DNA and proteins or in many chemical redox systems such as self assembled monolayers as well as the development of DNA hybridization probes and electrochemical sensors have employed a numerous of transition-metal complexes. These includes ruthenium,⁶⁰⁻⁶³ osmium,^{61,64} rhodium,^{62, 65} copper⁶⁶ and iron^{67,68,69} complexes. Ferrocene, most particularly, was often used as electrochemical probe for the detection of DNA sequences. DNA hybridization can be detected by changes in electrochemical voltage through the redox-active ferrocene that behaves differently in the presence of a DNA hybrid than it does in the presence of a single strand.⁷⁰ Ferrocene was also employed to measure the electron transfer rate using voltammetry in series of ferrocene-based monolayers (alkane, phenylethynyl) attached on gold electrode via thiol groups.^{71,72} Ferrocene derivatives have thus emerged as strong candidates for molecular electronic devices and electro optical materials.^{73,74}

4.1.2 Incorporation of ferrocene into DNA

Several methods for incorporating a ferrocene moiety into DNA exist. Fc-containing DNA oligonucleotides have been prepared, in which the ferrocenyl group is either linked to the N-3 position of a thymine base **28**⁷⁷ or conjugated to the nucleobase of deoxyuridine through an unsaturated bond **29**⁷⁸ or attached to the 2' position of the ribose ring through a butoxy linker **30**⁷⁹ (Figure 4.1).

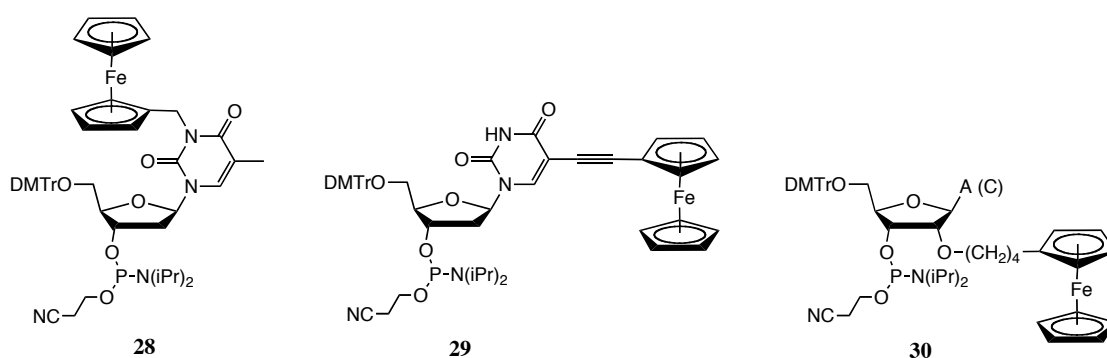
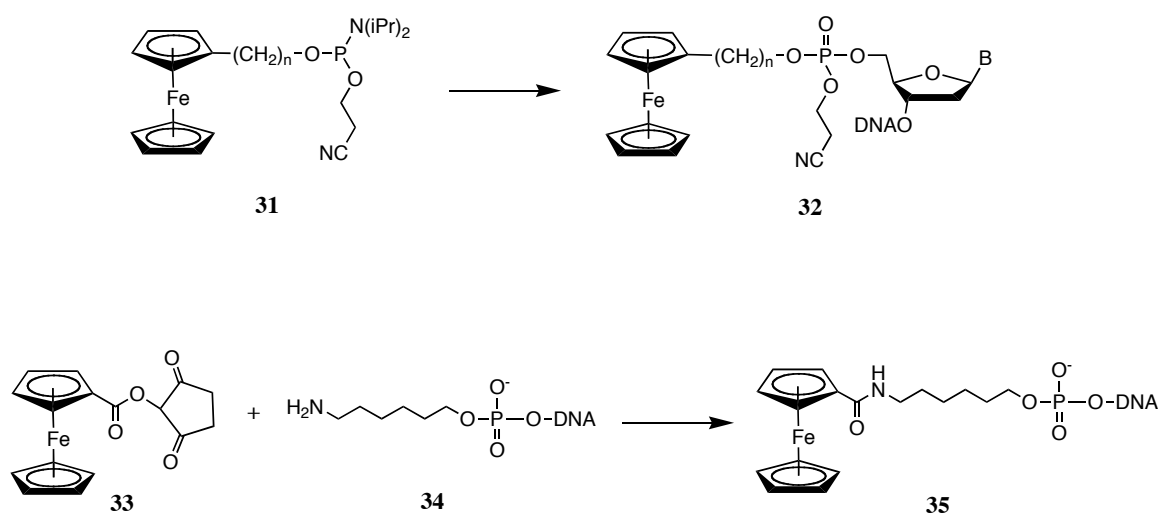


Figure 4.1 Fc-containing DNA phosphoramidites for incorporation into DNA

The incorporation of a ferrocenyl residue into oligodeoxyribonucleotides has been also achieved by coupling a ferrocenyl-phosphoramidite derivative **31** with the 5'-OH end of an oligonucleotide chain^{69,79} or by condensation of an activated ester of ferrocene-carboxylic acid **33** with the 5'-amino modified end of an oligodeoxyribonucleotide chain **34**^{67, 68, 80} (Scheme 4.1). A key advantage in those procedures is that, by attaching a conjugating molecule at the 5'-terminus of an oligomer, no modification in the standard automated solid-phase synthesis protocols⁸¹ has to be introduced.



Scheme 4.1 Other methods for incorporating ferrocene into DNA

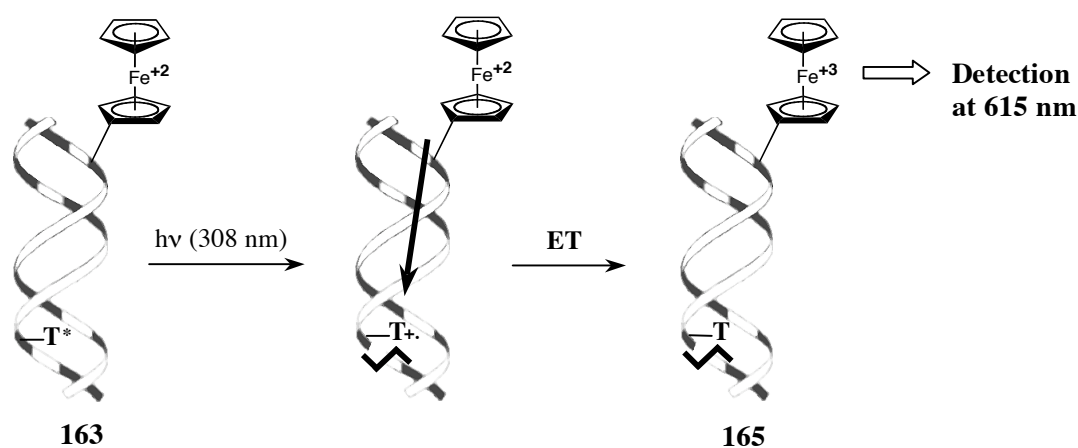
4.1.3 Why ferrocene?

The advantages of a ferrocene-based approach to investigate electron transfer are :

- Ferrocene is a unique class of one-electron donor due to its well established robust and reversible redox couple. Ferrocene and the corresponding ferrocenium salt differ from most other complexes since the central iron atom assumes the oxidation state +2 in ferrocene and the oxidation state +3 in ferrocenium ion. They contain two cyclopentadienyl rings in a sandwich-arrangement, so that the iron atom is highly bound and can scarcely participate in further coordination bindings.⁷⁵
- The oxidation potential of ferrocene ($E_{\text{ox}}^{\circ} = 0.40 \text{ V vs NHE}$ in acetonitrile)⁵⁷ is lower than the oxidation potential of guanine ($E_{\text{ox}}^{\circ} = 1.29 \text{ V vs NHE}$).¹⁷
- Ferrocene has a high degree of chemical and thermal stability (e.g. to air and water).⁵⁸
- Ferrocene is also an attractive probe because of its convenient synthetic chemistry: it is amendable to standard organic transformations, in particular typical coupling and protection/deprotection chemistry.
- Ferrocene possesses a unique spectroscopic property that should enable its sensitive and specific detection in a complex biological environment (Absorption of ferrocene: $\lambda_{\text{max}} = 440 \text{ nm}$ and ferrocenium : $\lambda_{\text{max}} = 615 \text{ nm}$).⁵⁸
- The redox potential can be easily tuned over a wide range by the choice of substituents on the rings of the ferrocene moiety.⁷⁶ Electron-donating groups, such as alkyls, shift the redox-potential of ferrocenyl derivatives to lower potential,^{69,70b} while electronwithdrawing groups such as carbamyls shift the redox potential to higher values.^{67, 68, 80}

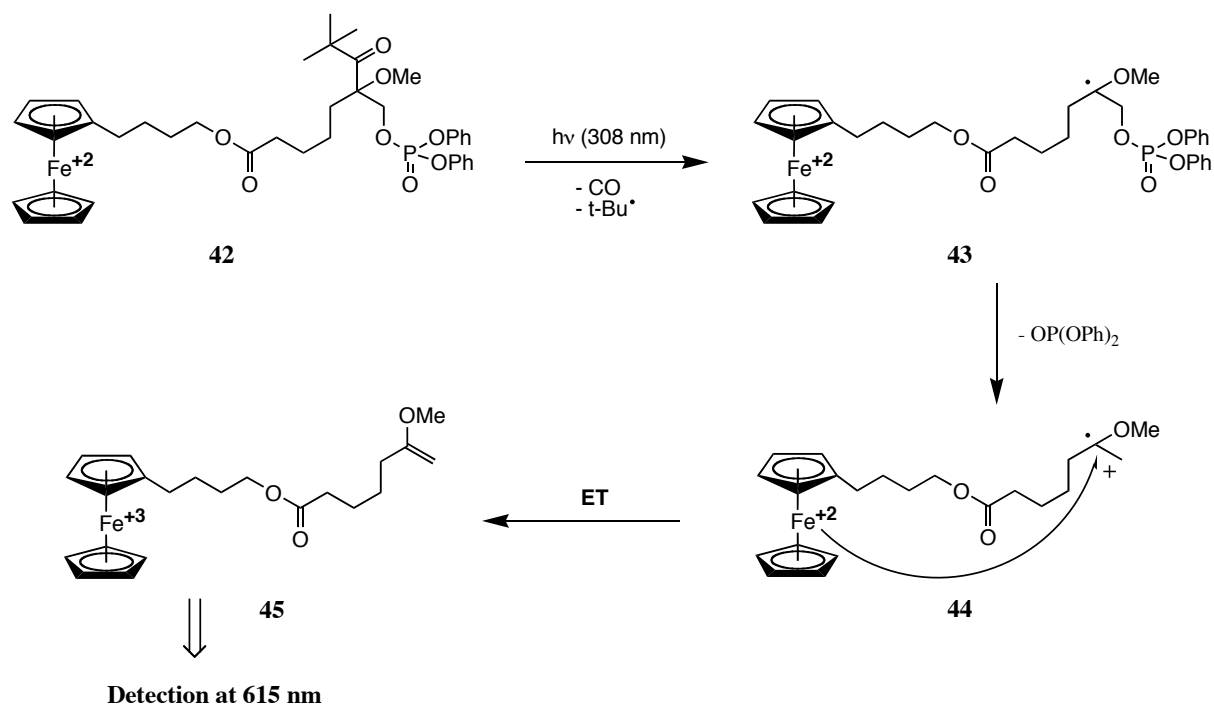
4.2 Our project

We plan to use ferrocene as redox-indicator to measure electron transfer through DNA as depicted in Scheme 4.2. Ferrocene is incorporated into DNA together with the charge injector T*. Upon irradiation at $\lambda \geq 308$ nm, a radical cation is generated on the charge injector (**163**→**164**) resulting from a Norrish type I cleavage of the pivaloyl group, followed by a spontaneous 3'-elimination (see Scheme 2.4 p. 11) and charge migration is initiated. We expect the positive charge to migrate towards ferrocene (**164**→**165**) which should be a thermodynamic sink for the positive charge⁵⁷. Ferrocene (+2) would thus be oxidized to ferrocenium (+3) and we intend to detect this oxidation using transient absorption spectroscopy.



Scheme 4.2 Electron transfer detection using ferrocene

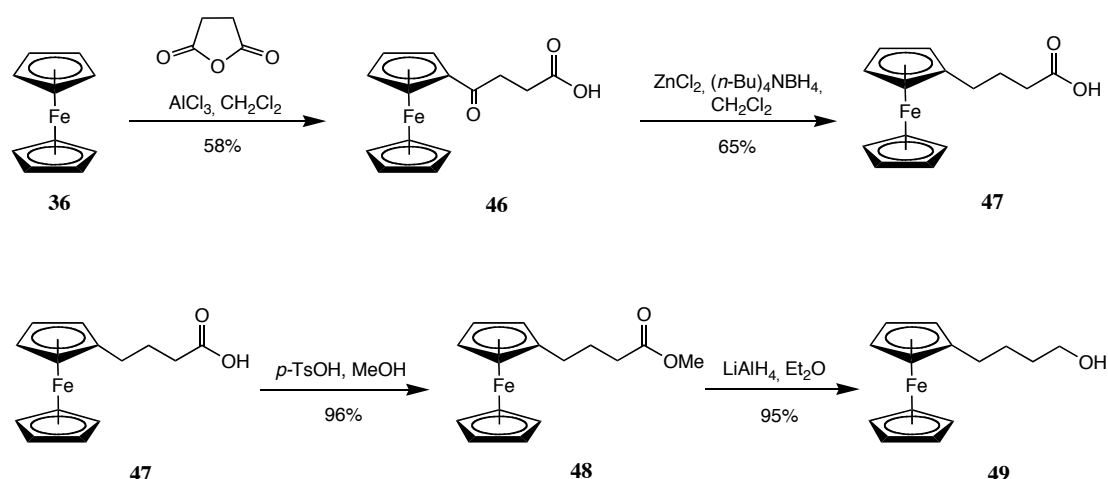
In order to test the principle before applying it to the DNA, a simple system **42** was designed, in which ferrocene is linked to a photolabile radical injector (Scheme 4.3). Irradiation of **42** at $\lambda \geq 308$ nm generates the radical cations **44** via Norrish type I cleavage and subsequent β -elimination of the phosphate leaving group.⁸² This radical cation has strong oxidizing properties.⁸³ We expect it to oxidize ferrocene (+2) to ferrocenium (+3) (**44**→**45**) and we intend to follow this process by transient absorption spectroscopy. Since ferrocenium has an absorption maximum at 615 nm⁵⁸, the absorbance at this wavelength will be monitored in order to obtain kinetic information about electron transfer in system **42**. If this experiment proves successful, ferrocene will then be used as redox-indicator in DNA systems.



Scheme 4.3 The ferrocenyl model system for ET investigation

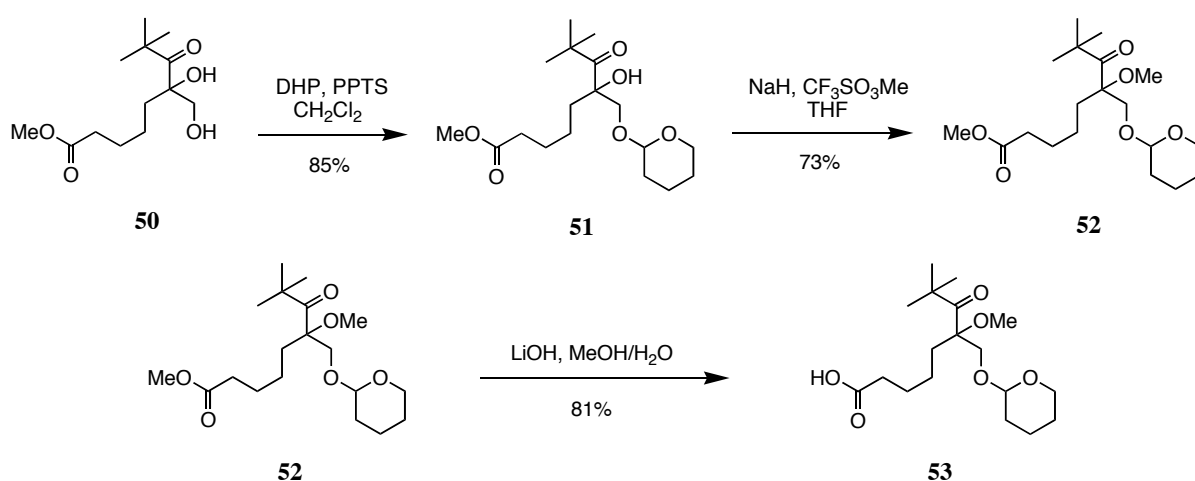
4.3 Synthesis of the ferrocenyl precursor

The ferrocenyl precursor **42** was synthesized via a 10 steps procedure. In the first step ferrocene **36** is reacted with succinic anhydride using Friedel–Craft’s catalyst AlCl_3 to provide the ketoacid **46** in 58% yield (Scheme 4.4).⁷⁹ Ketoacid **46** was then reduced with tetrabutylammonium borohydride and ZnCl_2 using a mild Clemmensen type reductive deoxygenation to furnish the acid **47**.⁸⁴ The carboxylic acid function which could not be directly reduced to the corresponding alcohol was first esterified with methanol in the presence of para-toluene sulfonic acid and thereafter reduced under suitable conditions by reaction with LiAlH_4 .



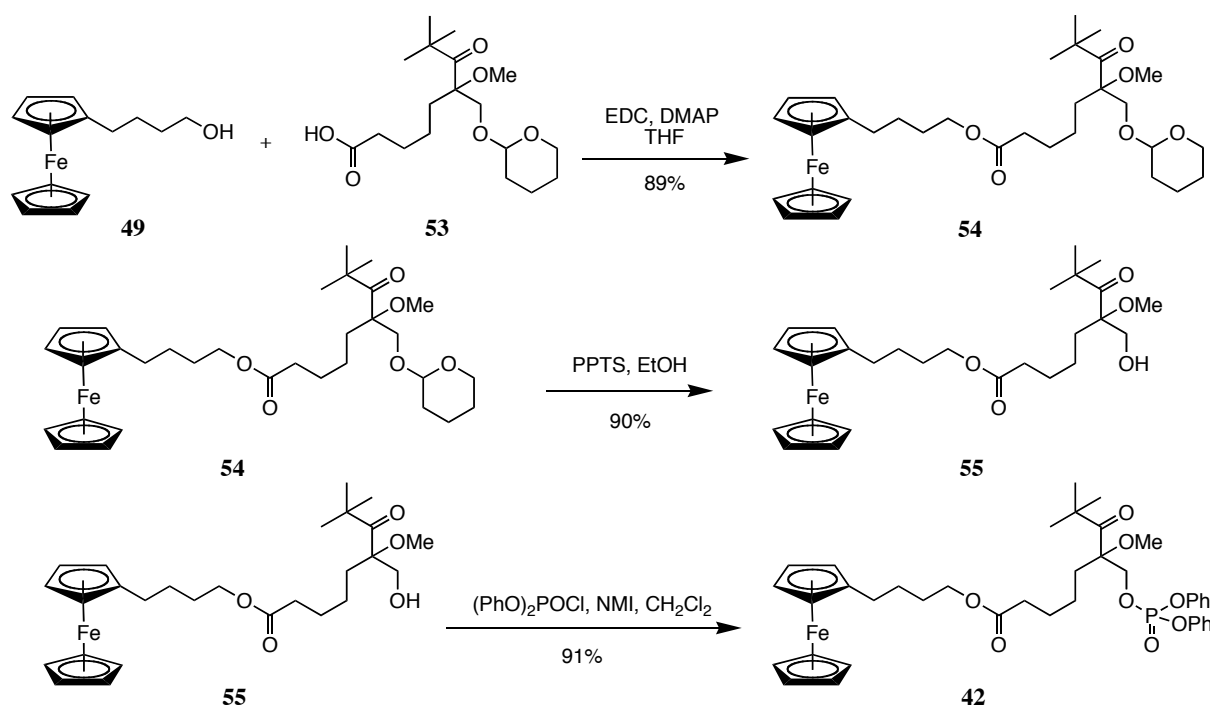
Scheme 4.4 Synthesis of ferrocenylbutanol

The synthesis of compound **50** has been developed in the Giese group.^{85,86} The tetrahydropyran protecting group seemed to be a good choice for the orthogonal protecting group strategy required in the following synthesis (Scheme 4.5) because it can selectively be introduced and removed under mild acidic conditions.⁸⁷ Protection of the primary alcohol function of **50** with dihydropyran catalysed with pyridinium paratoluene sulfonate gives compound **51** which was then converted to the methylether **52** by treatment with trifluoromethane sulfonic acid methyl ester. The ester function of compound **52** was saponified in the presence of lithium hydroxid to afford the carboxylic acid **53** in good yield.^{88,89}



Scheme 4.5 Synthesis of the radical cation injector

In order to get the target compound **42** we have to couple the alcohol **49** with the carboxylic acid **53** (Scheme 4.6). Alcohol **49** reacted with carboxylic acid **53** in presence of EDC and DMAP as catalyst to provide the desired ferrocenylester **54** in good yield.^{90,91} The tetrahydropyransyl protecting group was then removed under mild acidic conditions⁸⁷ to afford alcohol **55** and a suitable phosphate group was incorporated to give the photolytically active phosphorylated monomer **42**.⁹² This resulting conjugate containing both ferrocene and radical injector is now suitable for irradiation experiments in order to examine the charge transfer in our system.

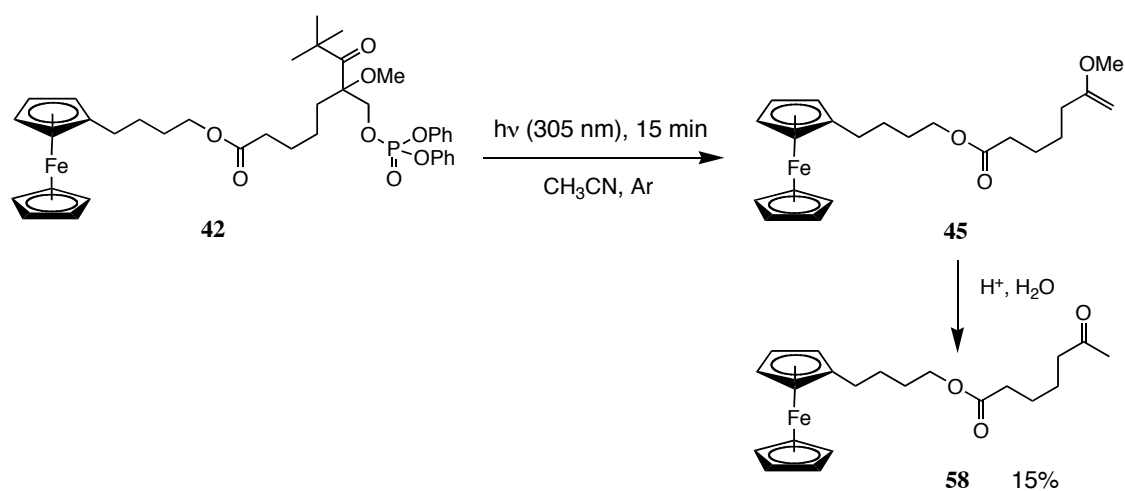


Scheme 4.6 Synthesis of the ferrocenyl precursor

4.4 Photolysis experiments

4.4.1 HPLC analysis

HPLC analysis was used as a first simple method to examine if ferrocene can act as an electron donor in system **42**. We hope by this way to detect the formation of the enol ether **45** which is the product of the electron transfer reaction. The irradiation of compound **42** was attempted using a mercury high pressure lamp with a 305 nm cut-off filter, under argon in acetonitrile (10^{-5} M) (Scheme 4.7). The photolysis solution was analyzed by RP18-HPLC and the products were identified by ESI-mass spectrometry if possible.



Scheme 4.7 Photolysis of the ferrocenyl precursor

The result as expected shows that enol ether **45** was formed under above experimental conditions but it is rapidly converted in presence of water to ketone **58** which has a retention time of 5.3 min.(Figure 4.2). Ketone **58** was obtained in 15% yield. The product was quantified by using an internal standard (see Experimental Part 7.3.1).

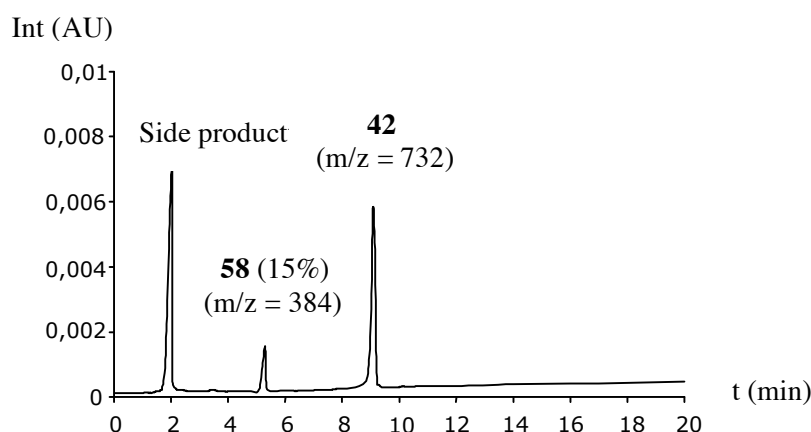
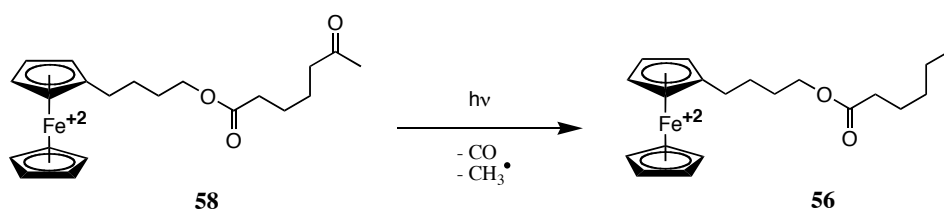


Figure 4.2 RP18-HPLC results of the irradiation experiment (solvent A: TEAA-Buffer, solvent B: Acetonitrile; Acetonitrile gradient 70% to 100% in 25 min)

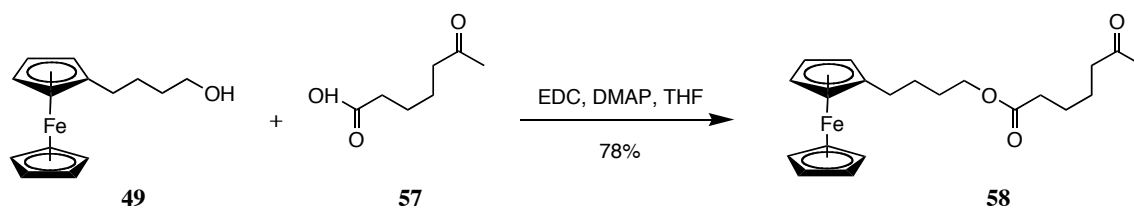
By longer irradiation time (≥ 15 min), the ketone **58** can undergo further Norrish Type I reaction to give product **56** (Scheme 4.8) but this product was not observed in our case.



Scheme 4.8 Norrish Type I reaction of ketone **58**.

4.4.1.1 Synthesis of the electron transfer product as reference

A product verification was made by co-injecting the independently formed ketone **58** with the irradiated solution of **42** into the RP18-HPLC. Ketone **58** was easily synthesized by coupling the previously synthesized ferrocenyl butanol with the commercial 6-oxoheptanoic acid (Scheme 4.9).



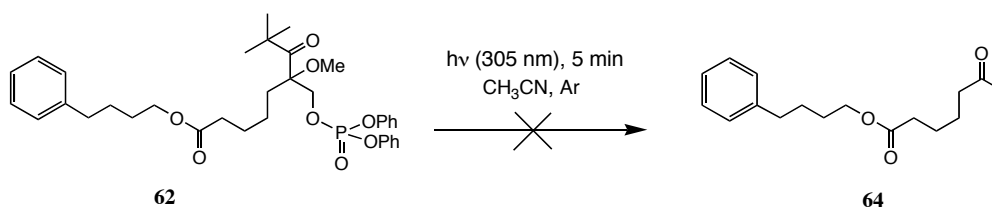
Scheme 4.9 Synthesis of the ketone reference

The co-injection of the synthesized ketone **58** confirmed its existence as electron transfer product by the presence of only one peak at 5.3 min with only one mass ($m/z = 384$) on the chromatogram.

The formation of ketone **58**, despite of its low yield, gives us a strong evidence that electron transfer occurs from ferrocene to radical cation **44** (see Scheme 4.3 p. 23). However in order to be sure that the electron comes really from ferrocene, we had to replace the ferrocene by a phenyl moiety that can not act as an electron donor as reported below.

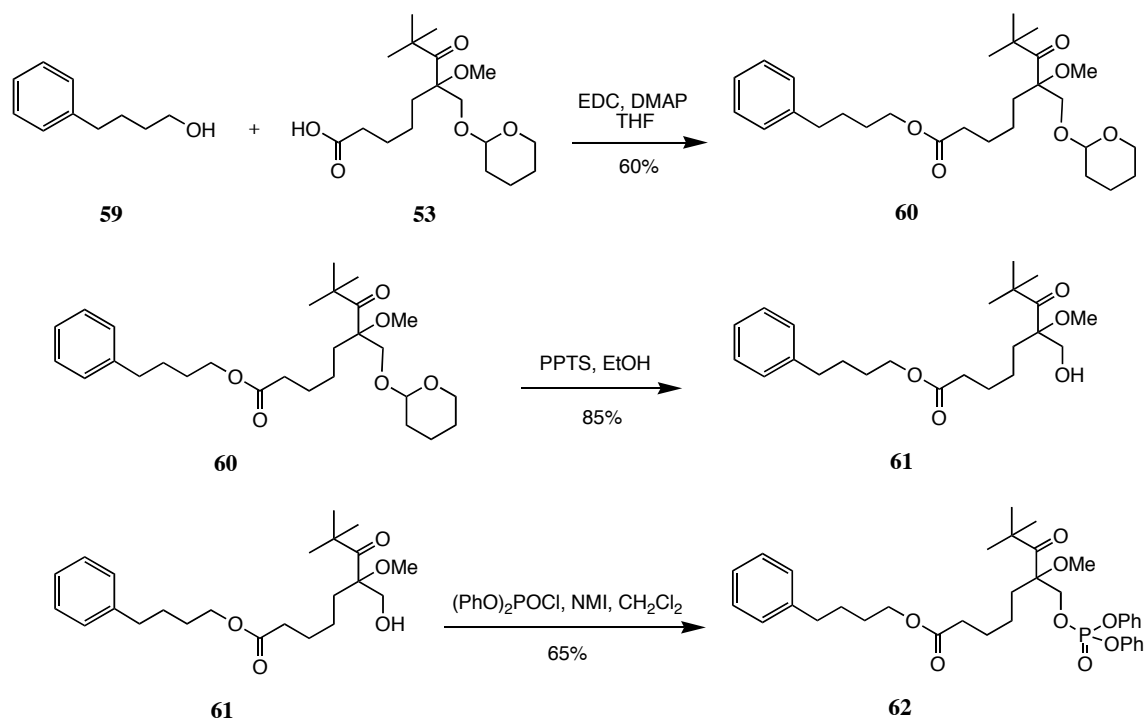
4.4.1.2 Blind test

Compound **62**, in which the ferrocene group has been replaced by a phenyl group was synthesized and subjected to the same irradiation conditions as compound **42** (Scheme 4.10). The phenyl group cannot be an electron donor so it should not generate electron transfer product in this case.



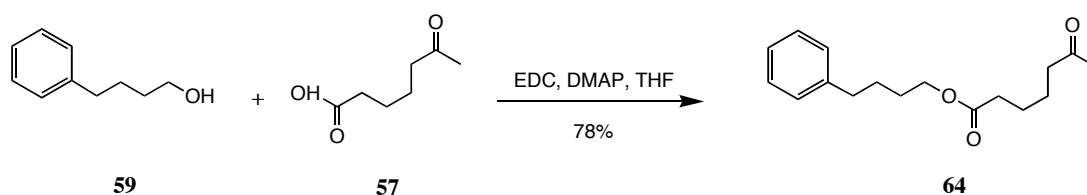
Scheme 4.10 Photolysis of the phenyl derivate **62** as blind test

Compound **62** was synthesized following the procedures used for compound **42** (Scheme 4.11). Phenylbutanol **59** was reacted with carboxylic acid **53** in presence of EDC and DMAP^{90,91} to afford compound **60** which was further deprotected and converted to the corresponding phosphorylated product **62**.⁹²



Scheme 4.11 Synthesis of the phenyl derivative

In case that electron transfer occurred in system **62**, the electron transfer product should be the ketone **64**. Thus, the ketone **64** was synthesized (Scheme 4.12) and injected into the RP18-HPLC as a reference (Figure 4.3B).

Scheme 4.12 Synthesis of reference compound **64**

Compound **62** was irradiated under the same irradiation conditions as compound **42** (under argon with mercury high-pressure lamp with a 305 nm cut-off filter) in acetonitrile (10^{-5}M). The sample was analyzed by RP18-HPLC (Figure 4.3A) and the products were identified by ESI-mass spectrometry. A product with a retention time of 2.1 min ($m/z = 308$) was isolated but, as expected, the ketone **64** which has a retention time of 3.8 min ($m/z = 276$) (Figure 4.3B) was not observed on the chromatogram. A product verification was made by co-injecting the independently formed ketone **64** into the RP18-HPLC.

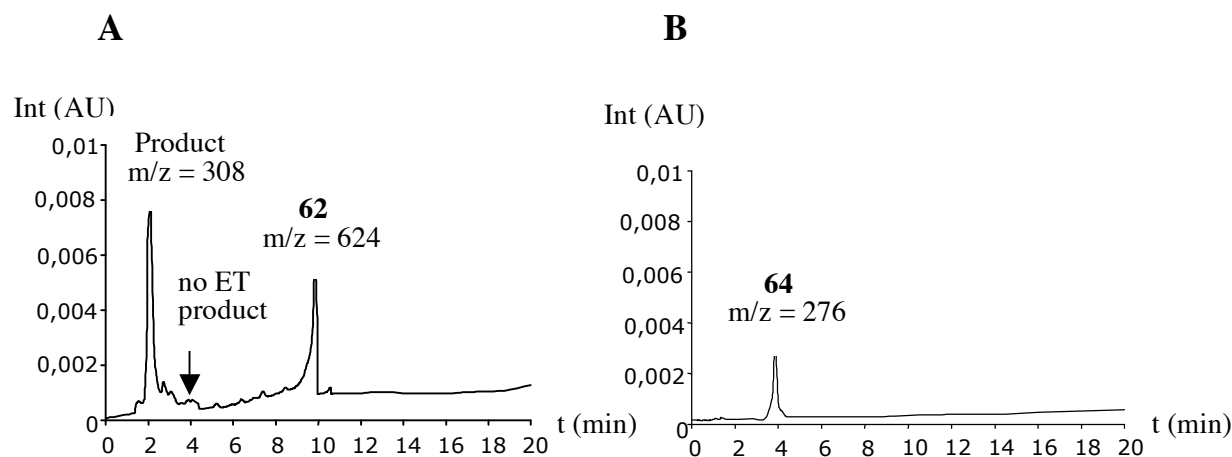
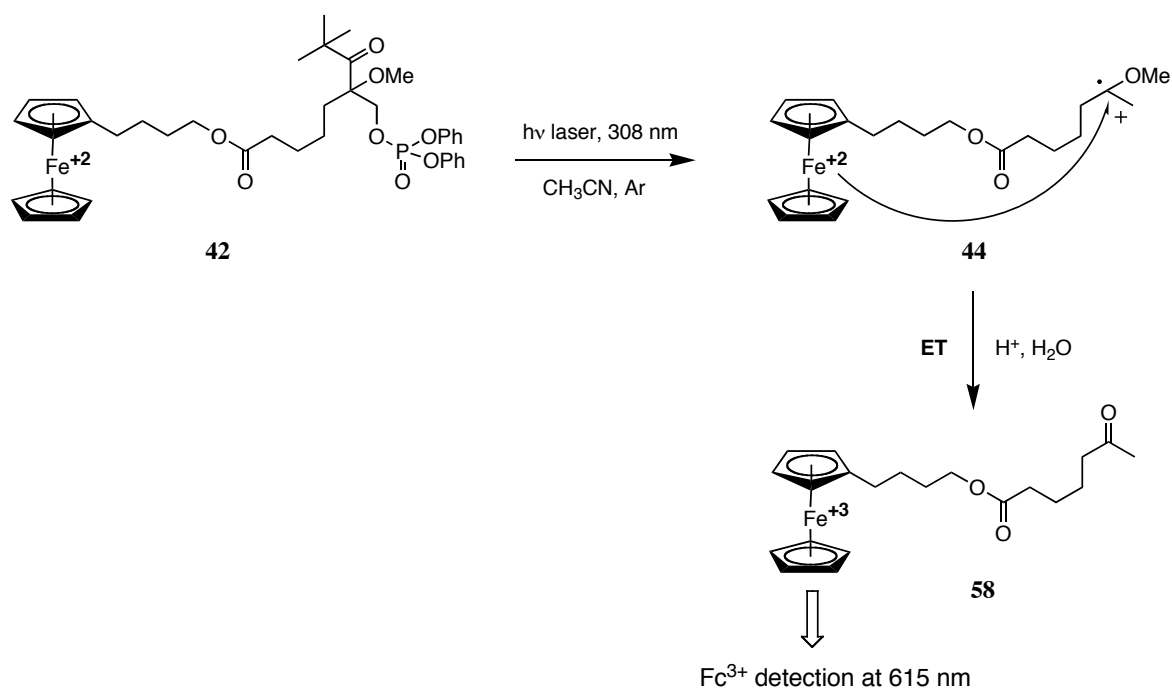


Figure 4.3 A) RP18-HPLC result of irradiation of compound **62**. B) Reference compound **64** (solvent A : TEAA-Buffer, solvent B : Acetonitrile ; Acetonitrile gradient 70% to 100% in 25 min)

These results prove, first that there is no electron transfer in a system like **62**, when ferrocene is replaced by a non-electron donating group and second, that the electron transfer observed in system **42** is due to ferrocene. According to the literature it is assumed that electron transfer occurs via an intermolecular process in compound **42** by low concentrations (10^{-5}M).¹⁴⁵ We can therefore conclude that ferrocene can be used as an electron donor in such photolysis experiments and although the yield of the electron transfer product is quite small, these results give us the opportunity to take the next step. We intend to use the spectroscopic properties of ferrocene to investigate electron transfer in system **42** using laser irradiation followed by transient absorption spectroscopy.

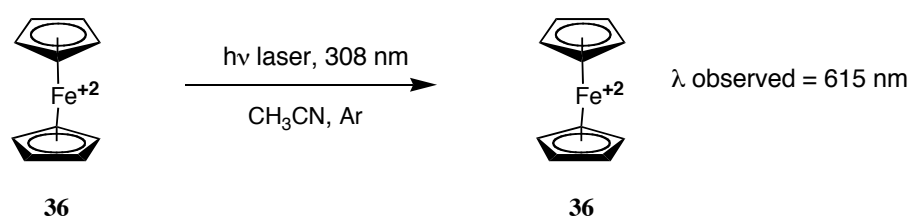
4.4.2 Laser experiment

The light-induced charge transfer in model system **42** was investigated using nanosecond flash photolysis (XeCl-excimer laser, $\lambda = 308$ nm).⁹³ In this way we attempt to detect spectroscopically the oxidation of ferrocene (+2) to ferrocenium (+3) resulting from the electron transfer from the ferrocene to the induced radical cation (Scheme 4.13). Absorbance at 615 nm was monitored in order to obtain kinetic information about electron transfer.



Scheme 4.13 Light-induced electron transfer in model system **42** using laser spectroscopy

Before starting the laser experiment with system **42** we first studied ferrocene **36** alone to be sure that no absorption could interfere at the detected wavelength (Scheme 4.14). A 8 mM solution of ferrocene **36** in acetonitrile was irradiated at 308 nm. As expected, no absorption was observed for irradiated ferrocene at 615 nm.



Scheme 4.14 Laser irradiation of ferrocene

In order to examine if electron transfer can be monitored through the oxidation of ferrocene to ferrocenium, system **42** was subjected to laser irradiation. Experiment consists of dissolving the compound **42** in degassed acetonitrile in order to obtain a 8 mM solution which was irradiated under argon with a XeCl-excimer laser at 308 nm. The reaction was observed at wavelength 615 nm corresponding to the absorbance maximum of ferrocenium.

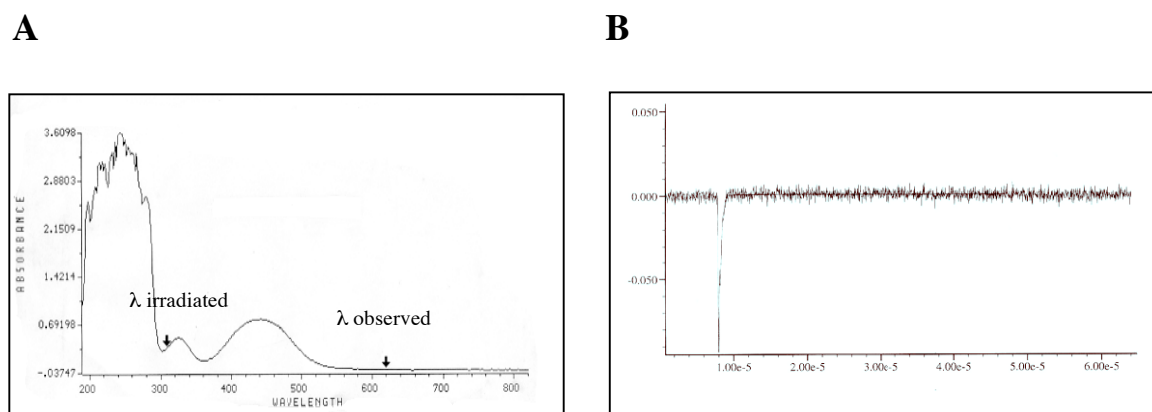


Figure 4.4 A) Absorbance spectrum of compound **42**. B) Time-resolved transient absorption at 615 nm for compound **42**

The spectrum shortly after the laser flash shows no transient absorption at 615 nm. A second series of laser irradiation were carried out but the transient absorption of the ferrocenium part was never detected probably because of the low extinction coefficient of ferrocenium. Extinction coefficient was found to be only $\epsilon = 420 \text{ M}^{-1} \cdot \text{cm}^{-1}$ for ferrocenium and $\epsilon = 100 \text{ M}^{-1} \cdot \text{cm}^{-1}$ for ferrocene.^{57,58} Considering these low extinction coefficients, the OD max for the transient absorption of ferrocenium in compound **42** was estimated to be in range of 0.004 when using such a laser (100mJ/pulse). This absorption is quite too small to be detectable.

4.5 Conclusion

The experiments in this chapter were carried out in order to show that ferrocene can be used as a charge trap in electron transfer processes and with the aim to use ferrocene as redox indicator for kinetic measurement of electron transfer, notably in DNA. The first results based on a RP-HPLC analysis of the irradiated products were very promising. They proved that electron transfer occurs from the ferrocene to the radical cation because enol ether, the product of electron transfer was clearly identified on the HPLC chromatogram. However, despite our first hopes, the second series of experiment were disappointing. The spectroscopic properties of ferrocene cannot be used to measure electron transfer using laser flash photolysis and transient absorption spectroscopy because of the too low extinction coefficient of the ferrocenium.^{57,58}

Another system using phenol as charge trap was therefore developed to measure electron transfer in DNA. The outcome of these experiments are discussed in the following chapter.

5. Phenol as charge acceptor

5.1 Introduction

Phenolic compounds such as anisol, p-cresol, tyrosine or tyrosylglycine have generated much interest, mainly due to their role as antioxidants in important biological and industrial processes. The mechanism of their action as antioxidants is primarily due to their ability to scavenge radicals by hydrogen abstraction or any electron transfer processes. Consequently, they are converted into phenoxyl radicals.⁹⁴⁻⁹⁹ In this respect, because of their low ionization potential, phenols are solutes with good electron donor properties.¹⁴¹ Early studies of phenols revealed phenoxyl radicals as the first observable products of one-electron-transfer oxidation.¹⁰⁰

The tyrosyl radical **65** (Figure 5.1) for example which is employed by nature for radical transport reactions in ribonucleotide reductase and in photosystem II,^{102, 103} can also be used as redox site to determine kinetics of charge separation and charge recombination in proteins using transient absorption spectroscopy.⁵⁹ The kinetic of electron transfer through oligopeptides was investigated in the Giese group on different systems comprising a tyrosine as charge acceptor connected to a photolabile radical injector.^{104,105} The electron transfer rate was determined by the direct observation of the transient absorption of the tyrosyl radical.

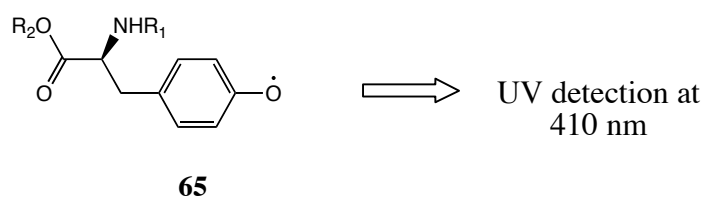


Figure 5.1 The tyrosyl radical

5.1 Our project

Based on these results we decided to use the UV properties of the phenoxy radical to measure the rate of electron transfer in the DNA. Our project consists in incorporating a phenol moiety into DNA through a modified nucleoside **100** (Figure 5.2). R is a protecting group which has to be removed once building block **100** is incorporated into DNA.

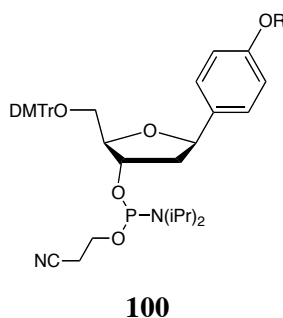
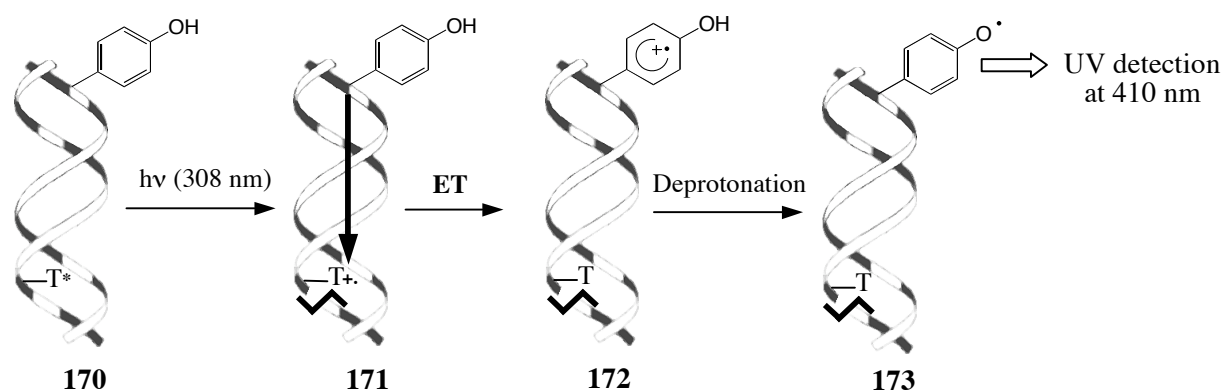


Figure 5.2 Phenol modified nucleoside ($R = Me, All, AOC$ or Ac)

Phenol possesses an oxidation potential ($E^{\circ}_{ox} = 0.86$ V vs NHE)¹⁴¹ which is considerably lower than the oxidation potential of the guanine ($E^{\circ}_{ox} = 1.29$ V vs NHE)¹⁷ and should therefore be oxidized to the phenoxy radical during the electron transfer process. The phenoxy radical has a characteristic absorption at $\lambda_{max} = 410$ nm and its molar extinction coefficient was found to be about 2.8×10^3 M⁻¹ cm⁻¹ at 410 nm.^{59,100}

The principle is straightforward. The phenol modified nucleoside is incorporated into DNA together with the charge injector T* and the subsequent strands are irradiated at $\lambda \geq 308$ nm (Scheme 5.1). Upon irradiation at this wavelength, a radical cation is generated on the charge injector (**170**→**171**) resulting from a Norrish type I cleavage of the pivaloyl group, followed by a spontaneous 3'-elimination (see scheme 2.4 p.11). We expect the positive charge to migrate through DNA towards the phenol moiety (**171**→**172**). In a proton-coupled electron transfer (PCET) reaction^{106,107} the phenoxy radical will be formed (**172**→**173**). Thus, we intend to detect the transient absorption of the phenoxy radical at 410 nm in order to obtain kinetic information about electron transfer.



Scheme 5.1 Charge transfer in DNA towards phenol

The synthesis of the phenol modified nucleoside **100** and its direct incorporation into oligonucleotides are described below.

5.3 Synthesis of the phenol modified nucleoside (100)

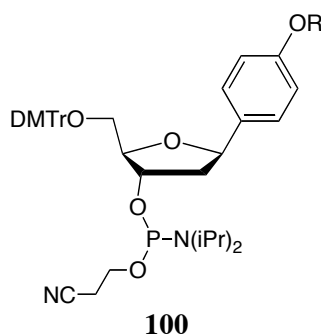
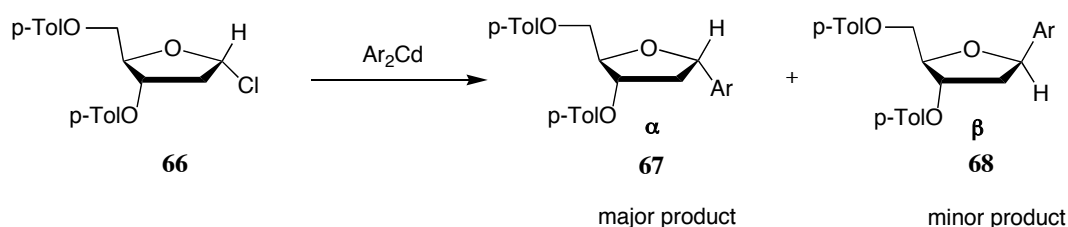


Figure 5.2 The phenol modified nucleoside

5.3.1 Synthesis background

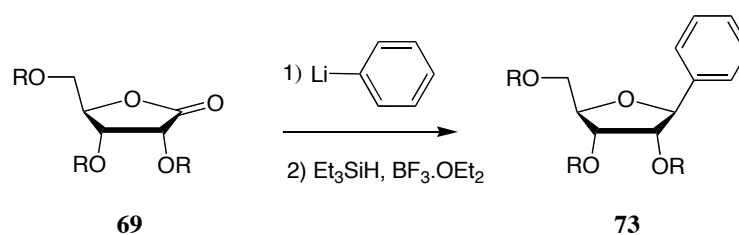
Kool has demonstrated that certain aromatic compounds like aryl C-nucleosides can function as artificial building blocks in DNA.^{108,109} For example, phenyl C-nucleosides can serve as replacements for natural pyrimidine nucleosides. Moreover, the aryl C-nucleosides maintain the ability for aromatic stacking.¹¹⁰

Despite the relatively straightforward structures of such compounds, efficient methods for the synthesis of simple aryl C-nucleosides are scarce. The key synthetic issue is the incorporation of the aryl moiety in the β -configuration, which mimics the anomeric stereochemistry of natural nucleosides. Previously, the most common method for the synthesis of aryl C-nucleosides involves the reaction of diarylcadmium or diarylzinc with 1,2-dideoxy-3,5-di-O-p-toluoyl- α -1-chloro-D-ribofuranose **66** (the so-called *Hoffer's* α -chlorosugar) (Scheme 5.2).^{109,111,112} Unexpectedly, these substitution reactions do not proceed with inversion but yield the α -anomer **67** as the major product in moderate yield. Although the α -anomer **67** could be equilibrated under acidic conditions to a mixture favoring the β -anomer **68**, the yields of β -anomer reported using this method are almost too low.¹¹²



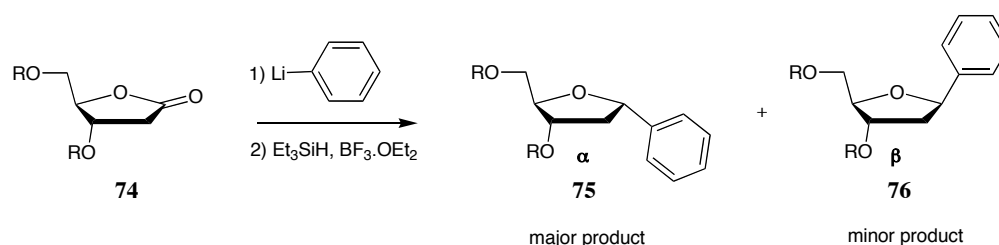
Scheme 5.2 Diarylcadmium coupling method for synthesis of aryl C-nucleosides

Kraus *et al*¹¹³ and Krohn *et al*¹¹⁴ reported a method for the synthesis of 1,2-dideoxy- β -1-phenyl-D-ribofuranose **73** based upon the addition of phenyllithium to a protected D-ribo-1,4-lactone **69** followed by stereoselective reduction of the resulting hemiacetal (Scheme 5.3).



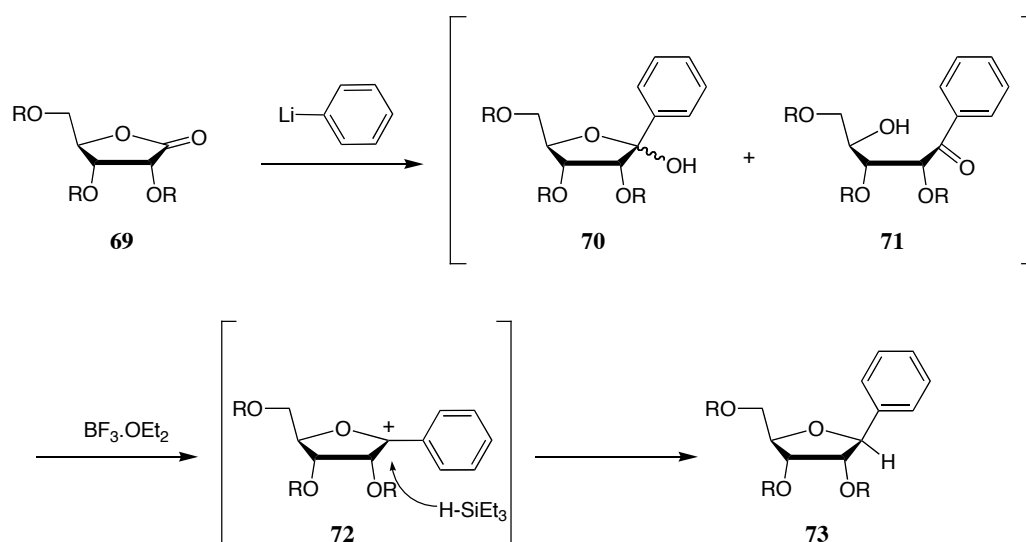
Scheme 5.3 Lithium coupling method for synthesis of aryl C-nucleosides

The lithium coupling approach has been applied by Matulic-Adamic, Beigelman, and coworkers¹¹⁵ to the syntheses of aryl C-2'-deoxyribonucleosides. However, it appeared that this method could not be successfully extended to the deoxyribose series because of the β -stereoselectivity in the absence of a 2'-substituent. (Scheme 5.4).



Scheme 5.4 Lack of β -stereoselectivity of the lithium coupling method for synthesis of aryl C-2'-deoxyribonucleosides

Presumably, this reaction proceeds through a 1'-carbocation intermediate **72** with delivery of the hydride from the α -face (Scheme 5.5). The α -2'-substituent could assist the approach of the silane from the more hindered face by control of the conformation of the ribofuranosyl ring or by direct interaction with the silicon center. So the acid-promoted S_N1-type additions to ribofuranosyl cations generally occur from the α -face.¹¹⁰



Scheme 5.5 Proposed mechanism for the lithium coupling method

Encouraged by these observations we decided to start the synthesis of our β -phenol C-2'-deoxyribonucleoside with a protected D-ribo-1,4-lactone rather than with a 2'-deoxy-D-ribonolactone.

5.3.3 Synthesis of the anisole nucleoside

The nucleoside with the methyl protecting group **100a** (Figure 5.3) was the first one that we synthesized following a method described by Leumann *et al* for the synthesis of pyridine C-nucleosides.¹¹⁷

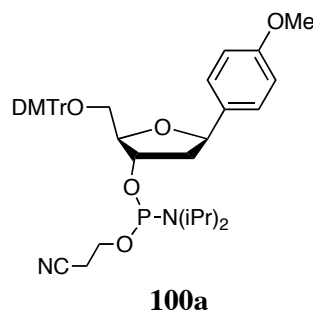
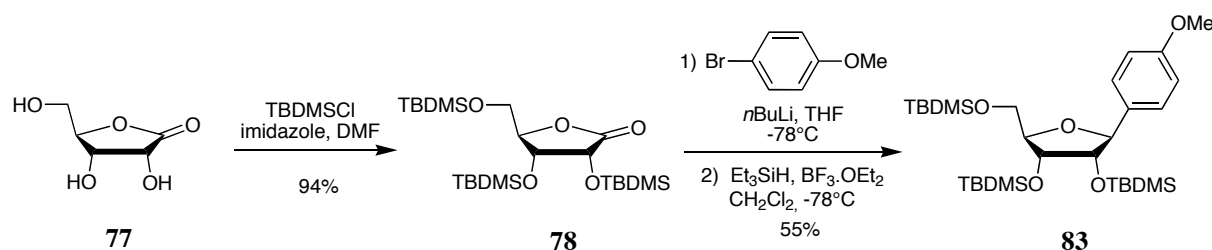


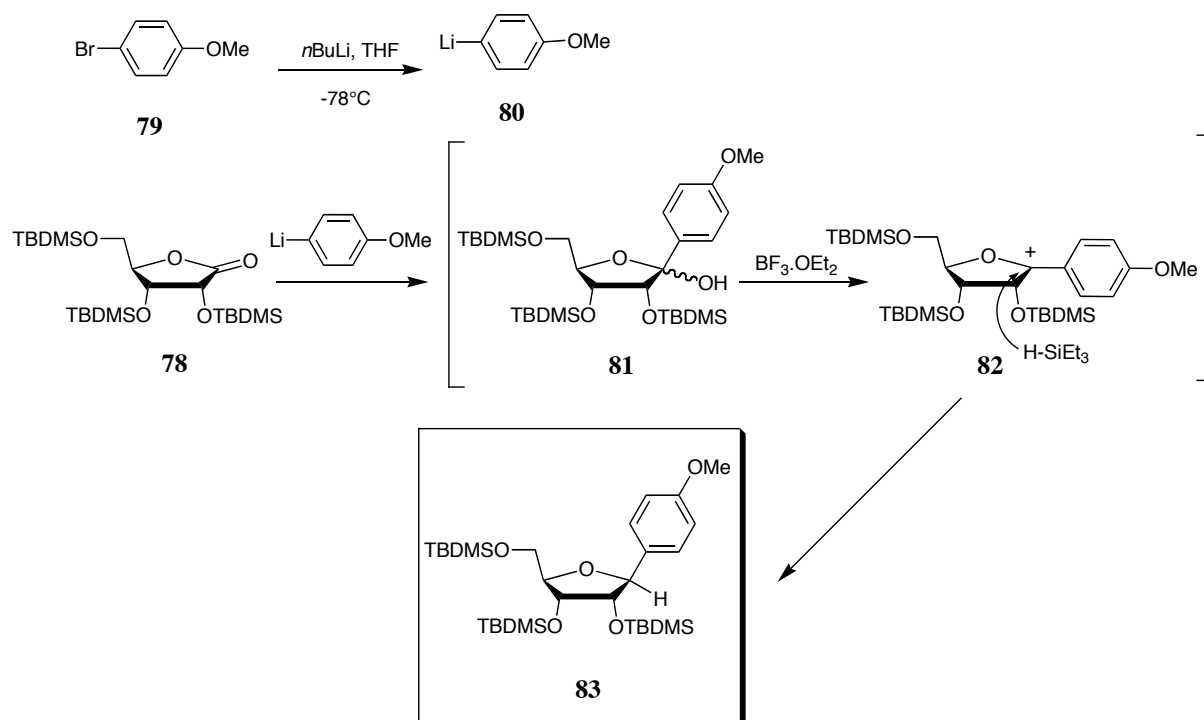
Figure 5.3 Anisole modified nucleoside

The first step consisted in a classic protection of the D-ribo-1,4-lactone **77** with *tert*-butyldimethylsilane in 94% yield (Scheme 5.7). Conversion of the protected ribonolactone **78** to the anisole C-nucleoside **83** was carried out using the lithium coupling procedure previously described for aryl C-nucleosides.^{110,113,114,116}



Scheme 5.7 Introduction of the anisole at the 1'- position of the D-ribose

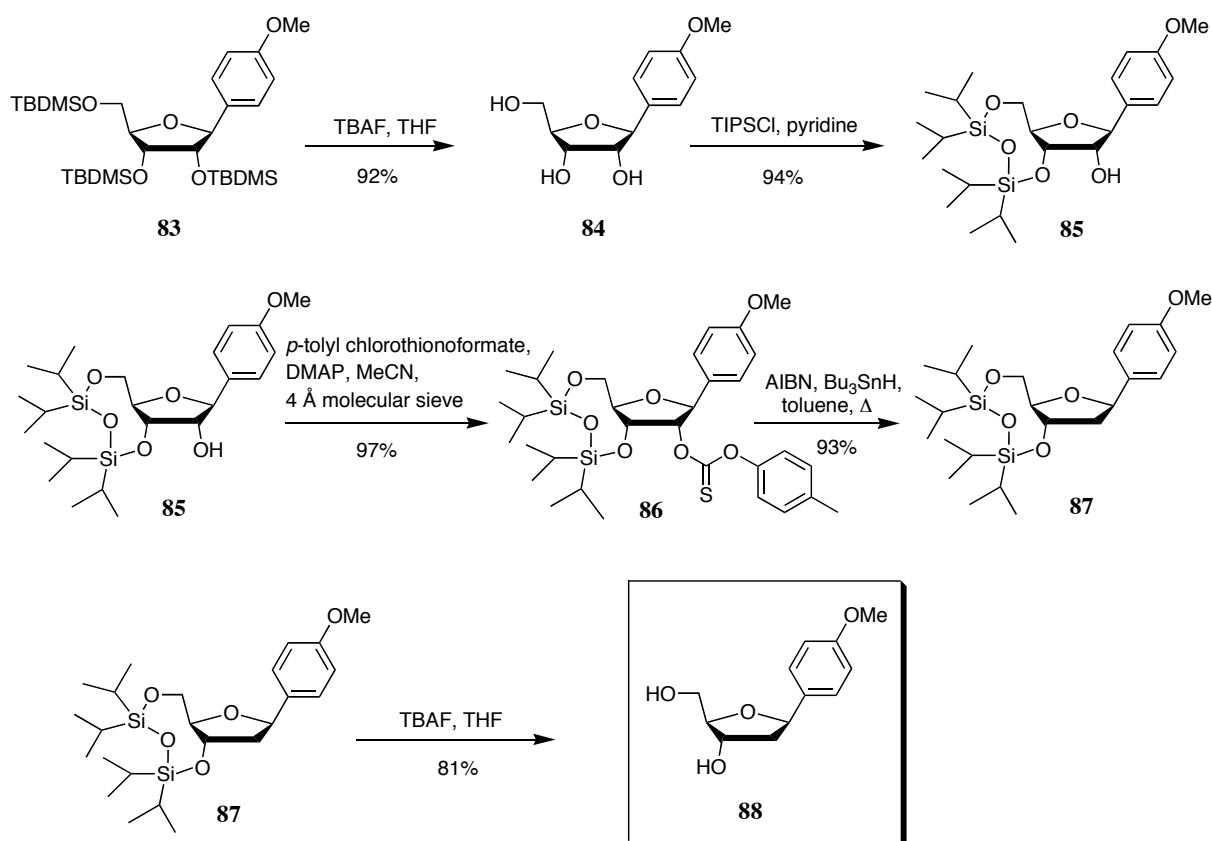
The anisole was introduced using a lithium salt of *p*-bromoanisole (Scheme 5.8). The lithiated anisole **80** reacted cleanly with the protected lactone **78** and give the hemiacetal **81**. This furanoside lactol **81** was not isolated but directly subjected to reduction under Lewis acidic conditions using triethylsilane as a hydride source, which led to the sterically uniform β -anisole C-ribofuranose **83** in 55 % yield.



Scheme 5.8 Coupling reaction of the sugar with the phenol moiety

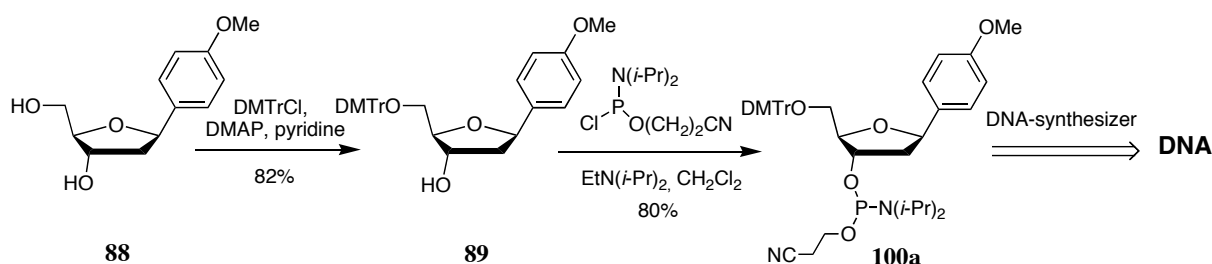
The end of the synthesis consisted in the removal of the 2'-hydroxyl group. A general procedure for the conversion of ribonucleosides to 2'-deoxyribonucleosides consists in a selective protection of the 3'- and 5'-hydroxyl functions of ribonucleosides with a cyclic disiloxane group followed by thioacylation, radical-induced reductive cleavage, and deprotection of the 3'- and 5'-hydroxyl functions.¹¹⁸

To do so, the TBDMS protecting groups were first removed with TBAF and the cyclic bifunctional disiloxane was selectively introduced by treatment of ribonucleoside **84** with 1,3-dichloro-1,1,3,3-tetraisopropylidisiloxane (TIPSCI) in pyridine¹¹⁹ to afford 3',5'-*O*-(1,1,3,3-tetraisopropylidisilox-1,3-diyl) (TIPS) derivative **85** in high yields (94%) (Scheme 5.9). Thioacylation of the 2'-hydroxyl group was achieved smoothly with *p*-tolyl chlorothionoformate in acetonitrile with DMAP as catalyst to provide clean conversion to the 2'-(*O-p*-tolylthionocarbonate) ester **86**. AIBN initiated homolytic deoxygenation of this thionocarbonate ester occurs under mild reaction conditions with tri-*n*-butyltin hydride in warm toluene. Deprotection with TBAF of the resulting compound **87** completed the four-stage conversion of ribonucleoside **84** to 2'-deoxyribonucleoside **88** in 68% overall yield.



Scheme 5.9 Conversion of the ribonucleoside to the 2'-deoxyribonucleoside

To incorporate the modified nucleoside **88** into a DNA fragment using an automatic DNA synthesizer, it had to be activated with suitable functional groups. Normally it should be protected with an acid labile trityl group at the 5'-position and a phosphoramidite at the 3'-position. The 5'-alcohol was protected with the dimethoxytrityl group using DMAP as catalyst in pyridine (Scheme 5.10). The subsequent product was phosphorylated using standard techniques with 2-cyanoethyl-*N,N*-diisopropylchlorophosphoramidite and Hünig's base^{120,81} to afford the building block **100a** in 80% yield.

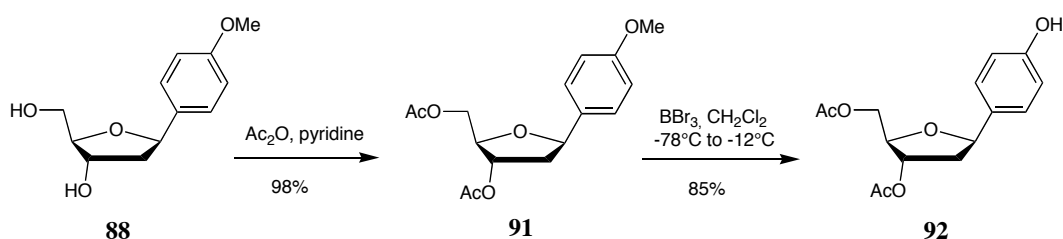


Scheme 5.10 Activation of the nucleoside with suitable functional groups for incorporation into DNA using a DNA synthesizer

5.3.4 Synthesis of the phenol protected nucleoside

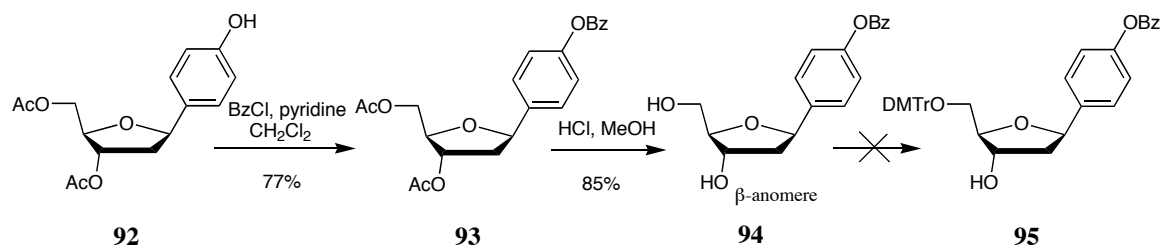
5.3.4.1 The anisole approach: cleavage of the methyl ether

A methyl is a permanent protecting group which cannot be removed once the anisole nucleoside is incorporated into DNA. To carry out assays with phenol as charge acceptor, the methyl has to be replaced by a protecting group which also withstands the automated DNA synthesis but which can be removed in DNA. We observed that the cleavage of the methyl ether was best carried out on compound **91** (Scheme 5.11). We therefore acetylated the dihydroxy compound **88** and subjected the resulting product **91** to treatment with excess boron tribromide in methylene chloride at -78°C ¹²¹ to afford the phenol **92** in 85% yield.



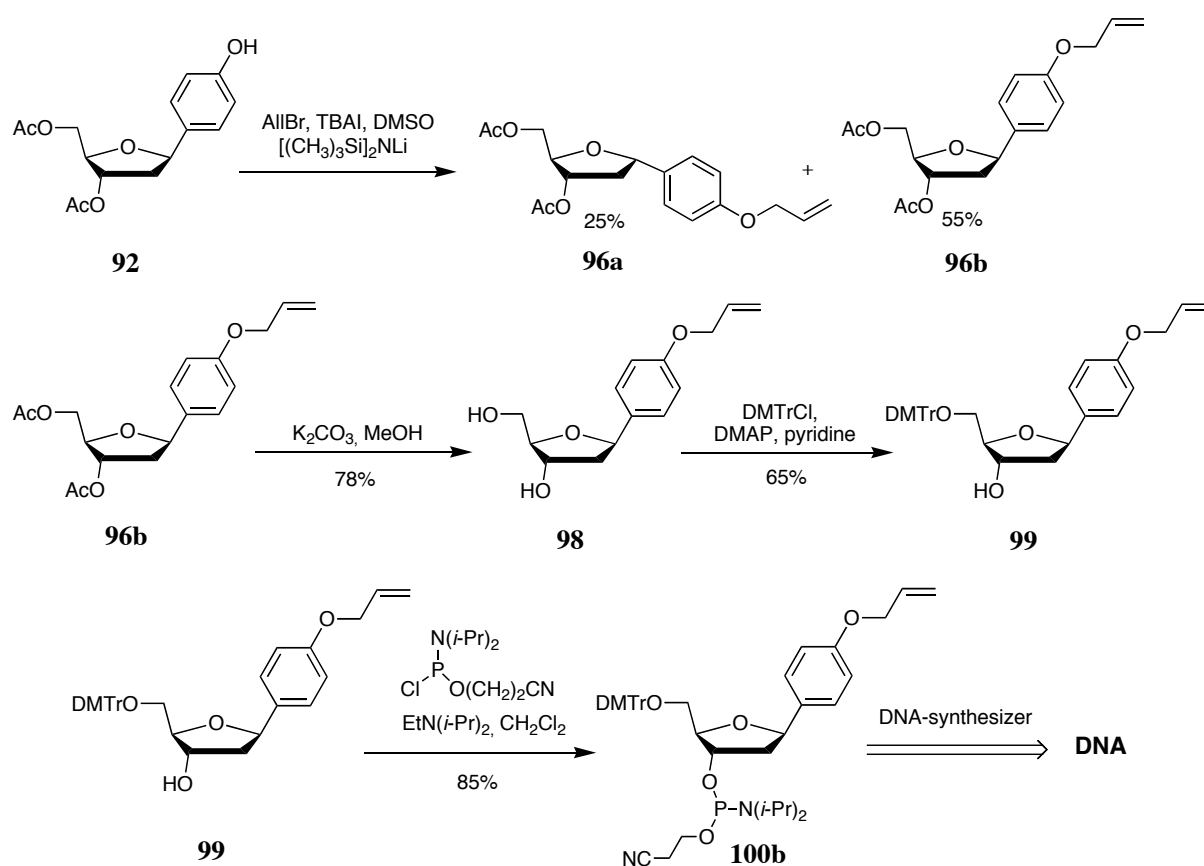
Scheme 5.11 Cleavage of the methyl ether

From there we could introduce different protecting groups and benzoyl was our first choice. The phenol modified nucleoside **92** was benzoylated and compound **93** was isolated in 77% yield (Scheme 5.12). Selective deprotection of the acetyls was managed under acidic conditions. However we observed about 20% anomerization. The β -anomer **94** was isolated and subjected to tritylation to prepare the building block for the DNA synthesizer but tritylation failed. The product decomposed systematically after the work-up. Benzoyl seems not to be the best protecting group for this kind of synthesis.



Scheme 5.12 The benzoyl protecting group strategy

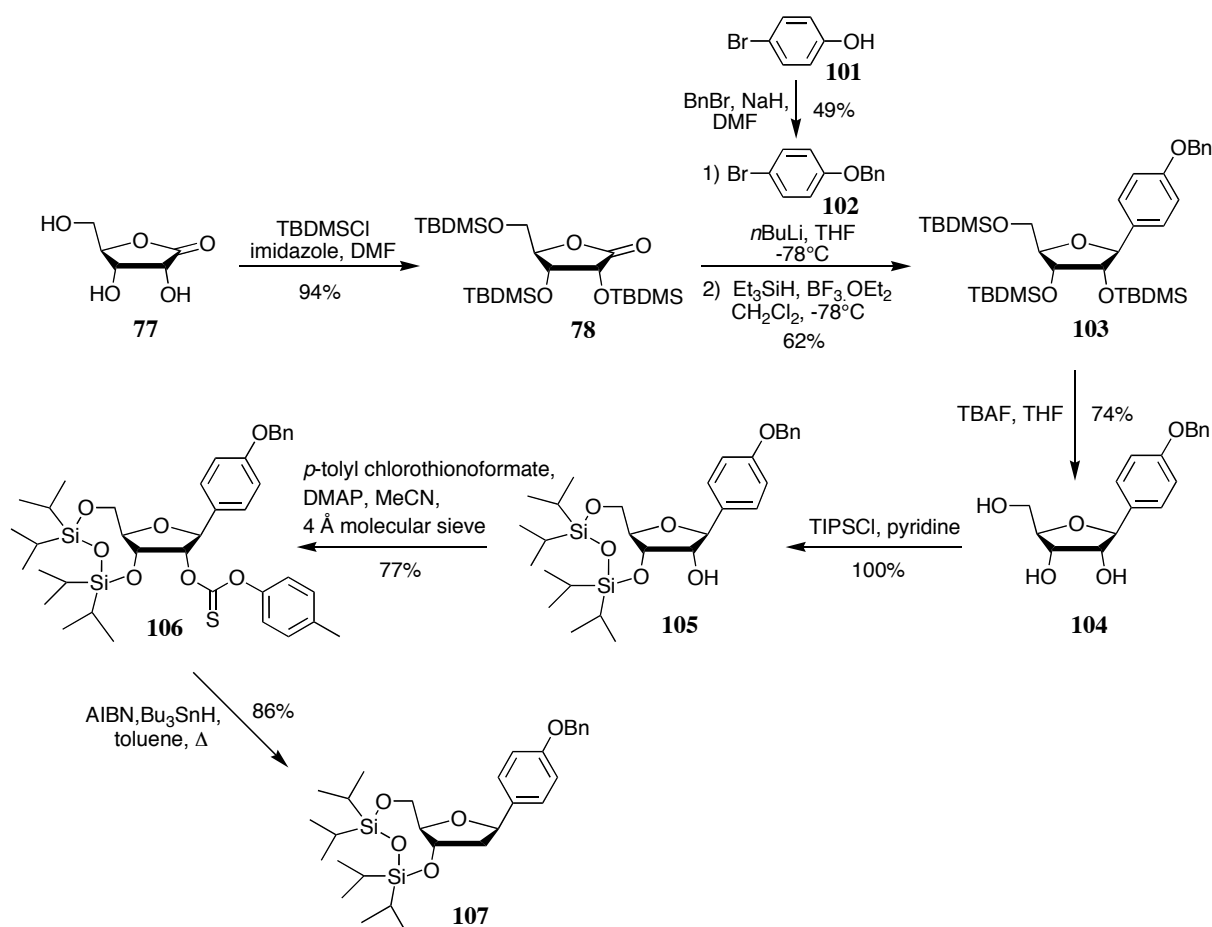
We then tried to introduce an allyl protecting group (Scheme 5.13). Alkylation of **92** in the presence of lithium bis(trimethylsilyl)amide as base in DMSO^{122,123} gave the desired product **96b** but also 25% of its α -anomer **96a**. The acetyl protecting groups were then removed from the isolated β -compound **96b** using basic conditions and the 5' alcohol was selectively protected with DMTrCl in pyridine to give the tritylated product **99**. Phosphorylation of **99** was performed according to standard procedures¹²⁰ with 2-cyanoethyl-*N,N*-(diisopropyl)-chlorophosphoramidite and Hünig's base and led to building block **100b** which is suitable for automated DNA synthesis.⁸¹ Although the synthesis of a phenol building block was achieved using this route, it was not very satisfactory (too much steps, low yields and C-1'-epimerization during allyl protection of the phenol) and we decided to develop a better pathway for such a class of compounds.



Scheme 5.13 The allyl protecting group strategy

5.3.4.2 A new approach: the benzyl approach

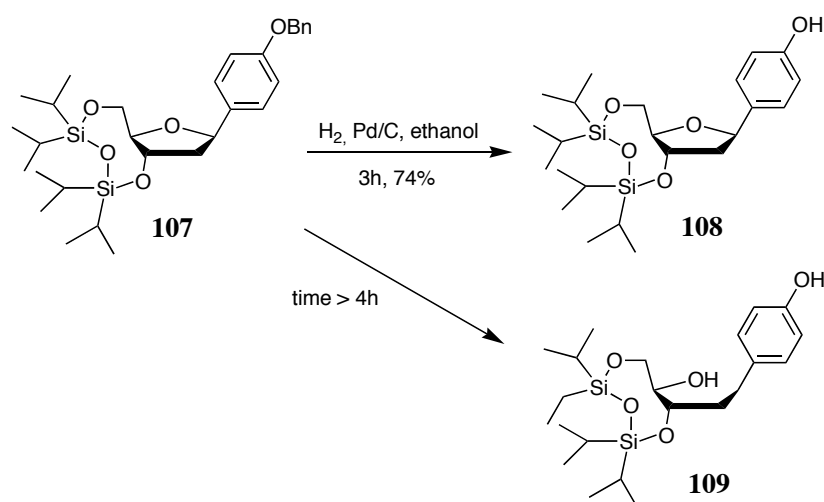
A new approach was designed for the synthesis of phenol modified nucleosides (Scheme 5.14). Back to the beginning of the first route we replaced the methyl protecting group by the more suitable benzyl protecting group. The benzyl protecting group also withstands the conditions of the base introduction. It is resistant to the 2'-OH removal synthesis and more importantly it can be removed by catalytic hydrogenation providing a phenol intermediate that can be protected with new protecting groups.



Scheme 5.14 Synthetic route to phenol modified nucleoside using benzyl as protecting group

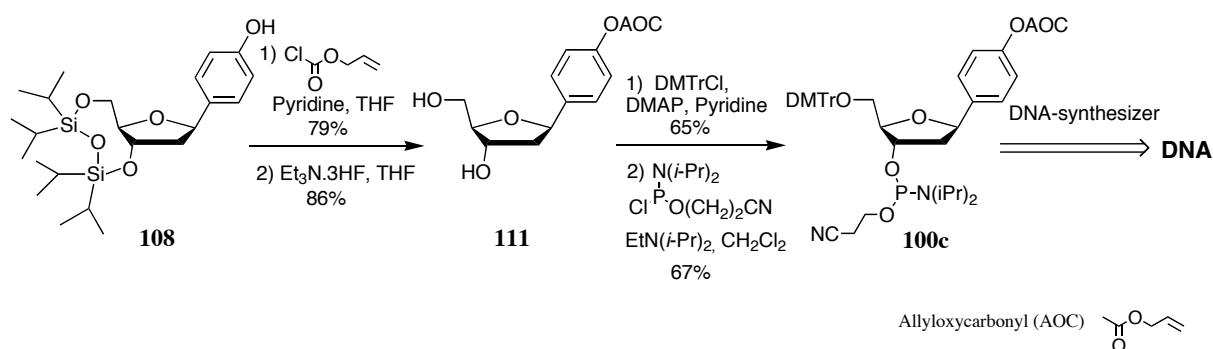
The starting ribono-1,4-lactone **77** was transformed into the corresponding deoxyribonucleoside **107** in 6 steps with 29 % overall yield. Conversion of the protected ribonolactone **78** to the benzyl protected phenol C-nucleoside **103** was attempted using the lithium coupling procedure previously described (Scheme 5.5). In this case the phenol moiety was introduced at the C-1' position with complete β -stereoselectivity using a lithium salt of 1-*O*-(benzyl)-4-bromophenol **102**. This method is the first reported for the synthesis of such class of phenol protected C-nucleosides. We also tried to introduce an allyl protected phenol but we failed. The benzyl protecting group appeared to be the best choice since it withstands the condition of the base introduction. The phenol ribonucleoside **103** was converted to phenol 2'-deoxyribonucleoside **107** following the four-step procedure described p. 41.

The benzyl protecting group was then removed using catalytic hydrogenation to afford the phenol nucleoside **108** in 74% yield (Scheme 5.15). In this reaction it is necessary not to exceed the reaction time of four hours otherwise the sugar ring will be opened because the sugar ring also possesses a benzylic system at its C-1' position which will be cleaved under this conditions.

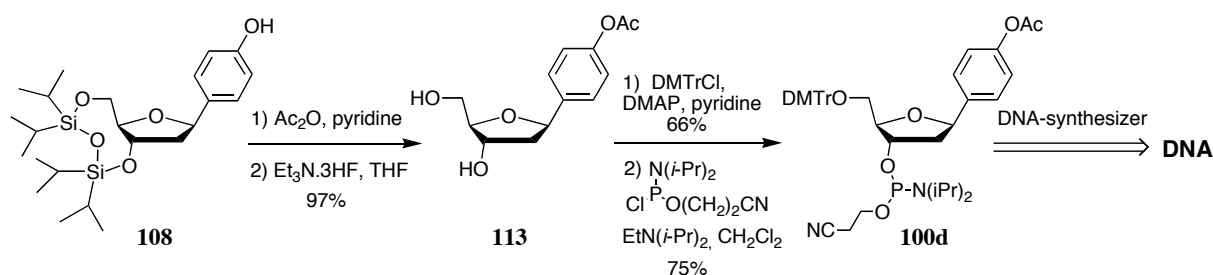


Scheme 5.15 Removal of the benzyl protecting group by catalytic hydrogenation

We could then introduce the desired protective groups into nucleoside **108**. We managed the allyloxycarbonation (Scheme 5.16) and the acetylation (Scheme 5.17). Both the allyloxycarbonyl protected and the acetyl protected phenol nucleoside **111** and **113** were converted to the suitable building blocks **100c** and **100d**, respectively.



Scheme 5.16 The allyloxycarbonyl protecting group strategy



Scheme 5.17 The acetyl protecting group strategy

5.3.5 Summary

Synthesis of the building blocks **100a-d** were achieved in good yields, starting from D-ribo-1,4-lactone and using a lithium coupling method for the selective introduction of the phenol at the C-1' position in the β -configuration and a standard radical-based procedure for the conversion of the C-ribonucleosides to the 2'-deoxyribonucleoside. Following this pathway, the anisole building block **100a** was synthesized in 9 steps with 21% overall yield, the allyl protected building block **100b** in 13 steps with 6,5% overall yield, the allyloxycarbonyl protected building block **100c** in 11 steps with 6.5% overall yield and finally the acetyl protected building block **100d** was synthesized in 10 steps with an overall yield of 10%. These four building blocks are now suitable for the introduction into synthetic oligonucleotides via automated solid-phase synthesis.

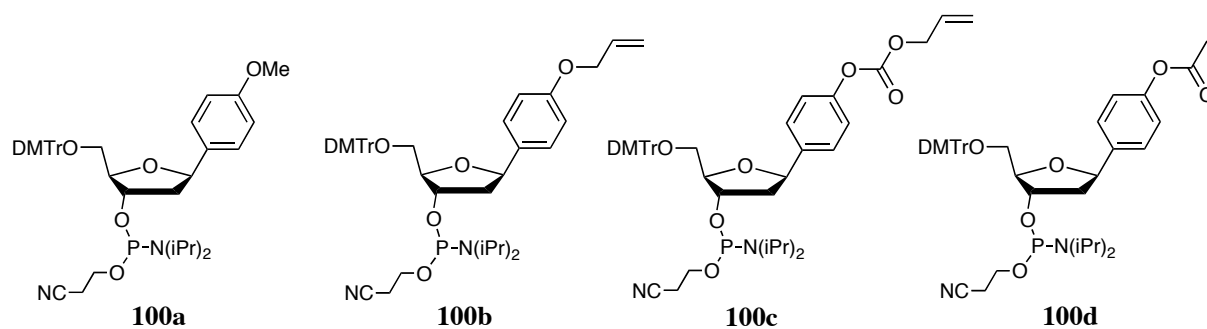


Figure 5.4 The four phenol building blocks for incorporation into DNA

5.4 Incorporation of the building blocks into DNA

5.4.1 Usual procedures for oligonucleotide synthesis

In principle, DNA synthesis is relatively simple. It involves the systematic addition of oligonucleotides to a growing DNA chain using automated Solid Phase DNA Synthesis.^{2, 81, 124} In solid-phase chemical synthesis of oligonucleotides, the 5' hydroxyl group of one nucleoside (immobilized onto a solid support) is coupled to the reactive 3' phosphorous group of the next nucleoside (introduced as a monomer in solution). Oligonucleotides are generally assembled from 3'-terminal to 5'-terminal. The synthesis cycle is performed via the addition of one nucleoside monomer at a time. The excess liquid phase-reagents are simply removed by filtration and washing with the solvent. Thus no purification steps are required between the cycles, the synthesis column is at the same time ready for the following reaction.

The synthesis is conducted with the growing DNA chain attached to a solid support made of controlled pore-glass (CPG) beads. The starting material is the solid support derivatized with the nucleoside, which will become the 3' hydroxyl end of the oligonucleotide. The nucleoside is bound to the solid support through a base labile succinyl linker attached at the 3' hydroxyl end. The 5'-hydroxyl is blocked with a dimethoxytrityl (DMTr) group. The synthesis proceeds with the following steps (Scheme 5.18):

- The first step of the synthesis cycle is detritylation. This is done via treatment of the derivatized solid support with trichloroacetic acid (TCA) to remove the DMTr group and to ultimately set free the 5'-hydroxyl group for the coupling reaction.
- An activated intermediate is formed by simultaneously adding the phosphoramidite nucleoside monomer and tetrazole to the reaction column. The tetrazole protonates the nitrogen of the phosphoramidite, making it susceptible to nucleophilic attack.
- Capping emerges as the next step in the synthesis cycle. This stage serves the purpose of terminating any chains that did not undergo coupling. Since the unreacted chains have free 5'-hydroxyl groups on them, they can easily be capped by acetylation. This capping is done with equal volumes of acetic anhydride and 1-methylimidazole. Capping minimizes the amount of the impurities and consequently eases product identification and purification.

5.4.2 Characterization of the modified oligonucleotides

5.4.2.1 The anisole nucleotides

After synthesis, the oligonucleotides should be cleaved from the solid support and deprotected. Strands **116** and **117** containing the anisole and the charge injector T* were subjected to standard ammonia treatment to release the oligonucleotide from the solid phase. Cleavage and deprotection are done simultaneously through the addition of concentrated ammonium hydroxide (32%) at 55°C. Ammonia treatment removes the cyanoethyl phosphate protecting groups and also the protecting groups on the exocyclic amines of the bases.⁸¹ After purification of the oligonucleotides, the DMTr group that was present at the final fragment of the DNA synthesis was removed under acidic conditions. At each of these two steps RP-HPLC purification was carried out. The purity of the oligonucleotides was checked by MALDI-ToF-MS (Table 5.1).

Sequence	[M-H] ⁻ calculated (m/z)	[M-H] ⁻ found (m/z)
116: 5'-TTTTTTTTTT(PhOMe)T*TTTTTTTTT-3'	6088.77	6087.52
117: 5'-TGCATCAT(PhOMe)T*TTATCAGAGC-3'	6148.89	6150.25

Table 5.1 Calculated and measured mass of strands containing anisole

5.4.2.2 Deprotection of the phenol nucleotides in DNA

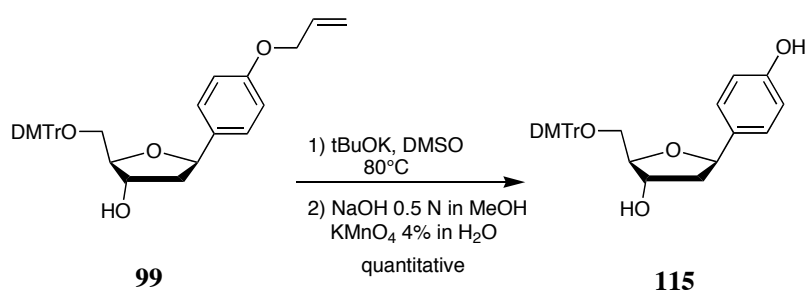
a) Allyl deprotection in DNA

The protecting groups on the phenol should also be removed. Various methods are described in the literature to remove the allyl protective group from phenol.¹²² We tried to apply some of these methods to our DNA system **118** (Tab.5.2). Strand **118** was beforehand released from the solid support using ammonia treatment (see chapter 5.4.2.1). After RP-HPLC purification the final DMTr group was removed and the strand was purified again.

Sequence	[M-H] ⁻ calculated (m/z)	[M-H] ⁻ found (m/z)
118 : 5'-TTTATATATATATA(PhOAll)ATATATATTTT-3'	7945.20	7948.03

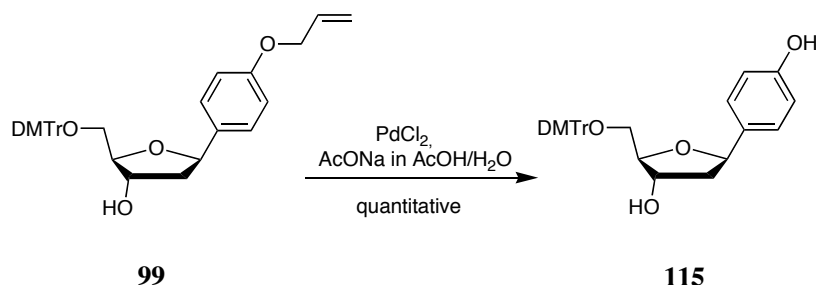
Table 5.2 Calculated and measured mass of strand **118** containing the allyl protected nucleoside

The allyl deprotection methods were first tested on the monomer **99** before applying them to DNA. The first method consists of using a strong base, potassium *tert*-butoxide, in polar solvent (DMSO) to isomerise the allyl phenyl ether to prop-1-enyl which is then cleaved by a oxidative method using a mixture KMnO₄/NaOH (Scheme 5.19).^{122,125,126} Compound **115** containing free phenol was obtained by using this cleavage method. Following this success we tried to apply this method to our DNA system, but it failed.



Scheme 5.19 Method 1 for allyl deprotection in the monomer **99**

Another procedure to remove the allyl protecting group is based on a catalytic process using palladium as transition metal catalyst (Scheme 5.20).^{122,126} The allyl protected nucleoside **99** was subjected to palladium treatment under acidic conditions and the phenol nucleoside **115** was isolated.

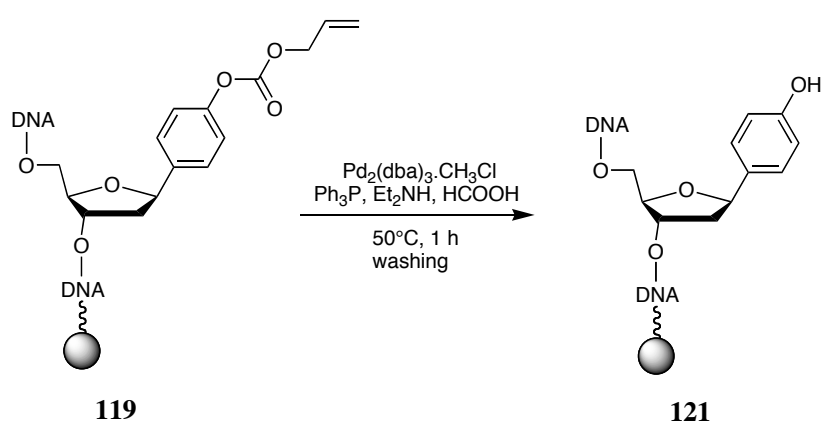


Scheme 5.20 Method 2 for allyl deprotection in the monomer **99**

Unfortunately we were unable to remove the allyl protecting group from the phenol incorporated in DNA using this method, we obtained very complex mixtures very difficult to exploit. We then turned our attention to the allyloxycarbonyl protecting group.

b) Allyloxycarbonyl deprotection in DNA

The allyloxycarbonyl protective group was removed from the DNA using a palladium catalyst (Scheme 5.21).¹²⁷ The interesting aspect is that this deprotection is carried out on solid support which simplifies the purification.



Scheme 5.21 Allyloxycarbonyl deprotection in DNA

After deprotection of the phenol, the strand **121** was cleaved from the solid support using ammonia treatment (see 5.4.2.1). After RP-HPLC purification the final DMTr group was removed and the strand was purified again.

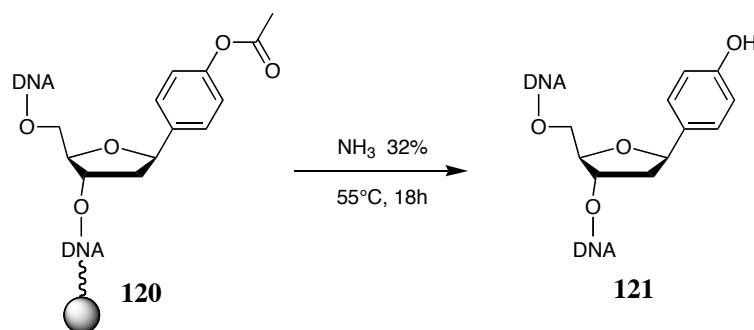
The purity of the deprotected strand **121** was checked by MALDI-ToF-MS (Table 5.3):

Sequence	[M-H] ⁻ Calculated (m/z)	[M-H] ⁻ Found (m/z)
121 : 5'-TTTATATATATATA(PhOH)ATATATATTTT-3'	7905.14	7908.12

Table 5.3 Calculated and measured mass of the phenol deprotected strand **121**

c) Acetyl deprotection

The acetyl protecting group is the optimal case as the acetyl is removed during the basic treatment used to cleave the DNA strand from the solid support. Cleavage and deprotection are done simultaneously through the addition of 32% ammonium hydroxide at 55°C (Scheme 5.22). Ammonia treatment removes the protecting groups on the phosphate, the protecting groups on the bases and finally the acetyl protecting group on the phenol. The final DMTr group was then removed under acidic conditions. After each of these two steps HPLC purification was carried out.



Scheme 5.22 Acetyl deprotection in DNA

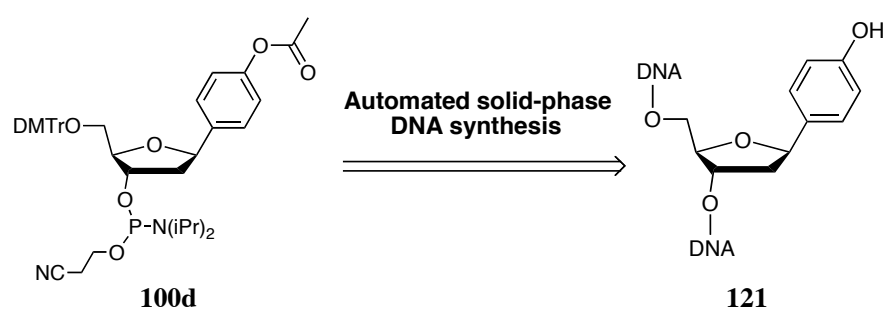
The purity of the deprotected strand **121** was checked by MALDI-ToF-MS (Table 5.4):

Sequence	[M-H] ⁻ Calculated (m/z)	[M-H] ⁻ Found (m/z)
121 : 5'-TTTATATATATATA(PhOH)ATATATATTTT-3'	7905.14	7906.01

Table 5.4 Calculated and measured mass of the phenol deprotected strand **121**

5.4.3 Summary

We reported here the first synthesis of phenol-labeled oligonucleotides. All the phenol protected building blocks that we have synthesized (see Figure 5.4) were successfully incorporated into DNA using automated solid-phase synthesis. However the acetyl protecting group strategy appeared to be the best approach (Scheme 5.23). First, the synthesis of the acetyl protected building block is shorter and has higher overall yields than the syntheses of the other building blocks. Second, the acetyl group can easily be removed once the nucleoside is incorporated into DNA strands. The acetyl protecting group removal requires one step less than the other protecting groups since it is achieved with the ammonia treatment used to cleave the DNA strand from the solid support. So the acetyl protection of the phenol is definitely the pathway to be used to incorporate phenol nucleosides in DNA strands.



Scheme 5.23 The acetyl protecting group strategy for incorporation of the phenol nucleoside into DNA using automated solid-phase DNA synthesis

The RP-HPLC chromatogram of the irradiated solution containing strand **122** is shown in figure 5.5. The detection was performed at 260 nm where the oligonucleotides have a maximal absorption. For all irradiation experiments the peaks were isolated and characterized by MALDI-ToF-MS with an accuracy of ± 5 m/z. Three main products were identified as 5'-phosphate **124**, 3'-phosphate **129** and enol ether **128**.

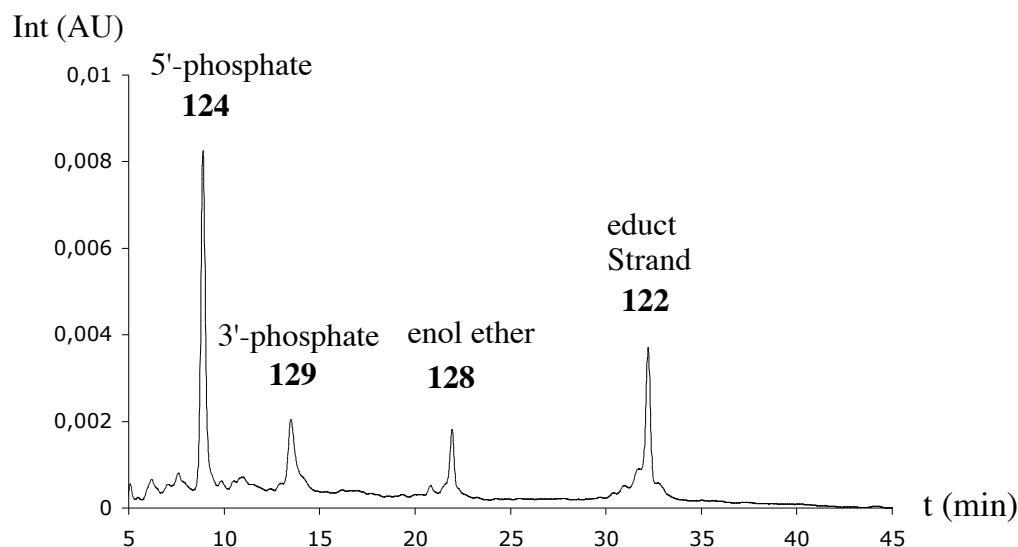


Figure 5.5 RP- HPLC-Chromatogram of the irradiation of **122**

Assuming that both electron transfer and water addition proceed irreversibly, the ratio of the water addition products (**124-128**) against the electron transfer product **128** is given by Eq. 5.1:

$$k_{ET,rel} = \frac{k_{ET}}{k_{H_2O}} = \frac{[\text{enol ether } \mathbf{128}]}{[\text{5'- phosphate } \mathbf{124}] - [\text{enol ether } \mathbf{128}]} \quad \text{Eq. 5.1}$$

The photolysis products were quantified by dividing the HPLC-peak areas by their calculated molar extinction coefficients and internal calibration. The molar extinction coefficients were calculated using the increment values of each base (see Experimental Part chapters 7.2.5 and 7.3).^{81b}

The $k_{ET,rel}$ values obtained for the strands **122 a-d** are given in table 5.3:

Sequence 122 5'-GCCTTATAPhOH(T) _n T*ATAAATCGT-3'	$k_{ET,rel}$
122a : n = 0	0.53
122b : n = 1	0.26
122c : n = 2	0.13
122d : n = 3	0.16

Table 5.3

Based on previous experiments using external electron donors such as methionine, selenomethionine or KI, we can assign a value for the rate of water addition at radical cation **123** of $k_{H_2O} = 1.10^8 \text{ s}^{-1}$.⁴⁹ With this value the electron-transfer rate from phenol to radical cation **123** can be estimated to be about $0.53 \cdot 10^8 \text{ s}^{-1}$ at a distance of 6.2 Å.¹³⁶

Although electron transfer is observed in all four cases, the results show that there are only little rate differences in strands **122a-d** where the phenol is separated by zero, one, two or three T's from the radical cation site. Thus, on addition of one or two T nucleotides between the phenol and the radical cation, the relative electron transfer rate decreases only slightly from $0.53 \times 10^8 \text{ s}^{-1}$ through $0.26 \times 10^8 \text{ s}^{-1}$ to $0.16 \times 10^8 \text{ s}^{-1}$. A further increase of one intervening T nucleotide has no decreasing effect on the electron-transfer rate.

Analogous experiments of charge transfer towards a guanine were carried out by Meggers and led to the same conclusion.^{31,49} The number of T nucleotides between the radical cation and the G has only a weak influence of the electron-transfer rate. We explain these results on the basis of the flexibility of the DNA single strand that can adopt conformations in which the distance between the electron donor, the phenol moiety or the guanine, and the electron acceptor, the radical cation, are short enough for a fast charge-transfer step, even if they are separated by several T units. Experiments by Kan and Schuster led to the same conclusion.⁵³

In order to verify that the electron-transfer rates obtained are not influenced by a guanine present in the sequence **122**, the experiment was repeated with poly A-T strands.

Sequence	$k_{ET, rel}$
132 : 5'-TTTTTATA(PhOH)TT*ATAATAAT-3'	0,20
133 : 5'-TTTATATATATATA(PhOH)AT*ATATATTTT-3'	0,22

Table 5.4 $k_{ET, rel}$ values for the poly A-T strands **132** and **133**

The relative electron-transfer rates obtained (Table 5.4) with the poly A-T single strands **132** (20mer) and **133** (26mer) in which phenol and T* are separated by one T are similar to the one found for strand **122b**. In **122b** phenol and T* are also separated by one T but G bases are present in the sequence (Table 4.3). We can therefore conclude that the G bases present in the sequences **122** have no influence on the measured electron transfer rates.

5.5.1.2 Anisole as electron donor

The single strands **116** and **117** in which anisole adjoining T* were irradiated under the same irradiation conditions that the phenol strands (320 nm, pH 5.0) and the photolysis products were analyzed by RP-HPLC.

116: 5'-TTTTTTTTT**PhOMeT***TTTTTTTTT-3'

117: 5'-TGCATCAT**PhOMeT***TTATCAGAGC-3'

In both cases, no electron transfer product (enol ether) was found, only water addition products 5'-phosphate and 3'-phosphate were observed (Figure 5.6 A). The irradiations were repeated in the presence of KI (0.2 M), a strong electron donor. The KI has the effect of transforming the radical cation formed directly into enol ether in a near diffusion-controlled reaction ($5 \times 10^9 \text{s}^{-1}$).¹⁴⁸ The enol ether peak revealed by the KI test (Figure 5.6 B) was never observed in the irradiation experiments of the single strands **116** and **117**.

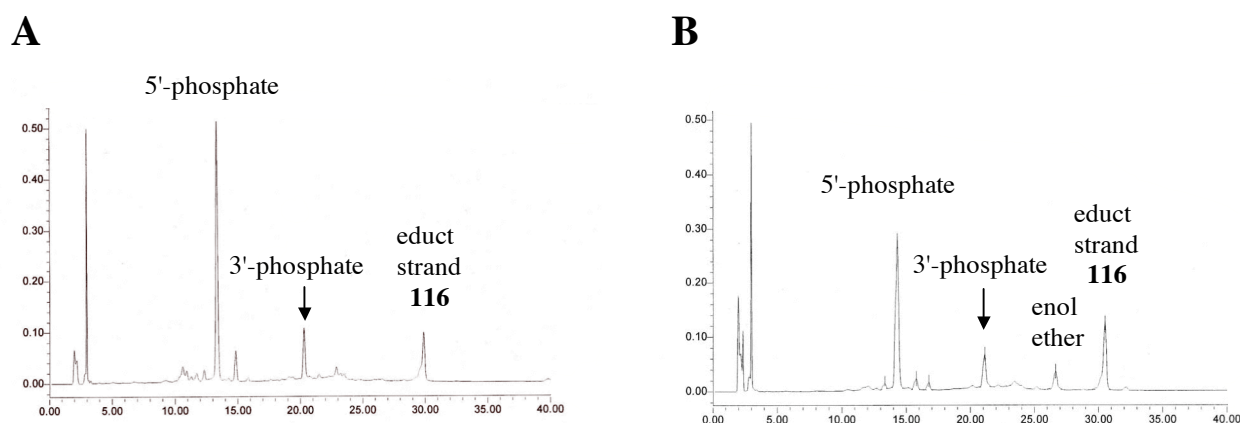


Figure 5.6 A) HPLC chromatogram of the irradiated strand **116**. The same experiments conducted with strand **117** also failed to reveal any ET product. B) HPLC chromatogram of the irradiated strand **116** + KI

These results can be explained regarding the oxidation potential of anisole and phenol. The oxidation of anisole to anisole radical cation in aqueous solutions has a potential $E^{\circ}_{\text{ox}}(\text{PhOMe}/\text{PhOMe}^{\bullet+}) = 1.52 \text{ V vs NHE}^{133}$ which is similar to the oxidation potential of phenol to phenol radical cation ($E^{\circ}_{\text{ox}}(\text{PhOH}/\text{PhOH}^{\bullet+}) = 1.50 \text{ V vs NHE}$).¹⁴² The enol ether radical cation ($E^{\circ}_{\text{red}}(\text{EE}^{\bullet+}) = 1.29\text{-}1.44 \text{ V vs NHE}$)¹³⁴ generated upon irradiation should not be capable of oxidizing phenol to phenol radical cation and anisole to anisole radical cation. However, the driving force in the phenol oxidation is the formation of the phenoxy radical by loss of the hydrogen which corresponds to a much lower oxidation potential ($E^{\circ}_{\text{ox}}(\text{PhOH} / \text{PhO}^{\bullet}) = 0.86 \text{ V vs NHE}$).¹⁴¹ Thus, oxidation of phenol in DNA systems could easily occur if the electron transfer is coupled with proton transfer to the solvent. This is not the case with anisole in systems **116** and **117**, the phenoxy radical cannot be formed by loss of the methyl moiety. The overall result is that upon irradiation the anisole cannot be oxidized and no electron transfer occurs. In regards of these results we decided to focus our attention on phenol as electron donor in double strand experiments.

5.5.2 Double strand experiments

5.5.2.1 Estimation of the $k_{ET,rel}$

In this chapter we examine the charge transfer of our system in double strands experiments. A DNA double strand has a well defined structure compared to DNA single strands, it's not flexible and can not bend over on itself, so we can assume that the distance between the electron donating phenol and the T* radical cation injector is defined.

Thus, strand **122b** was hybridized with its complementary strand **134X** to form double strand (Figure 5.6).

122b: 5'-GCC TTATAPhOH TT*ATAAATCGT-3'

134X:3'-CGG AATAT X AA TATT TAGCA-5'

Figure 5.6 DNA double strands

We checked the influence of the base (X) placed across the phenol on the electron transfer. The irradiation was performed following the procedure described in single strand experiments ($\lambda \geq 320$ nm, anaerobic conditions, citrate buffer pH 5.0). The analysis of the photolysis solution was done by RP-HPLC (Figure 5.7).

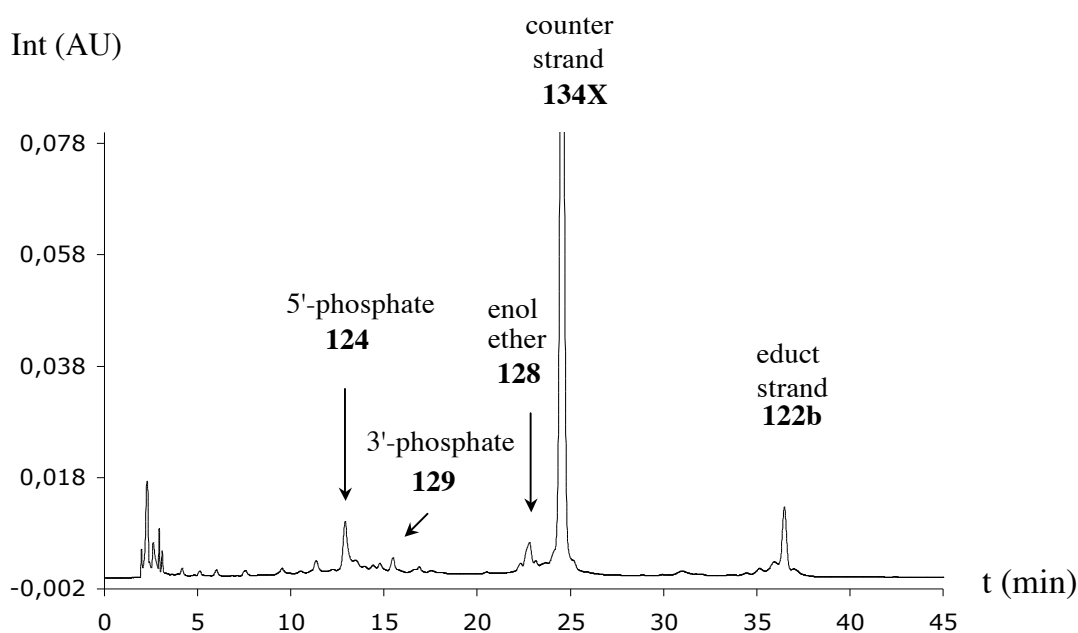


Figure 5.7 HPLC chromatogram of the irradiated double strand **122b/134X**

For X we incorporated A, T, C or an abasic site (Table 5.5). In all four systems electron transfer was observed but the rates obtained differed from each other. Thermal denaturation studies were done to compare the stability of the four 20mer double strands. In all cases the melting temperature (T_m) obtained are lower than that of a perfect match (unmodified strand). The T_m of an unmodified 20mer containing five to six G:C base pairs is estimated to be around 45°C. The destabilization might be due to the fact that the two modifications, phenol and T* are placed on the same strand and may be too close to each other.

X	T_m (°C)	$k_{ET, rel}$
A	26.8	1.14
T	28.8	1.49
C	37.1	0.84
Abasic	29.5	0.24

Table 5.5 Melting point and $k_{ET, rel}$ values for the double strand **122b/134X** (X = A, T, C or abasic)

However, when a cytosine C is placed across the phenol in the complementary strand, the T_m is 8 to 10°C higher than the other ones. This can be explained by formation of hydrogen bonds between the –OH group of the phenol and the ketone of the cytosine or between the –OH group and the imine of the cytosine (Figure 5.8). The hydrogen bonding would stabilize the double-helix structure and therefore lead to higher melting point. Based on this result we can suppose that phenol behaves more like guanine G and prefers to hybridize to C instead of A or T.

The $k_{ET, rel}$ found in double strand experiments are as large or larger than the one found in single strand experiments (Table 5.6). But the electron-transfer rate with an abasic site opposite the phenol is significantly smaller than the other ones. This suggests that the base placed across the phenol in the complementary strand has an influence on the electron-transfer rate. When an abasic site is placed across phenol no hydrogen bonding is possible. We can then imagine that phenol points outside of the DNA helix and forms an extra-helical bulge and this may account for the low rate observed in this case.

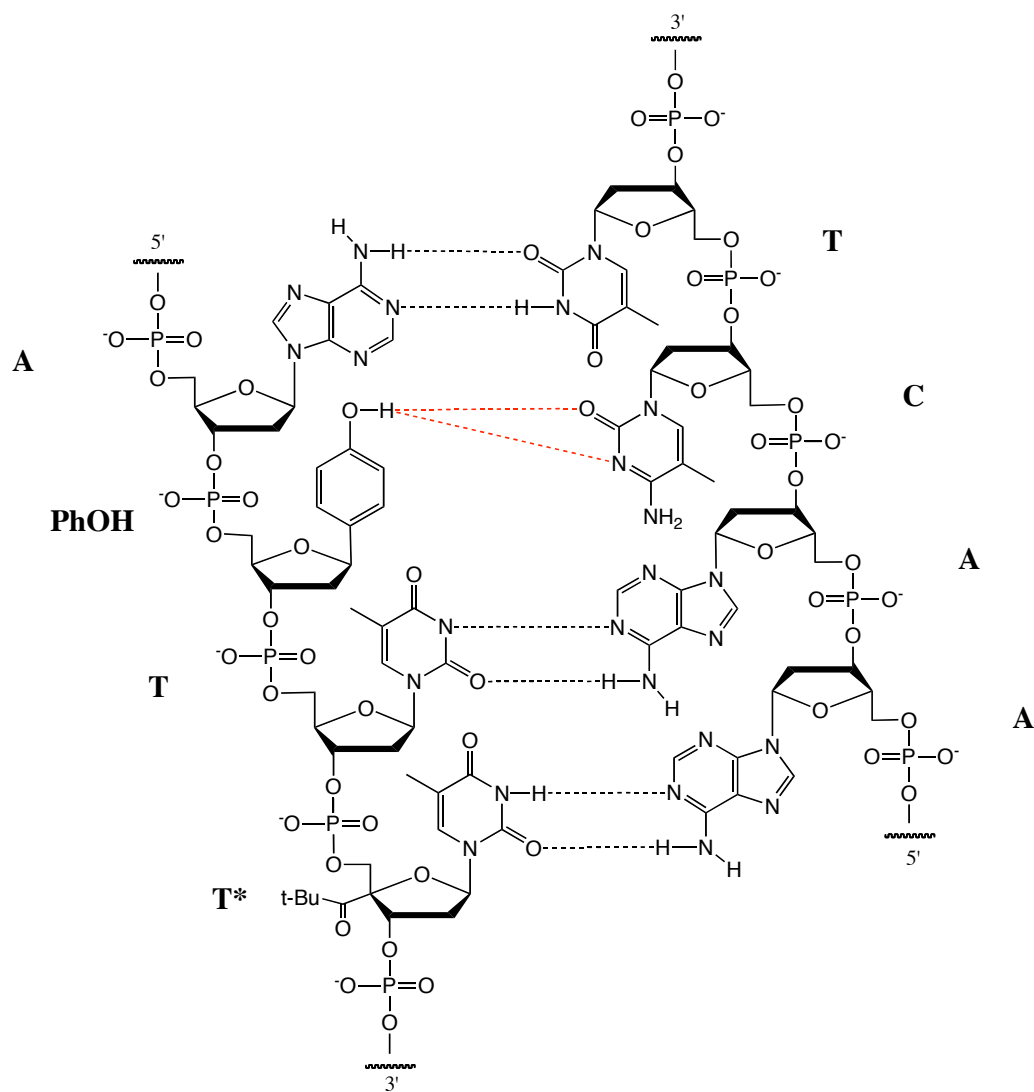


Figure 5.8 Possible hydrogen bonding between the $-OH$ of the phenol and the ketone or the imine of cytosine in double strand DNA **122b** /**134C**

5.5.2.2 Comparison with other electron donors and discussion

The $k_{ET,rel}$ values obtained with phenol as electron donor in DNA double strands **122/134C** were compared with the $k_{ET,rel}$ values reported for other electron donors in an identical DNA double strands system **178** (Figure 5.9). In this system the electron donor and the electron acceptor, the enol ether radical cation **9** resulting from T* irradiation (see Scheme 2.4) are separated by one T nucleotide. The electron donors are guanine (G), 7-deazaguanine (G^Z), 8-oxoguanine (G^{oxo}) and 8-Bromoguanine (G^{Br}) (Figure 5.10). In all cases a C nucleotide is placed opposite the electron donor.

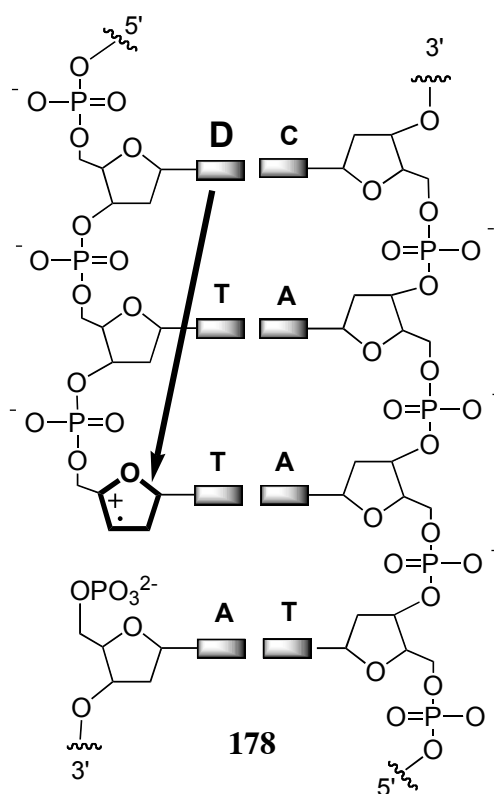


Figure 5.9 Influence of the electron donor on the electron-transfer rate in a D-B-A system **178** in DNA double strand ($D = \text{PhOH}, G^Z, G^{oxo}, G^{Br}, G$)

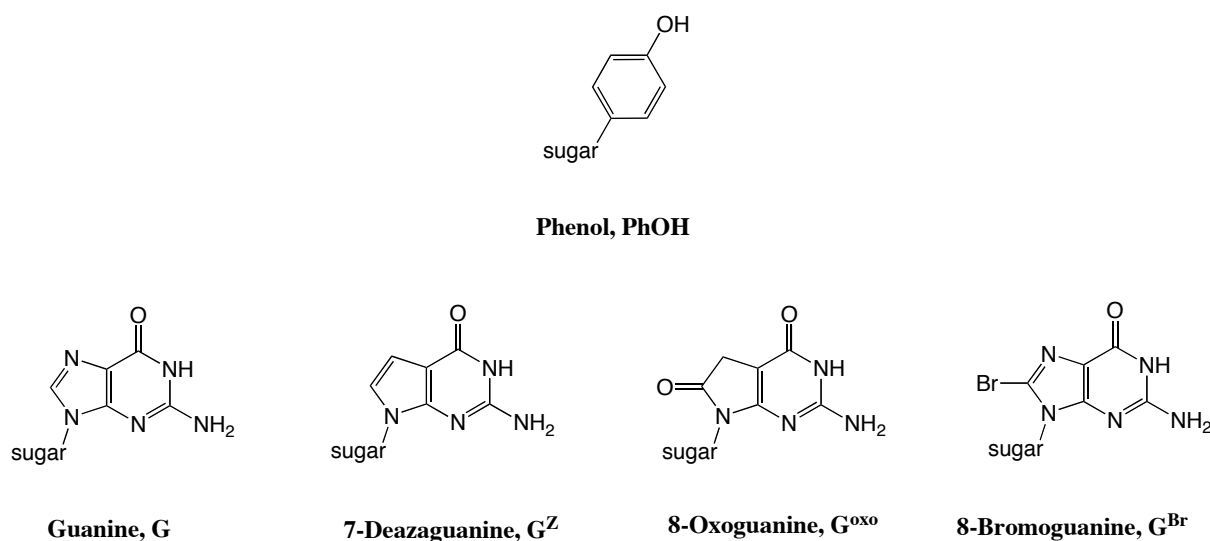


Figure 5.10 Structures of the electron-donors (D)

Table 5.6 displays the $k_{ET,rel}$ values obtained for the different electron donors in system **178** and the oxidation potential or ionization potential of the electron donors.

Donor (D)	$k_{ET,rel}$	E_{ox}° (in V vs NHE)	IP ¹²⁸ (eV)
PhOH	0.84	0.86 ¹⁴¹	
G ^Z	0.19 ¹²⁸		5.99
G ^{oxo}	0.046 ^{49,128}		6.19
G	0.012 ^{49,128}	1.29 ¹⁷	6.40
G ^{Br}	0.011 ¹²⁸		6.45

Table 5.6 Comparison between the $k_{ET,rel}$ obtained in DNA double strand with different electron donors. The ionization potentials (IP) were calculated as base pair with C in DNA using the UB3LYP/6-31G**.

Phenol appears to be the most efficient electron donor in this series. The $k_{ET,rel}$ value increases when the oxidation potential of the electron donor decreases. For example, electron transfer from phenol is 70 times faster than from guanine, which has a 0.45 V higher oxidation potential. These results are in agreement with the Marcus theory¹³⁰ for photoinduced electron-transfer reaction, as explained below.

According to Marcus, the rate constant of a single-step electron transfer reaction depends on the energy barrier (activation free energy) to pass the transition state (Eq. 5.2). A is a factor that depends on the nature of the charge transport reaction, R is the gas constant and T is the temperature of the reaction.

$$k_{ET} \propto A \cdot e^{-\frac{\Delta G^*}{RT}} \quad \text{Eq. 5.2}$$

The activation free energy ΔG^* may be expressed as following:

$$\Delta G^* = \frac{(\Delta G^\circ + \lambda)^2}{4\lambda} \quad \text{Eq. 5.3}$$

ΔG° is the reaction free energy (driving force) which corresponds to the energy difference between the minima of the parabolas (Figure 5.11) and λ the reorganization energy which is defined by the energy needed to change the nuclear coordinates of the reactant state (including contributions from the solvent) from its own minima configuration to the minima configuration of the product state.¹³⁰

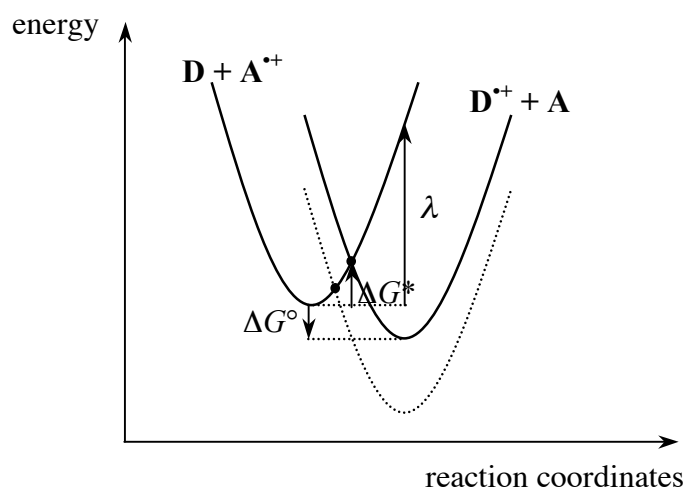


Figure 5.11 Illustration of the Marcus model for electron transfer from an electron donor D to an electron acceptor $A^{\cdot+}$

The reaction free energy ΔG° is given by Eq.5.4. E°_{ox} is the oxidation potential of the electron donor and E°_{red} the reduction potential of the electron acceptor, F is the Faraday constant.

$$\Delta G^\circ = F(E^\circ_{ox} - E^\circ_{red}) \quad (5-4)$$

The reaction free energy ΔG° is strongly dependent on the oxidation potential of the electron donor when the reduction potential of the electron acceptor doesn't change. In all the systems reported in Table 5.7, the electron acceptor is the enol ether radical cation **9** which was generated by photolysis of T* (see Scheme 2.4 p.11). Thus, the lower the oxidation potential of the electron donor is, the larger is $-\Delta G^\circ$ (see dashed line in Figure 5.11).

In order to discuss the influence of the oxidation potential and therefore of the reaction free energy ΔG° on the electron transfer-rate, we have to consider two cases (Figure 5.12):

- When, $-\Delta G^\circ < \lambda$, the electron transfer reaction takes place in the *normal Marcus region* as is generally the case for photoinduced electron-transfer reactions. In this case the sum $\Delta G^\circ + \lambda$ is positive and an increase of the driving force (more negative ΔG°) due to a lower oxidation potential of the electron donor, diminishes the sum $\Delta G^\circ + \lambda$ and therefore reduces ΔG^* . This leads to an increase of the electron-transfer rate.
- When, $-\Delta G^\circ > \lambda$, the electron transfer reaction takes place in the *inverted Marcus region*. In this case the sum $\Delta G^\circ + \lambda$ is negative and an increase of the driving force makes the sum $\Delta G^\circ + \lambda$ even more negative and due to the quadratic dependence increases ΔG^* . This leads to a decrease of the electron-transfer rate.

The optimal case would be $-\Delta G^\circ = \lambda$, corresponding on the top region of the Marcus parabola. In this case the electron transfer is barrierless.

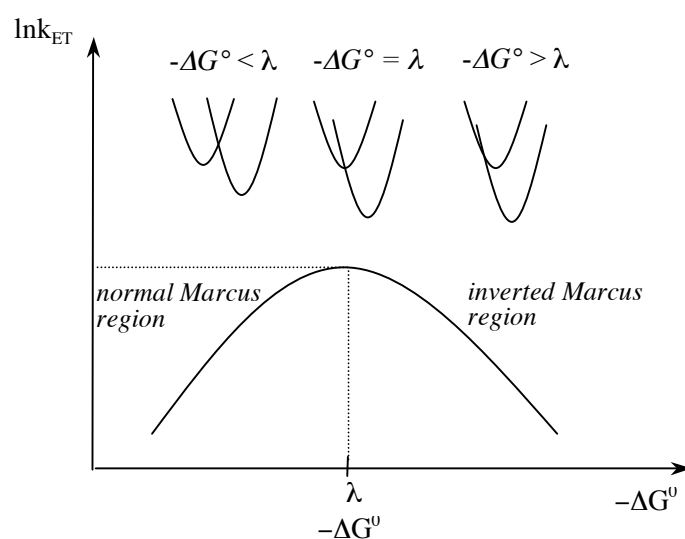


Figure 5.12 Dependence of the electron-transfer rate on the driving force ΔG°

The driving force of the electron transfer from phenol to enol ether radical cation can be estimated by considering the oxidation potential of phenol ($E^{\circ}_{\text{ox}}(\text{PhOH}) = 0.86 \text{ V vs NHE}$)¹⁴¹ and the reduction potential of the enol ether radical cation generated by photolysis ($E^{\circ}_{\text{red}}(\text{EE}^+) = 1.29\text{--}1.44 \text{ V vs NHE}$).¹³⁴ The estimated driving force is then $-\Delta G^{\circ} = 0.4\text{--}0.5 \text{ eV}$. The reorganization energy values λ reported from electron transfer in protein systems containing tyrosine are around 0.7 eV .¹³⁵ We assume that the λ value of phenol in DNA system **178** is in the same order. Based on these assumptions we can consider that electron transfer from phenol in system **178** takes place in the *normal Marcus region* $-\Delta G^{\circ} < \lambda$.

For G, G^{Br} , G^{oxo} and G^{Z} Biland reported a λ value of $0.4 \pm 0.02 \text{ eV}$ calculated with the same method as the oxidation potentials (UB3LYP/6-31G**).¹²⁸ The $\ln k_{\text{Et,rel}}$ values obtained for G, G^{Br} , G^{oxo} and G^{Z} are plotted against the oxidation potential (in eV) in figure 5.13, which exhibits a typical feature of the photoinduced electron-transfer processes in the *normal Marcus region*: the $\ln k_{\text{Et,rel}}$ increases with a decrease in the oxidation potential and therefore in the ΔG° value. Biland estimated that a decrease of 0.1 eV in the oxidation potential doubles the electron-transfer rate constant. For example the oxidation potential of G^{Z} was calculated to be 0.2 eV lower than the oxidation potential of G^{oxo} and the electron transfer is four times faster with G^{Z} than with G^{oxo} .

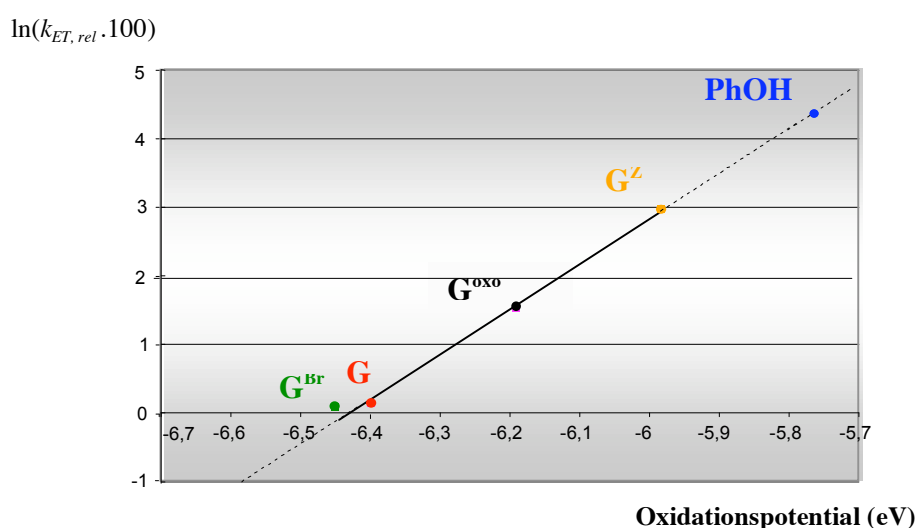


Figure 5.13 Influence of the oxidation potential on the electron-transfer rate

Interestingly, the relative electron-transfer rate with phenol is also about four times faster than the one with G^Z in system **178**. It is difficult to compare the oxidation potential of phenol given in V vs NHE with those of G^Z , G^{oxo} and G^{Br} given in eV as base-pair with C in DNA (Table 5.6). However we can suppose that the oxidation potential of phenol is lower than the oxidation potential of G^Z . The oxidation potential calculated by Lewis for G^Z , $E^{\circ}_{\text{ox}} = 0.95$ V vs SCE, would confirm our hypothesis.¹²⁹ Assuming that the distance between the phenol and the enol ether radical cation in system **178** is the same like the distance between G, G^{Br} , G^{oxo} , G^Z and the radical cation, we can speculate and report the $\ln k_{\text{ET,rel}}$ obtained with phenol on the trend line formed by G, G^{Br} , G^{oxo} and G^Z in Figure 5.13 (phenol in blue). The corresponding oxidation potential would be 5.78 eV. This value is very near the oxidation potential of 5.6 eV estimated by Biland,¹²⁸ to reach the maximum of the Marcus parabola where $-\Delta G^{\circ} = \lambda$ (Figure 5.14). According to Biland, the optimal oxidation potential should be approximately 0.75 eV lower than the oxidation potential of the guanine. Although this approximation is very speculative, phenol still appears from our experimental data as an excellent electron donor compared to the G series. Moreover the phenol modified nucleoside is also compatible with DNA.

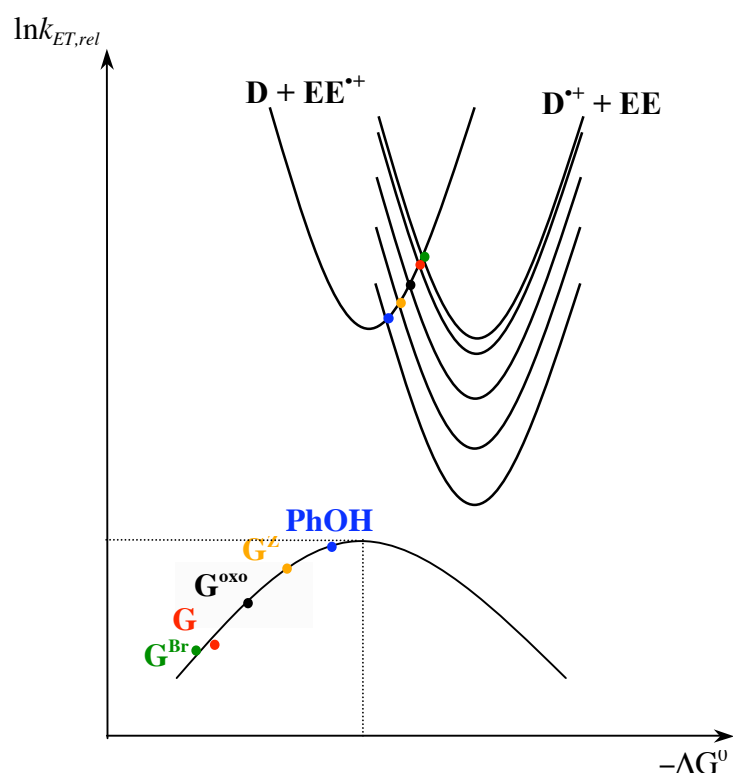
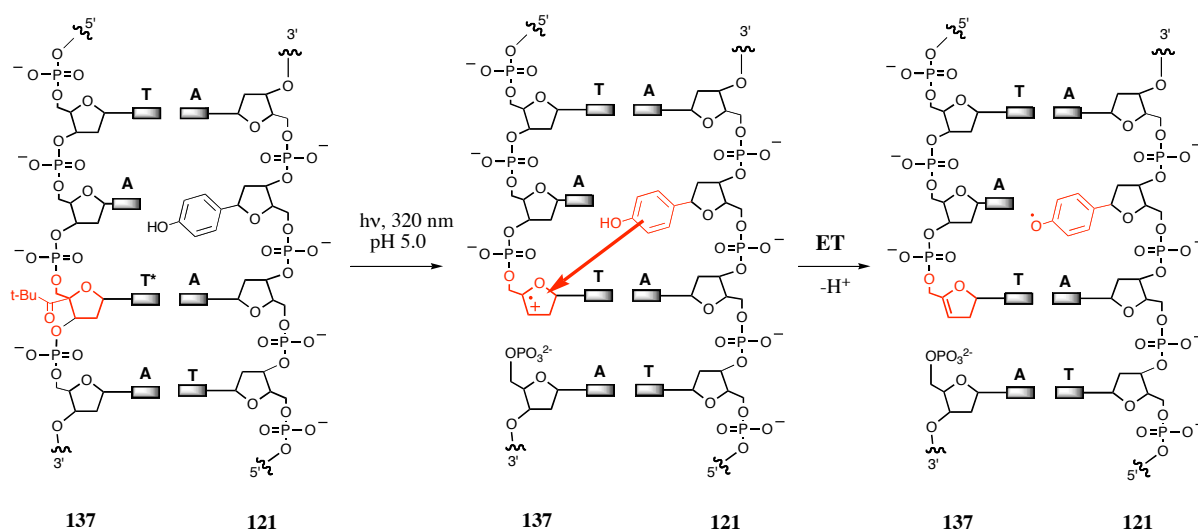


Figure 5.14 Schematic illustration of the Marcus model for electron transfer in the normal Marcus region from an electron donor D (G^{Br} , G , G^{oxo} , G^Z and phenol) to an electron acceptor EE^+ (the enol ether radical cation **9**)

5.5.2.3 Further experiments

In further experiment the charge transfer was investigated in a poly A:T double strand in which the charge is initiated in one strand and then transferred to the complementary strand. Strand **137** containing the radical cation injector T^* was annealed with its complementary strand **121** containing the phenol modification (Table 5.7). Photolysis of double strands **121/137** ($\lambda \geq 320\text{nm}$, anaerobic conditions, citrate buffer pH 5.0) generates the sugar radical cation in strand **137** (Scheme 5.25). The charge is then transferred to the phenol in the complementary strand **121**.



Scheme 5.25 Charge transfer from the sugar radical cation in strand **137** to the phenol placed in the complementary strand **121**

This double strand system displays again high electron transfer rate ($k_{ET,rel} = 0.68$) compared to similar system with G as electron donor (Table 5.7).

Sequence	$k_{ET,rel}$	Δr (\AA) ^a
121: 5'-TTTATATATATATA(PhOH)ATATATATTTT-3' 137: 3'-AAATATATATATAT* A TATATATAAAA-5'	0.68	11.5
138: 5'-GCTCTGATAAGTAGCTAGCA-3' 139: 3'-CGAGACTATT*CATCGATCGT-5'	0.015 ⁴⁵	9.6

Table 5.7 ET results in DNA double strands with phenol or guanine as electron donor. (a) The distance between phenol or G and T^* radical cation was estimated by computational *ab initio* calculations (macromodel 7.2).¹³⁶

Thermal denaturation studies^{137,138} were done to compare the melting temperatures (T_m) of duplex **121/137** containing the two modifications, phenol and T*, with unmodified duplex **135/136** and with duplexes **121/136** and **135/137** bearing just one of the both modifications (Table 5.8).

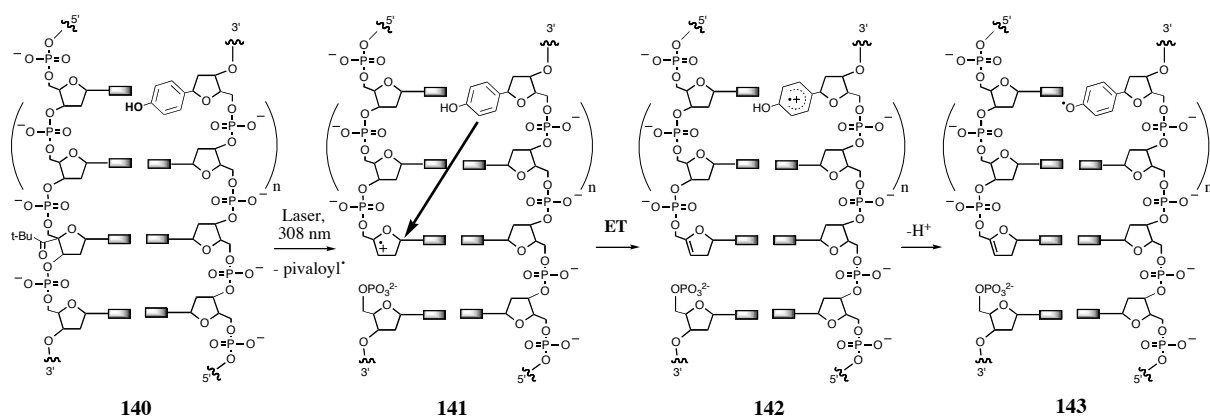
Sequence	T_m (°C)
121 : 5'- TTTATATATATATA(PhOH)ATATATATTTT-3' 137 : 3'-AAATATATATATAT T* A TATATATAAAA-5'	44.2
135 : 5'- TTTATATATATATATATATA TA TTTT-3' 136 : 3'-AAATATATATATATATATATATAAAA-5'	45.6
121 : 5'- TTTATATATATATA(PhOH)ATATATATTTT-3' 136 : 3'-AAATATATATATAT A TATATATAAAA-5'	45.1
135 : 5'- TTTATATATATA T A TATATATATTTT-3' 137 : 3'-AAATATATATAT AT * ATATATATAAAA-5'	40.6

Table 5.8 T_m studies of poly A:T double strands (26-mers) containing no, one or both modifications

The T_m value measured for duplex **121/137** containing both modifications (44.2 °C) is only 1°C lower than the T_m value of a perfect match **135/136** (45.6 °C). This indicates that the DNA structure is not destabilized when the two modifications are placed closed to each other in opposite strands. Interestingly, the T_m value obtained with duplex **135/137** containing only T* is 5°C lower (40.6°C) than that of a perfect match **135/136** (45.6°C) whereas the T_m value of duplex **121/136** containing only phenol is nearly the same (45.1°C). Moreover, the T_m value of duplex **121/137** containing both modifications is higher (44.2°C) than the T_m value of duplex **135/137** containing only T*(40.6°C). We can therefore conclude that T* destabilizes the DNA double-stranded structure whereas phenol stabilizes it.

5.6 Investigation of electron transfer using UV detection of the phenoxyl radical

In the previous chapter we have proved that phenol can act as a very good electron donor in electron transfer processes through DNA. In order to determine the rates of the electron transfer more precisely we propose to detect the phenoxyl radical using time resolved UV spectroscopy. Laser nanosecond flash-photolysis (XeCl-excimer laser, $\lambda = 308$ nm) of the DNA double strand **140** initiates charge transfer towards the phenol (**140**→**141**) which is oxidized to phenol radical cation (**141**→**142**). The phenoxyl radical is then generated by deprotonation of the phenol radical cation (**142**→**143**) (Scheme 5.26). The phenoxyl radical is UV active with a characteristic absorption maxima at 410 nm.



Scheme 5.26 Investigation of electron transfer through DNA using nanosecond flash-photolysis coupled with time-resolved UV

Although the experimental data we collected from our past studies indicated that we could base our assays on the principle described in Figure 5.26 we had to reconsider our proposal. When carrying out our preliminary experiments we became aware from studies related to electron transfer in protein systems¹⁰⁴ and using similar methodology, that the association pivaloyl and phenol is not suitable with the technique used. The pivaloyl chromophore resulting from the T* irradiation (see Figure 5.26) exhibited a strong fluorescence observed at 410 nm where the phenoxyl radical absorbs. The result is an overload of the photomultiplier which is blinded and requires 200 to 300 ns to give accurate values again.

Unable to correct this instrument problem we had to modify our system slightly and replace the phenol moiety by a trimethoxybenzene which absorbs at a different wavelength and seems to be an equally good electron donor.¹⁴⁷ The study of the new system and the development of the assay is carried out by Amiot in the Giese group.¹⁴⁹

5.7 Conclusion

Modifying an oligonucleotide with a specific chemical functionality, such as a photo-, redox- or chemically-active metal complex, is of wide-spread interest for mechanistic studies (electron transfer, structure-function), analytical applications (sequencing, hybridization assays) and therapeutic uses (anticancer, antiviral pharmaceuticals). In order to use phenol as electron donor to investigate electron transfer in DNA, we have reported the first DNA solid-phase synthesis of phenol labeled oligonucleotides using a novel phenol modified nucleoside phosphoramidite **100** (Figure 5.15) and a fully automated protocol.

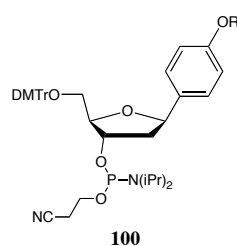
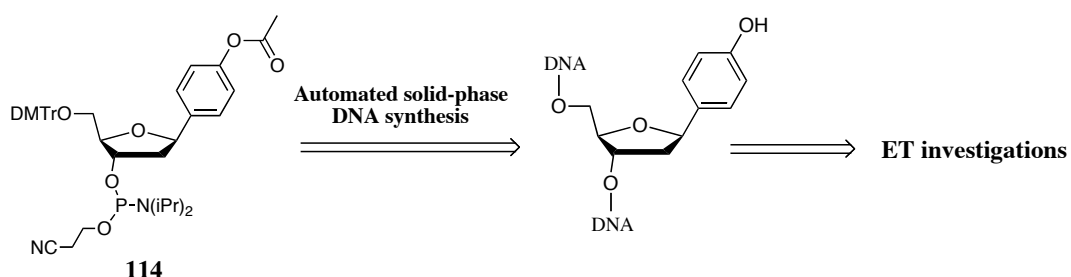


Figure 5.15 The phenol modified phosphoramidite

The choice of the phenol protecting group was a key point of the synthesis of the phenol modified nucleoside **100**. This protecting group had to withstand the nucleoside synthesis conditions, it also had to be compatible with the standard procedures for DNA synthesis and finally it had to be easily removed once the nucleoside was incorporated into DNA. The acetyl protecting group appeared to be ideal because it satisfied these three conditions, particularly it was removed during ammonia treatment used to cleave the DNA strand from the solid support. The synthesis of the acetyl protected building block **100d** was achieved successfully in 10% yield over 10 steps and its incorporation within oligonucleotides was performed with efficient coupling using standard automated DNA synthesis (Scheme 5.27).



Scheme 5.27 The acetyl protecting group strategy for incorporation of the phenol nucleoside into DNA using automated solid-phase DNA synthesis and further ET investigations

The pivaloyl modified thymine T* was incorporated into DNA at the same time as phenol and used as charge injector. Photolysis of single and double strand phenol-labeled oligonucleotides followed by HPLC analysis of the irradiated products demonstrated that phenol is a very good electron donor. The electron-transfer rates measured in single and double strand experiments are in agreement with the low oxidation potential of the phenol.

The system we have developed to investigate electron transfer in DNA is unique in that both the electron donor (phenol) and the electron acceptor (T*) are modified nucleic acids which are covalently linked to DNA. So only minor structural perturbations arise and no ambiguities occur with respect to distance separating the donor and the acceptor and the DNA assemblies are structurally well defined and well characterized. Such a system is ideal for electron transfer study because presents the advantage of locating precisely where the electron transfer starts and where it ends.

5.8 Further work and outlook

In the course of our assay development we found out that our phenol nucleoside **100** had to be replaced due to the fluorescence problem from the pivaloyl group at 410 nm where the phenoxy radical absorbs. The 2,4,6 trimethoxybenzene radical cation absorbs at 450 nm. At this wavelength the fluorescence of the pivaloyl doesn't interfere anymore on the rate measurement. In order to test the system, a simple dimer model was designed before applying the technique to the more expansive DNA (Figure 5.16). Dimer **145** containing both electron donor, the 2,4,6 trimethoxybenzene and radical cation precursor, the C4'-pivaloyl abasic nucleoside was synthesized in the Giese group by Amiot.¹⁴⁹

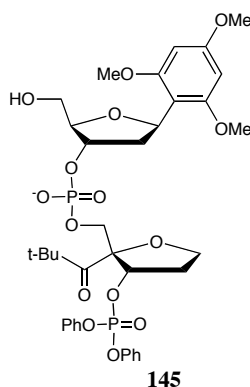


Figure 5.16 The 2,4,6 trimethoxy-nucleoside dimer

Laser irradiation of dimer **145** at $\lambda = 308$ nm (XeCl-excimer, citrate buffer pH 5.0) was followed by transient absorption spectroscopy. Figure 5.17B shows the formation and decay of the transient absorption signal obtained at 450 nm. The short-lived transient at 450 nm corresponds to the generated 2,4,6 trimethoxybenzene radical cation, where an absorbance maximum is observed (OD = 0.31).¹⁴⁹

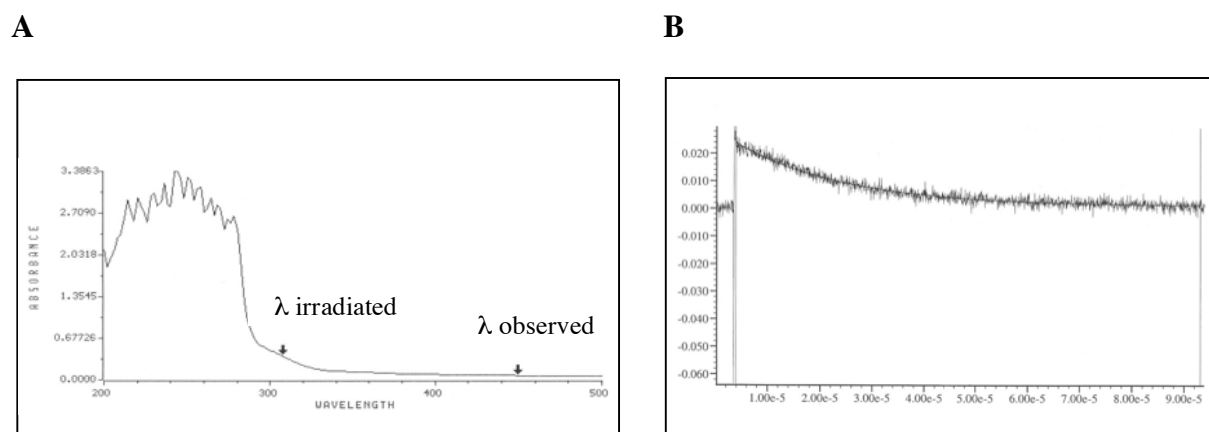


Figure 5.17 A) Absorbance spectrum of dimer **145**. B) Time-resolved transient absorption traces at 450 nm for the dimer **145**.

After this preliminary results were obtained we are confident that the replacement of the phenol by a trimethoxybenzene will lead to an excellent assay to study electron transfer into DNA using the technique of laser photolysis coupled with transient absorption spectroscopy. We are still currently working on the development of this assay.

Experimental Part

6. Instruments and materials

6.1 Physical Data

6.1.1 NMR Spectroscopy

¹H-NMR

Instruments: *Varian Gemini 300* (300 MHz), *Varian Gemini VXR 400* (400 MHz), *Bruker DRX500* (500 MHz).

The chemical shifts (δ) are given in ppm, referred to the internal standard tetramethylsilane ($\delta = 0.0$) or to the partially deuterated nucleus of d_1 -chloroform ($\delta = 7.26$), or to the partially deuterated methyl groups of d_4 -methanol ($\delta = 3.34$). All spectra are interpreted by first order, and the coupling constants (J) are given in Hertz. Split signals with defined multiplicity were characterized by the arithmetic middle of the signal lines. Multiplets are given as region in one-dimensional spectroscopy, but as value of the maximum in two-dimensional spectroscopy. Free hydroxy groups are assigned by proton-deuterium-exchange due to the addition of D_2O . When necessary, the classification of the signals was done by COSY and NOESY measurements. The signals were abbreviated as follow: s = singlet, bs = broad singlet, d = doublet, t = triplet, m = multiplet, ar = aromatic

¹³C-NMR

Instruments: *Varian Gemini VXR 400* (101.0 MHz), *Bruker DRX500* (125.8 MHz).

The chemical shifts (δ) are given in ppm and are referred to the signals of the solvents d_1 -chloroform ($\delta = 77.0$) or d_4 -methanol ($\delta = 49.9$). The spectra are proton broad band decoupled. When necessary the classification of the signals was done by APT or DEPT experiments. When carbon-deuterium coupling appeared, the chemical shifts (δ) are characterized by the arithmetic middle of the signal lines. The signals were abbreviated as follow: C_p = primary C-atom, C_s = secondary C-atom, C_t = tertiary C-atom, C_q = quarternary C-atom, C_{ar} = aromatic C-atom.

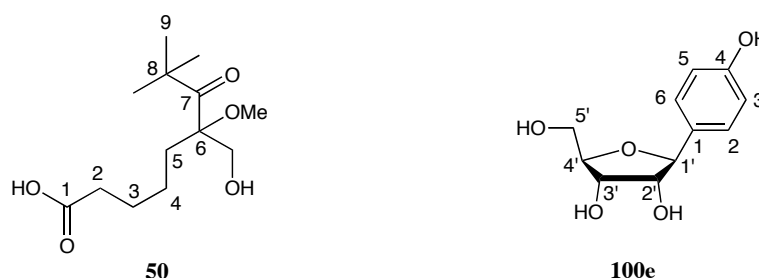
³¹P-NMR

Instrument: Varian Gemini VXR 400 (162.0 MHz)

The chemical shifts (δ) are given in ppm and are referred to the spectra reference of the external standard of 58% triphenylphosphate in chloroform ($\delta = -18$ Hz). The spectra are proton broad-band decoupled.

Numbering of the nuclei

The protons in the ¹H-NMR spectra are numbered with the same numbers as the related carbon atoms (Figure 6.1). If geminal hydrogen atoms show two distinguished signals, the high-field and the low-field shifted nuclei are told apart by an additional “a” or “b”. In compound **100e**, the protons of the nucleobase are listed with H-1 to H-n and the protons of the sugar with H-1' to H-n' according to the nomenclature of nucleosides.



Scheme 6.1 Numbering of the atoms of compound **50** and **100e**

6.1.2 Mass Spectroscopy

EI and FAB - Mass Spectroscopy

Instrument: Mass spectrometer VG70-250 and Finnigan MAT 312.

Mass spectra were carried out by Dr. H. Nadig at the Department of Chemistry at the University of Basel. The ion generation resulted via electron ionization (EI) or bombardment with fast xenon atoms (FAB), and the use of nitrobenzyl alcohol as matrix and sodium chloride as additive. The data are given in mass units per charge (m/z , intensity), and the intensities of the signals are indicated in percent of basis ion in brackets.

Electrospray - Mass - Spectrometry

Instrument: *Finnigan MAT LCQ, Octapole Mass-Spectrometer.*

The samples are directly injected in solution. The ion source resulted via electron ionization. All data refer to the atomic mass units per elemental charge (m/z , intensity). The intensities of the signals are indicated in percent of basis ion in brackets.

MALDI - TOF- Mass – Spectroscopy

Instrument: *Voyager Elite, Biospectrometry Research Station by Vestec.* Flight tube 2 m.

N_2 –Lazer (337 nm, 3 ns pulse duration, 0,2 mJ/pulse, accumulation of 10-100 puls). Acceleration voltage 25 kV, negative-ion mode.

Signals fit to unfragmented deprotonated molecule ion (M-H)⁻. All data refer to the atomic mass units per elemental charge (m/z , intensity).

6.1.3 UV/Vis – Spectroscopy

Instrument: *Perkin Elmer UV/Vis Spectrometre Lambda 2*

Extinction coefficients (ϵ) are given in $M^{-1}.cm^{-1}$.

6.1.4 Elemental Analysis

Instruments: *Leco CHN-900* (C-, H-, N-detection), *Leco RO-478* (O-detection).

The elemental analyses were carried out by W. Kirsch at the Departement of Chemistry at the University of Basel. The data are indicated in mass percents.

6.2 Chromatographic Methods

6.2.1 Thin Layer Chromatography (TLC)

Material: Silica gel 60 F254 aluminum sheets by *Merck* with a layer thickness of 0.2 mm.

The detection of UV-inactive compounds was carried out by dipping in:

- a solution of ceric ammonium sulfate dihydrate (10 g ceric (IV) sulfate tetrahydrate, 25 g ammonium molybdate tetrahydrate, 100 ml concentrated sulfuric acid and 900 mL water) and subsequent heating;

or

- a solution of permanganate (3 g potassium permanganate, 5 mL 5% sodium hydroxide, 20 g potassium carbonate and 300 ml water) and subsequent heating;

6.2.2 Flash Column Chromatography (FC)

Flash Column Chromatography was performed under high pressure (~1.5 bar, membrane pump) on silica gel C 560 KV (35-70 μm) by *Uetikon* or on silica gel 60 (40-63 μm) by *Merck*. The solvents were distilled before use. The ratio of the solvents in mixture is referred to the parts of the volume (v/v).

6.2.3 High Pressure Liquid Chromatography (HPLC):

Instrument: for strands purification : *Hewlett Packard 1050 Series*

for analytical : *Waters Alliance (2690 Separations Module) 2680 Dual Mode Detector*.

Column: - normal phase: *Merck LiChroCART 250-4 LiChrospher Si60* (5 μm), dimension: 250 mm x 4 mm, flow: 1 mL/min;

- reversed phase: *Merck LiChroCART 250-4 Lichrospher 100 RP-18* (5 μm), dimension: 250 mm x 4 mm, flow: 1 mL/min

6.3 Irradiation instruments

- **For analytical irradiation:** Irradiation bench by *Oriel* 68810, with mercury high pressure lamp by *Osram* 500 W, with 320 or 305 nm cut-off filter (2mm x 50 mm x 50 mm) by *Schott*. At given wavelength light transmittance is about 50% (Figure 6.2).

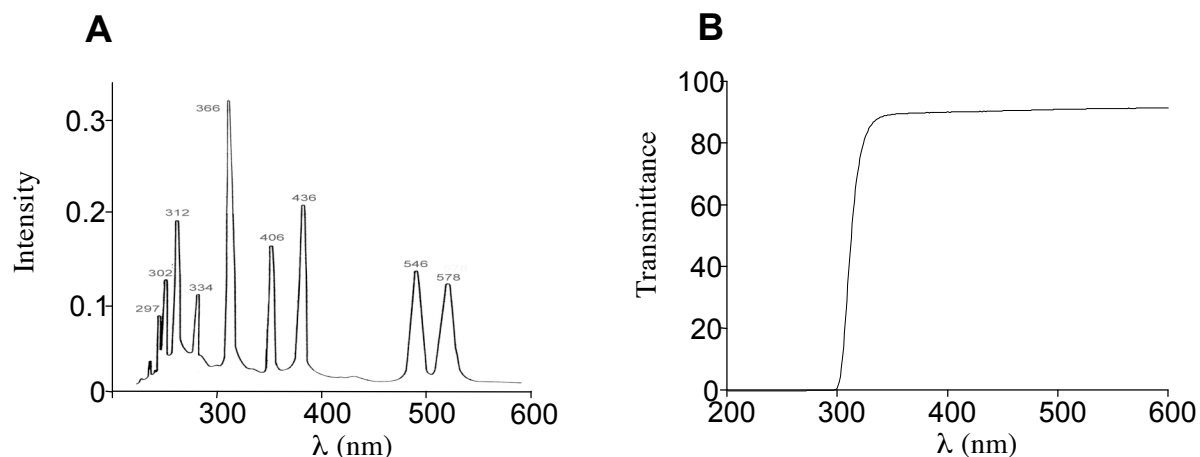


Figure 6.2 A) *Osram* 500 W lamp spectra. B) Light transmittance of a 320 nm cut-off filter.

- **For laser irradiation** : laser irradiations were carried out in the group of Prof J. Wirz (University Basel) with a COMpex 205 XeCl-Excimer Laser ($\lambda = 308$ nm, Laser power 100-150MJ/pulse, pulse duration 25 ns) from *Lambda Physik*. The samples were irradiated at RT in a quartz cuvette (4,5 cm x 1 cm x 1 cm). Before irradiation the samples were degassed by repeated freezing in liquid nitrogen followed by evaporation of the solvent with a diffusion pump. A monochromator xenon lamp (1P28 photomultiplier) was employed for kinetic measurements at the observed wavelength. Detection was performed with a iStar 720 ICCD Detector from *Andor*. The measuring data were analyzed with MacFitFlash 2.0.1.

6.3 DNA instruments

DNA synthesizer

Expedite 8909 by *Perspective Biosystems*. The reagents for the DNA synthesizer were ordered from *Glenresearch*.

Thermomixer and Vortexer

Thermomixer 5436 from *Eppendorf* and vortexer *Genie 2* from *Bender&Holbein AG*.

Lyophilisator

Speed Vac Plus from the firm *Savant*

Centrifuge

Centrifuge 5415 C from *Eppendorf*; *Picofuge* by *Stratagene*.

6.5 Chemicals and solvents

Chemicals: The reagents for the DNA synthesizer were ordered from *Eurogentech*. All other commercial substances were ordered from *Fluka Chemie AG* or *Aldrich* and applied without further purification if not specially mentioned.

Solvents: Diethyl ether and tetrahydrofurane were freshly absolved over sodium following the standard procedures. Other absolute solvents were bought from *Fluka Chemie AG*, *Rog mil Chemicals*, *Machler* and *J.T.Baker*, and used directly without further cleaning. Technical solvents for flash chromatographic separation procedures were distilled before use.

7. General methods

7.1 Synthesis

All the reactions were carried out under standard conditions in appropriate laboratory glassware. Reactions that were sensitive to water and oxygen were performed under argon atmosphere.

7.2 General oligonucleotide procedures

7.2.1 Synthesis

Synthesis:

The modified oligonucleotides were synthesized using an automated DNA solid-phase synthesizer. The oligonucleotides were assembled from 3'-terminal to 5'-terminal using a 0.2 μ M mass column (see Chapter 5.4.1). Amino derivatized borsilicate (Controlled Pore Glas: CPG) with a pore size of 1000 Å were used a solid phase support. The first nucleotide (in all cases thymidine) was already covalently attached at its 3' hydroxyl group to the solid-phase through a base labile succinyl linker. The synthesizer was set to standard Trityl-on mode. The modified nucleotides T* and phenol, which were before dried under high vacuum for 24 h, were dissolved in dry acetonitrile (0.08-0.1M) and the coupling times were enhanced from 2 min to 15 min for their incorporation.

Solid phase cleavage and deprotection:

Once the synthesis finished, the solid phase was dried under argon and the solid phase pores were added to 1 ml concentrated ammonia (32%) and stirred at 55°C overnight to remove the oligonucleotide from the solid phase. Ammonia treatment also removes the cyanoethyl phosphate protecting groups and the protecting groups on amines of the adenine, cytidine and guanine bases. The oligonucleotide was lyophilized and dissolved in 0.1 M TEAA-Buffer (pH 7.0) and further purified using RP-18 HPLC.

7.2.2 Purification

The oligonucleotides were purified by RP-18 HPLC. A RP-18 column from *Merk* (see Chapter 6.2.3) was used to separate the strands (Flow 1 ml/min). The column temperature was set at 55°C and the detection was made by UV-absorption at 260 nm. The oligonucleotides were eluted using an acetonitrile gradient composed by eluent A: 0.1 M triethylammoniumacetate buffer (TEAA) pH 7 and eluent B: Acetonitrile 190.

Trityl-on purification:

As the oligonucleotide synthesis was accomplished in Trityl-on mode, the last nucleotide of the sequence kept its 5'-trityl protecting group on. This helps to separate the incomplete, capped oligonucleotides which are primarily eluted by this first purification (trityl-on). An acetonitrile gradient of 15% to 40% in 30 minutes was used to isolate the modified strand which did generally eluate between 12 and 20 minutes.

Removal on the 5' trityl group:

The isolated fractions were lyophilized and then left to stand in 80% AcOH (200 µl) solution for 20 minutes at RT. After neutralizing with 3 M sodium acetate solution (50 µl) the dissolved strand was then placed in isopropanol (800 µl) and left standing over night at -20°C to precipitate the oligonucleotide. After centrifugation for 10 minutes at 10 000 rpm (14 000 g), the solution was decanted off.

Trityl-off purification:

The precipitate was then dissolved in nano-pure water and purified again by RP-18 HPLC. A typical gradient was 6% to 20% acetonitrile in 40 minutes (trityl-off), in order to achieve an optimal retention time of 13 to 18 minutes. The purity of the oligonucleotides was checked by MALDI-ToF MS.

7.2.3 Unmodified strands

All the unmodified oligonucleotides were purchased from *Microsynth* and *Qiagen/Operon* with beforehand PAGE - purification. Their purity was checked by RP-18 HPLC (Trityl-off mode) and MALDI-ToF MS.

7.2.4 Mass analysis

All mass analyses of oligonucleotides single strands were done by MALDI-ToF MS. To do so, 1 μ l of the trityl-off purified solution was taken with a micropipette and mixed with 1 μ l of the matrix solution (0.5 M 2,4-dihydroxyacetophenone and 0.3M ammoniumtartrate in nanopure water/acetonitrile 3/1) and placed on the metal plate to dry. After the sample has crystallized, the sample plate is placed into the mass spectrometer for analysis.

7.2.5 Quantification by UV-absorption

The molar extinction coefficient of the oligonucleotides were calculated using the increment values of the next formula :

$$\epsilon_{260} = (\epsilon_A \times N_A + \epsilon_C \times N_C + \epsilon_G \times N_G + \epsilon_T \times N_T) \times 0.9 + \epsilon_{\text{modification}} \quad \text{Eq. 7.1}$$

N is the number of each bases in the oligonucleotide and ϵ its corresponding molar extinction coefficient. The following standard ϵ_{260} values were used for each base (the values were determined using absorption of 260 nm)⁸¹ and the ϵ value for the phenol was determined experimentally at 260 nm with the compound **92**.

Nucleobases	ϵ_{260} (in $M^{-1} \cdot cm^{-1}$)
Adenine	15400
Guanine	11500
Cytosine	7400
Thymine	8700
Phenol (92)	195

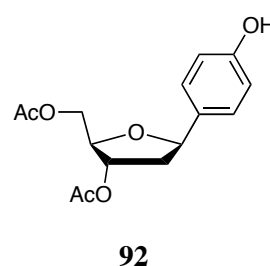


Table 7.1 Increment values of the nucleobases

Oligonucleotide solution was placed in a plastic cuvette (1 ml, 1cm) and absorption was measured at 260nm. The concentration of the nucleotide was determined using the Beer-Lambert law (7.2):

$$A = \epsilon_{260} \times C \times l \quad \text{Eq. 7.2}$$

A is the measured absorbance at 260 nm, ϵ_{260} the molar extinction coefficient at 260 nm ($M^{-1}.cm^{-1}$), C the concentration ($mol.l^{-1}$) and l the path length of the cuvette (cm).

7.2.6 Hybridization

The double strands were annealed by placing the modified strand (1 nmol) and its complementary strand (1.1-1.2 nmol) in a citrate buffer solution (pH 5.0, in addition to 100 mM NaCl, 200 μ l) for 3 minutes at 80°C and then letting slowly cool down to RT for 3 hrs.

7.2.7 Melting point determination by UV/Vis - Spectroscopy

The measurement of the melting point was carried out at 260 nm with a temperature gradient of 1°C/min. The modified strand (1 nmol) and its complementary strand (1.1-1.2 nmol) were dissolved in a citrate buffer solution (pH 5.0, in addition to 100 mM NaCl, 1000 μ l). The melting point (T_m) is given as a mean value of the heating and cooling down temperature curves (first order derivative).

7.2.8 Photolysis

The strands, -both double and single, were dissolved in a citrate buffer (200 μ l, 20 mM sodium citrate, 100 mM NaCl, pH 5.0) in a 1.5 ml polymethylmethacrylate cuvette from Semadeni containing a rubber septum. Argon was bubbled through the solution for 15 min under low pressure to degas the solution. The cuvettes, still under an argon atmosphere, were placed on the appropriate position and irradiated behind a cut-off filter (320 nm) with a 500 W mercury high-pressure lamp for 5 min. The thermostat set at 15 °C to keep any evaporation to a minimum. After the photolysis was finished, the solvent was evaporated in vacuum, and the residue purified with HPLC.

7.3 Quantification of the photolysis products by HPLC

7.3.1 Ferrocene derivatives photolysis

The photolysis products were isolated by RP-18 HPLC using an acetonitrile gradient 70% to 100% in 25 min (solvent A: TEAA-Buffer, solvent B: Acetonitrile) and quantified by using the area factor F_p given in Eq. 7.3:

$$F_x = \frac{n(X) \times \text{area}(S)}{n(S) \times \text{area}(X)} \quad \text{Eq. 7.3}$$

$n(X)$: mol quantity of the educt before photolysis.

$\text{area}(X)$: chromatogram peak area of the educt.

$n(S)$: mol quantity of the co-injected standard.

$\text{area}(S)$: chromatogram peak area of the co-injected standard.

The yield (%) of the photolysis product Y is given by Eq. 7.4:

$$Y(\%) = F_Y \times \frac{n(S) \times \text{area}(Y)}{\text{area}(S)} \quad \text{Eq. 7.4}$$

7.3.2 Phenol oligonucleotides photolysis

The photolysis products Y were isolated by RP-18 HPLC using an acetonitrile gradient 6% to 20% in 40 min (solvent A: TEAA-Buffer, solvent B: Acetonitrile) and quantified by dividing the peak areas by their calculated extinction coefficients (see 7.2.5) and internal calibration:

$$Y(\%) = \frac{\text{area}(Y)}{\epsilon(Y)} \times \frac{n(S) \times \epsilon(S)}{\text{area}(S)} \quad \text{Eq. 7.5}$$

$\text{area}(Y)$: chromatogram peak area of the photolysis product.

$\epsilon(Y)$: extinction coefficient of the photolysis product.

$n(S)$: mol quantity of the co-injected standard, generally the counter strand.

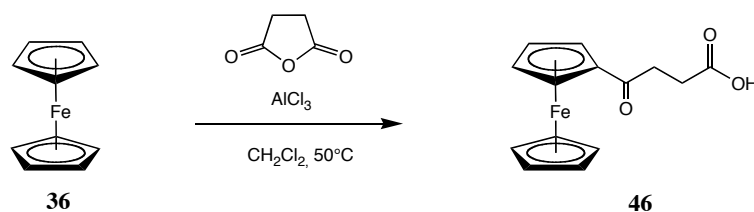
$\epsilon(S)$: extinction coefficient of the co-injected standard.

$\text{area}(S)$: chromatogram peak area of the co-injected standard

8 Synthesis of the ferrocenyl derivatives

8.1 Synthesis of the ferrocenyl linker, the 4-Ferrocenylbutanol (49)

3-Ferrocenoylpropylic acid (46)



A mixture of ferrocene **36** (2.51 g, 13.5 mmol) and glutaric acid anhydride (1 g, 10 mmol) in dichloromethane (50 ml) was added dropwise to aluminium trichloride (1.73 g, 13 mmol) in anhydrous dichloromethane (50 ml). The yellow solution turns violet. After refluxing for 3 h, the batch was hydrolysed (100 ml water) and the resulting solution was filtered through frit to remove reaction products which are not soluble in either aqueous phase or organic phase. The aqueous phase was separated and the organic phase was washed with water (3 x 50 ml), dried over Na_2SO_4 and concentrated under reduced pressure. The residue was purified by column chromatography on silica gel (Dichloromethane/Methanol 95/5) to give 2.24 g (7.83 mmol, 58%) of pure product **46** as an orange powder.

$\text{C}_{14}\text{H}_{14}\text{FeO}_3$: 286.11 g.mol⁻¹

R_f (Dichloromethane/Methanol 95/5) = 0.26

¹H-NMR (400 MHz, CDCl_3 , δ /ppm):

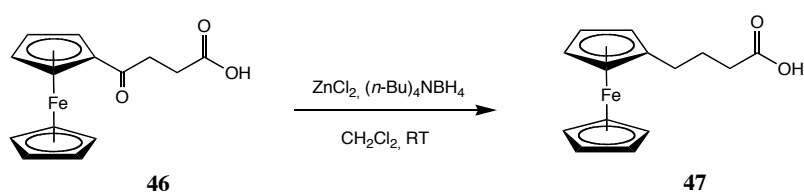
4.11 (s, 5H, Fc); 4.05 (s, 4H, Fc); 2.72 (t, $J = 6.6$ Hz, 2H, Fc-CO- $\underline{\text{CH}}_2$); 2.36 (t, $J = 6.4$ Hz, 2H, $\underline{\text{CH}}_2\text{COOH}$).

^{13}C -NMR (101 MHz, CDCl_3 , δ/ppm):

198.8 ($\text{C}_q, \text{C}=\text{O}$); 180.2 (C_q, COOH); 87.9 (C_q, Fc); 68.9 ($\text{C}_t, 5 \underline{\text{C}}\text{H Fc}$); 68.5, 67.8 ($\text{C}_t, 4 \underline{\text{C}}\text{H Fc}$); 34.1 ($\text{C}_s, \text{Fc}-\text{CO}-\underline{\text{C}}\text{H}_2$); 29.8 ($\text{C}_s, \underline{\text{C}}\text{H}_2\text{COOH}$).

MS (ESI, MeOH/ CH_2Cl_2 1/1) : 309.5 $[\text{M} + \text{Na}]^+$

4-Ferrocenylbutyric acid (**47**)



To a solution of compound **46** (286 mg, 1 mmol) and tetrabutylammonium borohydride (257 mg, 1 mmol) in dichloromethane (3 ml) cooled in an ice-water bath was added slowly a 1.0 M ZnCl_2 solution in ether (2.1 ml, 2.1 mmol). The mixture was stirred at RT for 1 h and poured into water (5 ml). The organic layer was separated, dried over Na_2SO_4 , and concentrated under reduced pressure. The crude product was purified by flash chromatography on a silica gel column (Dichloromethane/Methanol 95/5) to afford 177 mg (0.65 mmol, 65%) of product **47** as an orange solid.

$\text{C}_{14}\text{H}_{16}\text{FeO}_2$: 272.13 $\text{g}\cdot\text{mol}^{-1}$

R_f (Dichloromethane/Methanol 95/5) = 0.49

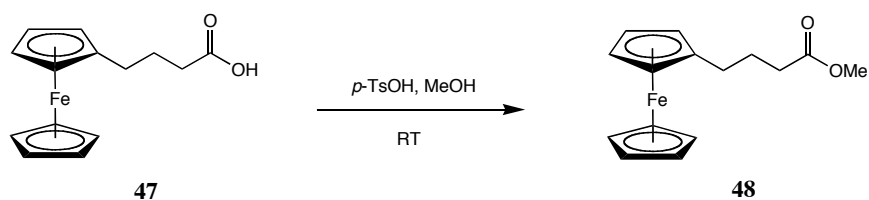
^1H -NMR (400 MHz, CDCl_3 , δ/ppm):

4.12 (s, 5H, Fc); 4.03 (s, 4H, Fc); 2.37 (m, 4H, $\text{Fc}-\underline{\text{C}}\text{H}_2, \underline{\text{C}}\text{H}_2\text{COOH}$); 1.87 (m, 2H, $\underline{\text{C}}\text{H}_2$).

^{13}C -NMR (101 MHz, CDCl_3 , δ/ppm):

179.9 (C_q, COOH); 87.9 (C_q, Fc); 68.8 ($\text{C}_t, 5 \underline{\text{C}}\text{H Fc}$); 68.1, 67.2 ($\text{C}_t, 4 \underline{\text{C}}\text{H Fc}$); 33.6 ($\text{C}_s, \underline{\text{C}}\text{H}_2\text{COOH}$); 28.6 ($\text{C}_s, \text{Fc}-\underline{\text{C}}\text{H}_2$); 26.0 ($\text{C}_s, \text{CH}_2-\underline{\text{C}}\text{H}_2-\text{CH}_2$).

MS (ESI, MeOH/ CH_2Cl_2 1/1): 272.3 $[\text{M}]^+$

4-Ferrocenylbutyric acid methyl ester (48)

Acid **47** (252 mg, 0.93 mmol) was dissolved in methanol (5 ml) and *p*-toluene sulfonic acid was added (catalytic amount). The reaction mixture was stirred for 4 h at RT under argon, then concentrated under reduced pressure and chromatographed directly on a silica gel column (Dichloromethane). The desired product **48**, 254 mg (0.89 mmol, 96%), was isolated as an orange oil.

C₁₅**H**₁₈**FeO**₂: 286.16 g.mol⁻¹

*R*_f (Dichloromethane) = 0.38

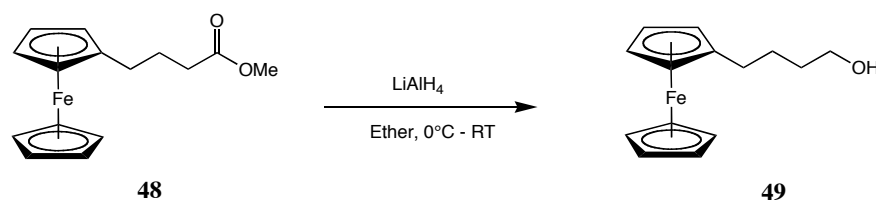
¹**H**-NMR (400 MHz, CDCl₃, δ/ppm):

4.12 (s, 5H, Fc); 4.06 (s, 4H, Fc); 3.68 (s, 1H, OCH₃); 2.38 (m, 4H, Fc-CH₂, CH₂COOH); 1.86 (m, 2H, CH₂).

¹³**C**-NMR (101 MHz, CDCl₃, δ/ppm):

174.0 (C_q, COOH); 88.1 (C_q, Fc); 68.5 (C_t, 5 CH); 68.1, 67.2 (C_t, 4 CH Fc); 51.5 (C_p, OCH₃); 33.7 (C_s, CH₂COOH); 29.0 (C_s, Fc-CH₂); 26.1 (C_s, CH₂-CH₂-CH₂).

MS (ESI, MeOH/ CH₂Cl₂ 1/1): 286.3 [M]⁺

4-Ferrocenylbutanol (49)

LiAlH₄ (50 mg, 1.32 mmol) was added to a stirred solution of compound **48** (340 mg, 1.19 mmol) in diethylether (18 ml) cooled to 0°C. The reaction mixture was stirred for 1h at RT under argon and the batch was slowly hydrolysed (20 ml water). Dichloromethane was added (40 ml) and the mixture was neutralized with a 2 M solution of hydrochloric acid (15 ml). The organic layer was separated, washed 3 times with water (3 x 30 ml), dried over Na₂SO₄ and concentrated. Column chromatography over silical gel (Pentane/AcOEt 2/1) afford 291 mg (1.13 mmol, 95%) of the desired alcohol **48** as an orange solid.

C₁₄H₁₈FeO: 258.15 g.mol⁻¹

R_f (Pentane/ AcOEt 2/1) = 0.34

¹H-NMR (400 MHz, CDCl₃, δ/ppm):

4.11 (s, 5H, Fc); 4.05 (s, 4H, Fc); 3.55 (t, *J* = 6.15 Hz, 2H, CH₂OH); 2.35 (t, *J* = 7.2 Hz, 2H, Fc-CH₂); 1.58 (m, 4H, CH₂); 1.33 (s, 1H, OH).

¹³C-NMR (101 MHz, CDCl₃, δ/ppm):

89.0 (C_q,Fc); 68.5 (C_t, 5 CH Fc); 68.1, 67.1 (C_t, 4 CH Fc); 62.8 (C_s, CH₂OH); 32.6, 29.4, 27.2 (3C_s, 3 x CH₂).

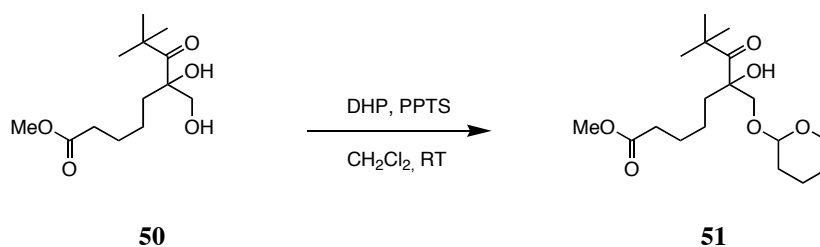
MS (ESI, MeOH/ CH₂Cl₂ 1/1): 258.3 [M]⁺

Elemental analysis: calculated: C 67.62, H 7.09, O 5.63.

found: C 66.33, H 6.12, O 5.75.

8.2 Synthesis of the radical injector (53)

(rac)-8,8-Dimethyl-6-hydroxy-7-oxo-6-[(tetrahydro-2H-pyran-2-yloxy) methyl] nonanoic acid-methyl ester (51)



To a solution of alcohol **50**⁸⁵ (200 mg, 0.77 mmol) and dihydropyran (174 μl , 1.92 mmol) in dichloromethane (6ml) was added pyridinium *p*-toluenesulfonate (48 mg, 0.192 mmol) and the mixture was stirred at RT for 1.5 h. Saturated NaHCO_3 solution was added (15 ml) and the aqueous layer was extracted with dichloromethane (3 x 10 ml). The collected organic layer was dried over MgSO_4 , filtered and concentrated. The crude product was purified by flash chromatography on a silica gel column (Pentane/AcOEt 4/1) to afford 224 mg (0.65 mmol, 85%) of the product **52** as a colorless oil.

$\text{C}_{18}\text{H}_{32}\text{O}_6$: 344.45 $\text{g}\cdot\text{mol}^{-1}$

R_f (Pentane/ AcOEt 4/1) = 0.28

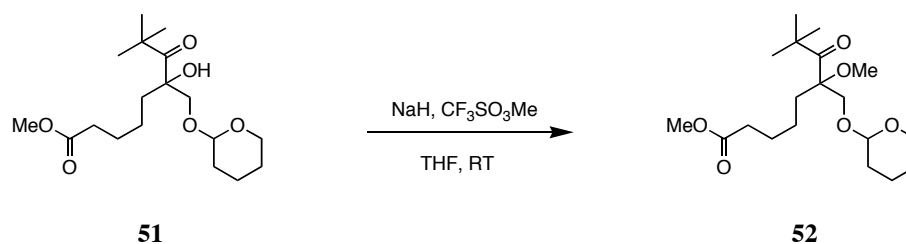
$^1\text{H-NMR}$ (400 MHz, CDCl_3 , δ/ppm):

mixture of both diastereoisomers : 4.59 (dd, 1H, THP); 4.02 (d, $J = 10.1$ Hz, 1H, $\text{CH}_2\text{H}_b\text{OTHP}$); 3.95 (d, $J = 10.1$ Hz, 1H, $\text{CH}_2\text{H}_a\text{OTHP}$); 3.65 (s, 3H, OCH_3); 3.55 (d, $J = 10.12$ Hz, 2H, THP); 2.28 (t, $J = 7.5$ Hz, 2H, H-2); 1.76 -1.48 (m, 12H, 6H THP, 2 x H-3, 2 x H-4, 2 x H-5); 1.25 (s, 9H, H-9).

$^{13}\text{C-NMR}$ (101 MHz, CDCl_3 , δ/ppm):

mixture of both diastereoisomers : 218.5 (C_q , C-7); 173.9 (C_q , C-1); 99.8 (C_t , THP); 84.0 (C_q , C-6); 74.5 (C_s , CH_2OTHP); 63.3 (C_s , THP); 51.4 (C_p , OCH_3); 44.7 (C_q , C-8); 36.9 (C_s , C-5); 33.9 (C_s , C-2); 30.7 (C_s , THP); 27.1 (C_p , 3 x C-9); 25.7 (C_s , THP); 25.4 (C_s , C-3); 23.2 (C_s , C-4); 19.8 (C_s , THP).

MS (ESI, MeOH/ CH_2Cl_2 1/1): 367.3 $[\text{M}+\text{Na}]^+$

(rac)-8,8-Dimethyl-6-methoxy-7-oxo-6-[(tetrahydro-2H-pyranloxy) methyl] nonanoic acid-methyl ester (52)

A mixture of alcohol **51** (200 mg, 0.58 mmol) and sodiumhydride (60% in mineral oil, 46 mg, 1.16 mmol) in diethylether (8 ml) was stirred for 3 h at RT and trifluoromethane sulfonic acid methyl ester (127 μ l, 1.16 mmol) was added. The reaction mixture was stirred for 20 min under argon at RT. Water (10 ml) was then added as well as diethylether (20 ml). The organic layer was washed with saturated NaHCO_3 solution (20 ml), with saturated NH_4Cl solution (20 ml) and with brine (20 ml). The organic phase was then dried over MgSO_4 , filtered and the solvents were removed. The residue was purified by flash chromatography on a silica gel column (Pentane/AcOEt 4/1) to afford 152 mg (0.42 mmol, 73%) of the desired methyl ether **52** as a colorless oil.

$\text{C}_{19}\text{H}_{34}\text{O}_6$; 358.47 $\text{g}\cdot\text{mol}^{-1}$

R_f (Pentane/ AcOEt 4/1) = 0.40

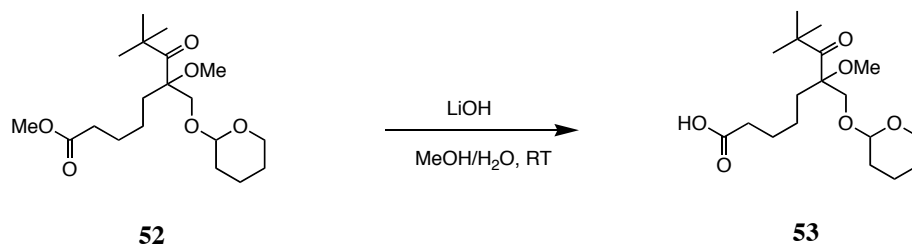
$^1\text{H-NMR}$ (400 MHz, CDCl_3 , δ/ppm):

mixture of both diastereoisomers : 4.59 (dt, 1H, THP); 3.92 (d, $J = 10.6$ Hz, 1H, $\text{CH}_a\text{H}_b\text{OTHP}$); 3.82 (d, $J = 10.6$ Hz, 1H, $\text{CH}_a\text{H}_b\text{OTHP}$); 3.65 (s, 3H, OCH_3 ester); 3.43 (d, $J = 10.6$ Hz, 2H, THP); 3.28 (s, 3H, OCH_3 ether); 2.27 (t, $J = 7.9$ Hz, 2H, H-2); 1.69 -1.47 (m, 12H, 6H, THP, 2 x H-3, 2 x H-4, 2 x H-5); 1.21 (s, 9H, H-9).

$^{13}\text{C-NMR}$ (101 MHz, CDCl_3 , δ/ppm):

mixture of both diastereoisomers: 217.7 (C_q , C-7); 173.9 (C_q , C-1); 99.1 (C_t , THP); 89.9 (C_q , C-6); 69.7 (C_s , CH_2OTHP); 61.5 (C_s , THP); 51.4 (C_p , OCH_3 ester); 49.4 (C_p , OCH_3 ether); 45.1 (C_q , C-8); 33.8 (C_s , C-5); 31.8 (C_s , C-2); 30.7 (C_s , THP); 26.9 (C_p , 3 x C-9); 25.4 (C_s , THP); 25.2 (C_s , C-3); 23.1 (C_s , C-4); 18.8 (C_s , THP).

MS (ESI, MeOH/ CH_2Cl_2 1/1): 381.3 $[\text{M}+\text{Na}]^+$

(rac)-8,8-Dimethyl-6-methoxy-7-oxo-6-[(tetrahydro-2H-pyran-2-yl)oxy] methyl] nonanoic acid (53**)**

Ester **52** (152 mg, 0.42 mmol) was dissolved in a mixture of methanol/H₂O 3/1 (4 ml) and lithium hydroxide (53 mg, 1.27 mmol) was added. The reaction mixture was stirred for 4 h at RT under argon, then concentrated under reduced pressure and chromatographed on a silica gel column (Pentane/AcOEt 1/1 + 0.1 % AcOH) to afford 118 mg (0.34 mmol, 81%) of the acid **53** as a colorless oil.

C₁₈**H**₃₂**O**₆: 344.45 g.mol⁻¹

R_f (Pentane/ AcOEt 1/1) = 0.31

¹**H-NMR** (400 MHz, CDCl₃, δ/ppm):

mixture of both diastereoisomers : 4.56 (dt, 1H, THP); 3.92 (d, *J* = 10.6 Hz, 1H, CH_aH_bOTHP); 3.82 (d, *J* = 10.6 Hz, 1H, CH_aH_bOTHP); 3.43 (d, *J* = 10.8 Hz, 2H, THP); 3.29 (s, 3H, OCH₃ ether); 2.31 (t, *J* = 7.5 Hz, 2H, H-2); 1.72 -1.49 (m, 12H, 6H THP, 2 x H-3, 2 x H-4, 2 x H-5); 1.21 (s, 9H, H-9).

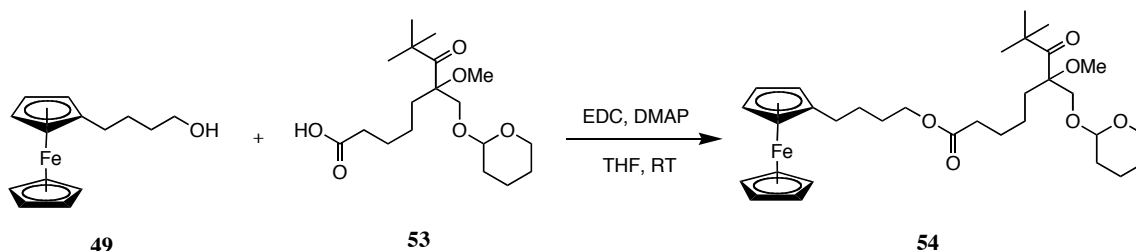
¹³**C-NMR** (101 MHz, CDCl₃, δ/ppm):

mixture of both diastereoisomers : 217.7 (C_q, C-7); 179.1 (C_q, C-1); 98.5 (C_t, THP); 89.9 (C_q, C-6); 69.7 (C_s, CH₂OTHP); 61.5 (C_s, THP); 49.4 (C_p, OCH₃ ether); 45.2 (C_q, C-8); 33.8 (C_s, C-5); 31.8 (C_s, C-2); 30.7 (C_s, THP); 26.9 (C_p, 3 x C-9); 25.4 (C_s, THP); 25.2 (C_s, C-3); 23.1 (C_s, C-4); 18.8 (C_s, THP).

MS (ESI, MeOH/ CH₂Cl₂ 1/1): 367.4 [M+Na]⁺

8.3 Synthesis of the ferrocenyl precursor (42)

(rac)-8,8-Dimethyl-6-methoxy-7-oxo-6-[(tetrahydro-2H-pyran-2-yl)oxy]methyl nonanoic acid-4-(ferrocenyl)butyl ester (54)



To a solution of alcohol **49** (39 mg, 0.15 mmol) and acid **53** (57 mg, 0.165 mmol) in abs. THF (4 ml) EDC (38 mg, 0.2 mmol) and DMAP (9 mg, 0.075 mmol) were added. The mixture was stirred under argon at RT for 17 h and saturated NaHCO₃ solution (10 ml) was added. The mixture was extracted with AcOEt (3 x 10 ml) and the combined organic layers were washed with saturated NH₄Cl solution (2 x 10 ml), dried over MgSO₄ and concentrated under reduced pressure. The crude product was purified by flash chromatography on a silica gel column (Pentane/AcOEt 4/1 v/v) to give 78 mg (0.13 mmol, 89%) of the desired ester **54** as a yellow oil.

C₃₂**H**₄₈**FeO**₆: 584.59 g.mol⁻¹

*R*_f (Pentane/AcOEt 5/1) = 0.34

¹H-NMR (400 MHz, CDCl₃, δ/ppm):

mixture of both diastereoisomers: 4.61 (dt, 1H, THP); 4.08 (s, 5H, Fc); 4.04 (s, 4H, Fc); 3.92 (d, *J* = 10.6 Hz, 1H, CH_aH_bOTHP); 3.83 (d, *J* = 10.6 Hz, 1H, CH_aH_bOTHP); 3.42 (d, *J* = 10.8 Hz, 2H, THP); 3.3 (s, 3H, OCH₃ ether); 2.35 (t, *J* = 7.7 Hz, 2H, H-2); 2.27 (t, *J* = 6.8 Hz, 2H, Fc-CH₂); 1.72 -1.49 (m, 16H, 6H THP, 2 x H-3, 2 x H-4, 2 x H-5, 4 x H CH₂ Fc); 1.23 (s, 9H, H-9).

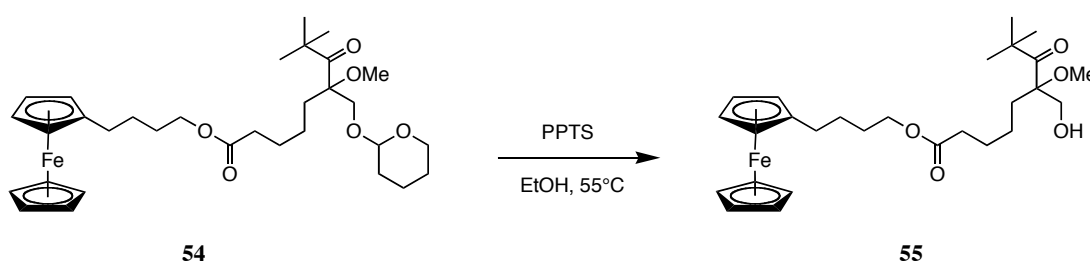
¹³C-NMR (101 MHz, CDCl₃, δ/ppm):

mixture of both diastereoisomers: 217.7 (C_q, C-7); 173.5 (C_q, C-1); 98.6 (C_t, THP); 89.9 (C_q, C-6); 88.7 (C_q, Fc); 69.8 (C_s, CH₂OTHP); 68.5 (C_t, 5 CH Fc); 68.0, 67.1 (C_t, 4 CH Fc); 64.1 (C_s, CH₂OC=O); 61.1 (C_s, THP); 49.4 (C_p, OCH₃ ether); 45.1 (C_q, C-8); 34.1 (C_s, C-5); 32.5 (C_s,

Fc-CH₂); 31.8 (C_s, C-2); 30.4 (C_s, THP); 29.6 (C_s); 27.2 (C_s); 26.9 (C_p, 3 x C-9); 25.4 (C_s, THP); 25.2 (C_s, C-3); 23.2 (C_s, C-4); 18.9 (C_s, THP).

MS (ESI, MeOH/ CH₂Cl₂ 1/1): 584.6 [M]⁺

(rac)-8,8-Dimethyl-6-hydroxymethyl-6-methoxy-7-oxo-nonanoic acid-4-(ferrocenyl)butyl ester (55)



Compound **54** (39 mg, 67 μ mol) was dissolved in ethanol (0.5 ml) together with pyridinium p-toluenesulfonate (2 mg, 7 μ mol) and the reaction mixture was stirred at 55°C for 4 h. The solution was then treated with water (2 ml) and the mixture was extracted with dichloromethene (3 x 5 ml). The combined organic extracts were dried over MgSO₄ and concentrated, yielding an oil that was purified by flash chromatography on silica gel (Pentane/AcOEt 3/1) to give 30 mg (60 μ mol, 90%) of compound **55** as a yellow oil.

C₂₇H₄₀FeO₅: 500.47 g.mol⁻¹

R_f (Pentane/AcOEt 3/1) = 0.31

¹H-NMR (400 MHz, CDCl₃, δ /ppm):

4.09 (s, 5H, Fc); 4.05 (s, 4H, Fc); 3.70 (dd, 2H, CH₂OH); 3.3 (s, 3H, OCH₃ ether); 2.35 (t, *J* = 7.6 Hz, 2H, H-2); 2.28 (t, *J* = 7.4 Hz, 2H, Fc-CH₂); 1.75 -1.50 (m, 10H, 2 x H-3, 2 x H-4, 2 x H-5, 4 x H CH₂ Fc); 1.22 (s, 9H, H-9).

$^{13}\text{C-NMR}$ (101 MHz, CDCl_3 , δ/ppm):

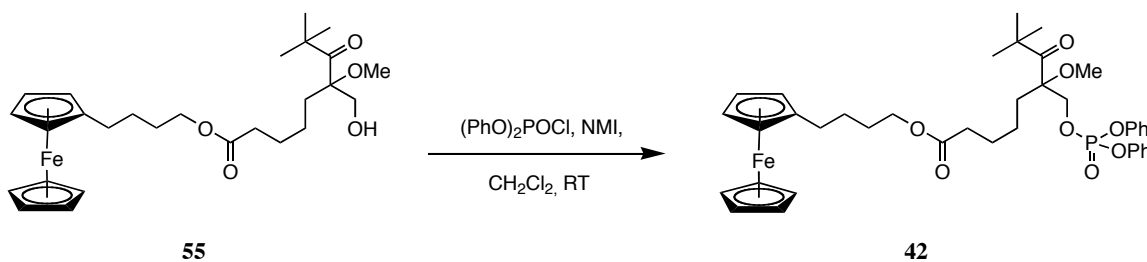
217.9 (C_q , C-7); 173.4 (C_q , C-1); 90.4 (C_q , C-6); 88.7 (C_q ,Fc); 68.7 (C_t , 5 $\underline{\text{C}}\text{H}$ Fc); 67.8 (C_s , $\underline{\text{C}}\text{H}_2\text{OH}$); 65.0 (C_t , 4 $\underline{\text{C}}\text{H}$ Fc); 63.2 (C_s , $\underline{\text{C}}\text{H}_2\text{OC}=\text{O}$); 49.9 (C_p , $\text{O}\underline{\text{C}}\text{H}_3$ ether); 45.2 (C_q , C-8); 34.4 (C_s , C-5); 33.0 (C_s , Fc- $\underline{\text{C}}\text{H}_2$); 32.0 (C_s , C-2); 29.6 (C_s); 27.8 (C_s); 27.2 (C_p , 3 x C-9); 25.6 (C_s , C-3); 23.8 (C_s , C-4).

MS (ESI, MeOH/ CH_2Cl_2 1/1): 500.4 $[\text{M}]^+$

Elemental analysis: calculated: C 61.72, H 4.71, O 7.47

found: C 61.66, H 4.65, O 7.44

(rac)-8,8-Dimethyl-6-methoxy-7-oxo-6-[(diphenylphosphoryloxy)methyl] nonanoic acid-4-(ferrocenyl)butyl ester (42)



To a solution of **55** (15 mg, 30 μmol) and *N*-methylimidazole (14 μl , 180 μmol) in dichloromethane (0.2 ml) under argon was added diphenyl phosphochloridate (16 μl , 75 μmol). The mixture was stirred at RT for 18 h. The reaction was then quenched with a 10% tartaric acid solution in water (2 ml). The aqueous layer was extracted with dichloromethane (3 x 5 ml). The organic phase was dried over MgSO_4 , filtered and the solvent removed under reduced pressure. The residue was purified by column chromatography on silica gel (Pentane/AcOEt 3/1) to afford 20 mg (27 μmol , 91%) of compound **42** as a yellow oil.

$\text{C}_{39}\text{H}_{50}\text{FeO}_8\text{P}$: 732.65 $\text{g}\cdot\text{mol}^{-1}$

R_f (Pentane/AcOEt 3/1) = 0.26

¹H-NMR (400 MHz, CDCl₃, δ/ppm):

7.20 (m, 4H_{ar}, Ph); 7.18 (m, 6H_{ar}, Ph); 4.33 (d, *J* = 4.6 Hz, 2H, CH₂OP); 4.14 (bs, 11H_{ar}, Fc); 3.21 (s, 3H, OCH₃ ether); 2.25 (m, 4H, 2 x H-2, 2 x H Fc-CH₂); 1.55 (m, 10H, 2 x H-3, 2 x H-4, 2 x H-5, 4 x H CH₂ Fc); 1.17 (s, 9H, H-9).

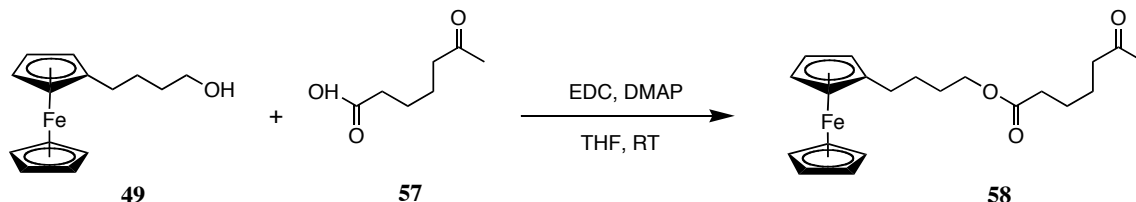
¹³C-NMR (101 MHz, CDCl₃, δ/ppm):

215.6 (C_q, C-7); 173.3 (C_q, C-1); 150.4 (C_q, Ph); 129.8 (C_t, 4 CH_{ar} meta Ph); 125.4 (C_t, 2 CH_{ar} para Ph); 120.05 (C_t, 4 CH_{ar} ortho Ph); 89.0 (C_q, C-6); 88.9 (C_q, Fc); 69.4 (C_t, 9 CH Fc); 69.3 (C_s, CH₂OP); 64.2 (C_s, CH₂O Fc); 49.9 (C_p, OCH₃ ether); 45.2 (C_q, C-8); 33.9 (C_s, C-5); 31.2 (C_s, CH₂ Fc); 29.2 (C_s, C-2); 28.4 (C_s); 27.4 (C_s); 26.8 (C_p, 3 x C-9); 25.1 (C_s, C-3); 23.1 (C_s, C-4).

³¹P-NMR (162 MHz, CDCl₃, δ/ppm):

-15.35

MS (ESI, MeOH/ CH₂Cl₂ 1/1): 755.3 [M + Na]⁺

8.4 Synthesis of the ketone reference (58)**6-Oxoheptanoic acid-4-(ferrocenyl) butyl ester**

To a solution of alcohol **49** (52 mg, 0.2 mmol) and 6-oxoheptanoic acid **57** (35 mg, 0.24 mmol) in abs. THF (5 ml) was added EDC (54 mg, 0.28 mmol) and DMAP (10 mg, 0.08 mmol). The mixture was stirred under argon at RT for 18 h and saturated NaHCO_3 solution (10 ml) was added. The mixture was extracted with AcOEt (3 x 10 ml) and the combined organic layers were washed with saturated NH_4Cl solution (2 x 10 ml), dried over MgSO_4 and concentrated under reduced pressure. The crude product was purified by flash chromatography on a silica gel column (Pentane/AcOEt 3/1) to give 60 mg (0.15 mmol, 78%) of the desired ester **58** as a colorless oil.

$\text{C}_{21}\text{H}_{28}\text{FeO}_3$: 384.31 g.mol⁻¹

R_f (Pentane/AcOEt 3/1) = 0.44

¹H-NMR (400 MHz, CDCl_3 , δ /ppm):

4.08 (s, 5H, Fc); 4.04 (s, 4H, Fc); 2.37 (t, $J = 6.8$ Hz, 2H, CH_2COCH_3); 2.35 (t, $J = 7.6$ Hz, 2H, OCOCH_2); 2.30 (t, $J = 7.1$ Hz, 2H, Fc- CH_2); 2.12 (s, 3H, COCH_3); 1.61 (m, 8H, CH_2).

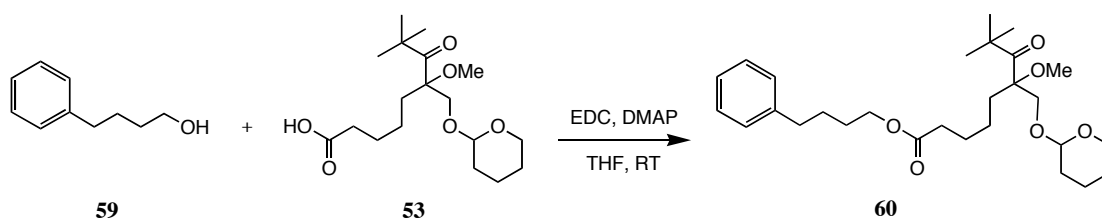
¹³C-NMR (101 MHz, CDCl_3 , δ /ppm):

208.4 (C_q , CO ketone); 173.4 (C_q , CO ester); 88.7 (C_q , Fc); 69.8 (C_s , CH_2OTHP); 68.4 (C_t , 5 CH Fc); 68.0, 67.1 (C_t , 4 CH Fc); 64.2 (C_s , $\text{CH}_2\text{OC=O}$); 43.2 (C_s , CH_2COCH_3); 34.0 (C_s , OCOCH_2); 29.8 (C_t , COCH_3); 29.1 (C_s); 28.5 (C_s , Fc- CH_2); 27.4, 24.4, 23.2 (C_s).

MS (ESI, MeOH/ CH_2Cl_2 1/1): 384.5 [M]⁺

8.5 Synthesis of the phenyl derivatives for the blind test

(rac)-8,8-Dimethyl-6-methoxy-7-oxo-6-[(tetrahydro-2H-pyran-2-yl)oxy]methyl nonanoic acid-4-(phenyl)butyl ester (**60**)



To a solution of 4-phenylbutanol **59** (30 mg, 0.2 mmol) and acid **53** (69 mg, 0.2 mmol) in abs. THF (4 ml) was added EDC (42 mg, 0.22 mmol) and DMAP (12 mg, 0.1 mmol). The mixture was stirred under argon at RT for 17 h and saturated NaHCO₃ solution (10 ml) was added. The mixture was extracted with AcOEt (3 x 10 ml) and the combined organic layers were washed with saturated NH₄Cl solution (2 x 10 ml), dried over MgSO₄ and concentrated under reduced pressure. The crude product was purified by flash chromatography on a silica gel column (Pentane/AcOEt 4/1) to give 58 mg (0.12 mmol, 60%) of the desired ester **60** as a colorless oil.

C₂₈**H**₄₄**O**₆: 476.65 g.mol⁻¹

*R*_f(Pentane/AcOEt 5/1) = 0.31

¹H-NMR (400 MHz, CDCl₃, δ/ppm):

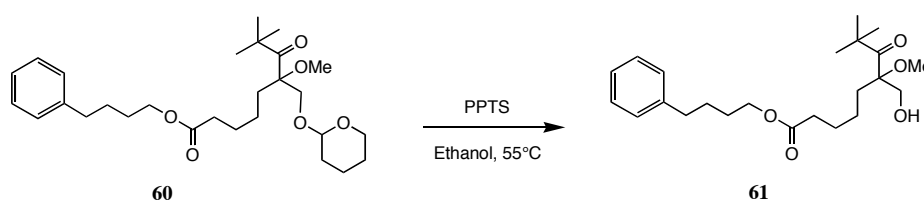
mixture of both diastereoisomers : 7.25 (m, 5H, Ph); 4.61 (dt, 1H, THP); 4.08 (t, *J* = 6.3 Hz, CH₂OC=O); 3.94 (d, *J* = 10.6 Hz, 1H, CH₄H_bOTHP); 3.89 (d, *J* = 10.6 Hz, 1H, CH_aH_bOTHP); 3.42 (d, *J* = 10.7 Hz, 2H, THP) ; 3.24 (s, 3H, OCH₃ ether) ; 2.61 (t, *J* = 6.8 Hz, 2H, Ph-CH₂); 2.26 (t, *J* = 7.7 Hz, 2H, H-2); 1.72 -1.49 (m, 16H, 6H THP, 2 x H-3, 2 x H-4, 2 x H-5, 4 x H Ph linker); 1.20 (s, 9H, H-9).

$^{13}\text{C-NMR}$ (101MHz, CDCl_3 , δ/ppm):

mixture of both diastereoisomers: 217.3 (C_q , C-7); 173.5 (C_q , C-1); 142.0 (C_q , Ph); 128.3, 127.5, 125.8 (C_t , Ph); 98.8 (C_t); 90.0 (C_q , C-6); 69.8 (C_s , CH_2OTHP); 64.1 (C_s , $\text{CH}_2\text{OC=O}$); 61.1 (C_s , THP); 49.6 (C_p , OCH_3 ether); 45.2 (C_q , C-8); 35.4 (C_s , Ph- CH_2); 34.1 (C_s , C-2); 31.7 (C_s , C-5) 28.4 (C_s , THP); 27.7 (C_s , THP); 26.9 (C_p , 3 x C-9); 25.4 (C_s , THP); 25.2 (C_s , C-3); 23.2 (C_s , C-4); 18.9 (C_s , THP).

MS (ESI, MeOH/ CH_2Cl_2 1/1): 476.6 $[\text{M}]^+$

(rac)-8,8-Dimethyl-6-hydroxymethyl-6-methoxy-7-oxo-nonanoic acid-4-(phenyl)butyl ester (61)



Compound **60** (55 mg, 114 μmol) was dissolved in ethanol (1 ml) together with pyridinium p-toulenesulfonate (catalytic amount) and the reaction mixture was stirred at 55°C for 4 h. The solution was then treated with water (2 ml) and the mixture was extracted with dichloromethane (3 x 5 ml). The combined organic extracts were dried over MgSO_4 and concentrated, yielding an oil that was purified by flash chromatography on silica gel (Pentane/AcOEt 4/1) to give 38 mg (97 μmol , 85%) of **61** as a yellow oil.

$\text{C}_{23}\text{H}_{36}\text{O}_5$: 392.53 $\text{g}\cdot\text{mol}^{-1}$

R_f (Pentane/AcOEt 4/1) = 0.18

¹H-NMR (400 MHz, CDCl₃, δ/ppm):

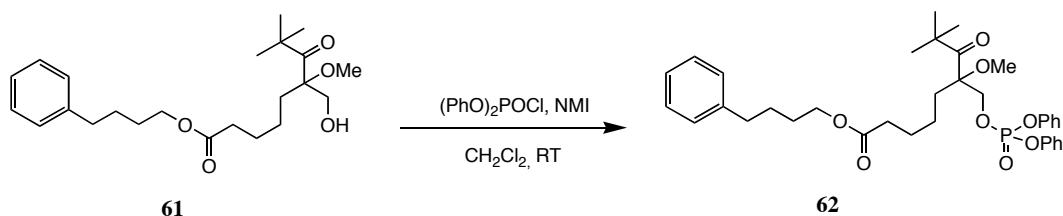
7.25 (m, 5H, Ph); 4.08 (t, *J* = 6.3Hz, CH₂OC=O); 3.68 (dd, 2H, CH₂OH); 3.28 (s, 3H, OCH₃ ether); 2.58 (t, *J* = 7.0 Hz, 2H, Ph-CH₂); 2.32 (t, *J* = 7.5 Hz, 2H, H-2); 1.75 -1.50 (m, 10H, 2 x H-3, 2 x H-4, 2 x H-5, 4 x H Ph linker); 1.22 (s, 9H, H-9).

¹³C-NMR (101 MHz, CDCl₃, δ/ppm):

217.8 (C_q, C-7); 173.4 (C_q, C-1); 142.1 (C_q, Ph); 128.3, 127.4, 125.6 (C_i, Ph); 90.2 (C_q, C-6); 67.9 (C_s, CH₂OH); 63.2 (C_s, CH₂OC=O); 49.9 (C_p, OCH₃ ether); 45.2 (C_q, C-8); 35.4 (C_s, Ph-CH₂); 34.2 (C_s, C-2); 32.0 (C_s, C-5); 27.2 (C_p, 3 x C-9); 25.6 (C_s, C-3); 23.8 (C_s, C-4).

MS (ESI, MeOH/ CH₂Cl₂ 1/1): 415.5 [M+Na]⁺

(rac)-8,8-Dimethyl-6-methoxy-7-oxo-6-[(diphenylphosphoryloxy)methyl] nonanoic acid-4-(phenyl)butyl ester (62)



To a solution of **61** (21 mg, 53 μmol) and *N*-methylimidazole (25 μl, 317 μmol) in dichloromethane (0.5 ml) under argon was added diphenyl phosphochloridate (28 μl, 132 μmol). The mixture was stirred at RT for 18 h. The reaction was then quenched with a 10% tarttric acid solution in water (2 ml). The aqueous layer was extracted with dichloromethane (3 x 5 ml). The organic phase was dried over MgSO₄, filtered and the solvent removed. The residue was purified by column chromatography on silica gel (Pentane/AcOEt 3/1) to afford 21 mg (34 μmol, 65%) of compound **62** as a colorless oil.

C₃₅H₄₆O₈P: 624.71 g.mol⁻¹

R_f (Pentane/AcOEt 3/1) = 0.20

$^1\text{H-NMR}$ (400 MHz, CDCl_3 , δ/ppm):

7.18 (m, 15 H_{ar} , Ph); 4.34 (d, $J = 4.5$ Hz, 2H, CH_2OP); 4.06 (t, $J = 6.4$ Hz, $\text{CH}_2\text{OC}=\text{O}$); 3.21 (s, 3H, OCH_3 , ether); 2.65 (t, $J = 7.0$ Hz, 2H, Ph- CH_2); 2.26 (t, $J = 7.5$ Hz, 2H, H-2); 1.66 (m, 10H, 2 x H-3, 2 x H-4, 2 x H-5, 4 x H Ph linker); 1.16 (s, 9H, H-9).

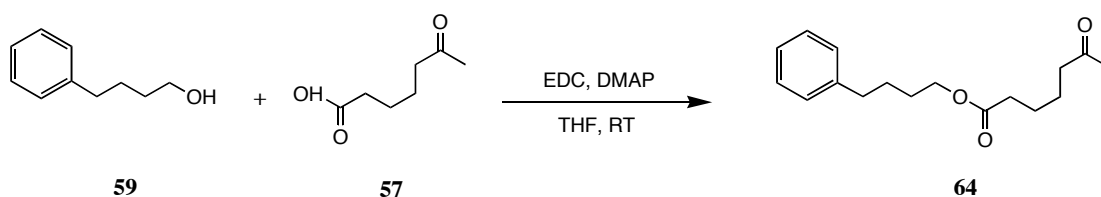
$^{13}\text{C NMR}$ (101 MHz, CDCl_3 , δ/ppm):

217.6 (C_q , C-7); 173.3 (C_q , C-1); 150.4 (C_q , Ph); 142.1 (C_q , Ph); 129.7, 128.4, 127.4, 125.8, 125.4, 120.1 (C_r , Ph); 89.0 (C_q , C-6); 69.3 (C_s , CH_2OP); 64.2 (C_s , $\text{CH}_2\text{OC}=\text{O}$); 49.5 (C_p , OCH_3 , ether); 45.2 (C_q , C-8); 35.4 (C_s , Ph- CH_2); 33.9 (C_s , C-2); 31.2 (C_s , C-5); 26.8 (C_p , 3 x C-9); 25.1 (C_s , C-3); 23.0 (C_s , C-4)

$^{31}\text{P NMR}$ (162 MHz, CDCl_3 , δ/ppm): -15.35

MS (ESI, MeOH/ CH_2Cl_2 1/1): 647.4 $[\text{M} + \text{Na}]^+$

6-Oxo-heptanoic acid-4-(phenyl)butyl ester (**64**)



To a solution of alcohol **59** (45 mg, 0.3 mmol) and 6-oxoheptanoic acid **57** (52 mg, 0.36 mmol) in abs. THF (5 ml) was added EDC (75 mg, 0.39 mmol) and DMAP (18 mg, 0.15 mmol). The mixture was stirred under argon at RT for 18 h and saturated NaHCO_3 solution (10 ml) was added. The mixture was extracted with AcOEt (3 x 10 ml) and the combined organic layers were washed with saturated NH_4Cl solution (2 x 10 ml), dried over MgSO_4 and concentrated. The crude product was purified by flash chromatography on a silica gel column (Pentane/AcOEt 9/1) to give 76 mg (0.27 mmol, 92%) of the desired ester **64** as a colorless oil.

$\text{C}_{17}\text{H}_{24}\text{O}_3$; 276.37 g.mol⁻¹

R_f (Pentane/AcOEt 3/1) = 0.40

¹H-NMR (400 MHz, CDCl₃, δ/ppm):

7.20 (m, 5H_{ar}, Ph); 4.06 (t, $J = 6.4$ Hz, CH₂OC=O); 2.65 (t, $J = 7.0$ Hz, 2H, CH₂COCH₃); 2.45 (t, $J = 6.8$ Hz, 2H, OCOCH₂); 2.29 (t, $J = 7.1$ Hz, 2H, Ph-CH₂); 2.11 (s, 3H, COCH₃); 1.59 (m, 8H, CH₂)

¹³C-NMR (101 MHz, CDCl₃, δ/ppm):

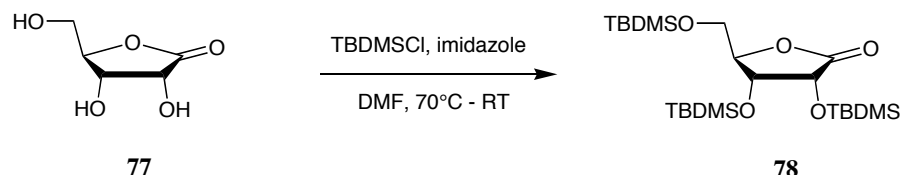
208.4 (C_q, CO ketone); 173.4 (C_q, CO ester); 141.9 (C_q, Ph); 128.3, 125.7 (C_p, Ph); 64.2 (C_s, CH₂OC=O); 43.2 (C_s, CH₂COCH₃); 35.6 (C_s, Ph-CH₂); 34.0 (C_s, OCOCH₂); 29.8 (C_t, COCH₃); 29.1, 27.4, 24.3, 23.1 (C_s)

MS (ESI, MeOH/ CH₂Cl₂ 1/1): 299.3 [M+Na]⁺

9. Synthesis of the phenol nucleoside

9.1 The benzyl approach

3',4',5'-Tris-O-(*tert*-butyldimethylsilyl)-D-ribofuran-1'-one (**78**)



Ribonolactone **77** (3.56 g, 24 mmol) was dissolved in abs. *N,N*-dimethylformamide (50 mL). Imidazole (13.9 g, 204 mmol) as well as *n*-butyldimethylsilylchloride (12.7 g, 82 mmol) were added. The reaction was stirred for 1h at 70°C and then overnight at RT. The reaction mixture was then diluted with diethylether (100 ml) and washed with water (50 ml). The aqueous layer was then extracted with diethylether (2 x 50 ml). The collected organic phase was dried over MgSO₄, filtered and the solvent removed. The residue was crystallized with methanol to give 10.95 g (22.3 mmol, 93%) of compound **78** as white crystals.

$\text{C}_{23}\text{H}_{50}\text{O}_5\text{Si}_3$: 490.90 g.mol⁻¹

R_f (Dichloromethane/Acetone 98/2) = 1

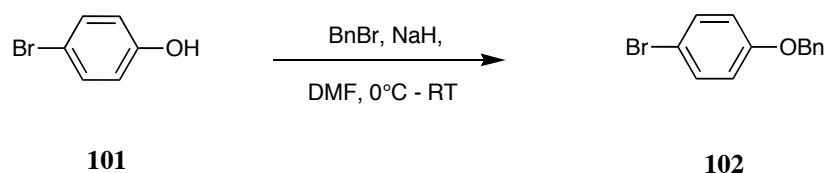
¹H-NMR (300 MHz, CDCl₃, δ/ppm):

4.56 (d, *J* = 4.95 Hz, 1H, H-2'); 4.28 (m, 2H, H-3', H-4'); 3.82 (m, 2H, H-5'); 0.91(m, 27H, *t*-BuSi); 0.01-0.19 (6s, 18H, MeSi).

¹³C-NMR (101 MHz, CDCl₃, δ/ppm):

175.5 (C_q, C=O); 86 (C_t, C-2'); 72.3 (C_t, C-4'); 71 (C_t, C-3'); 62.8 (C_s, C-5'); 26.2 (C_p, 9C, SiC(CH₃)₃); 18.7 (C_q, 3C, SiC(CH₃)₃); -4.17 to -5.3 (C_p, 6C, SiCH₃).

MS (FAB, KCl): 491 [M+H]⁺; 529 [M+K]⁺

1-O-Benzyl-4-bromophenol (102)

4-Bromophenol **101** (1g, 5.78 mmol) was dissolved in dimethylformamide (20 ml) and the temperature was cooled down to 0°C. Sodiumhydride (60% in mineral oil, 277 mg, 6.94 mmol) was added and the reaction mixture was stirred for 15 min. Benzylbromide (0.8 ml, 6.94 mmol) was then added and the ice bath was removed. The reaction mixture was stirred for 15 h under argon at RT. Water (10 ml) was added to destroy the excess of sodiumhydride and the reaction mixture was diluted with diethylether (50 ml) and washed with water (50 ml). The aqueous layer was then extracted with diethylether (3 x 50 ml). The collected organic phase was dried over MgSO₄, filtered and the solvent removed. The residue was crystallized in methanol to give 0,75 g (2.85 mmol, 49%) of compound **102** as white crystals.

C₁₃H₁₁BrO: 263.13 g.mol⁻¹

R_f (Toluene) = 0.77

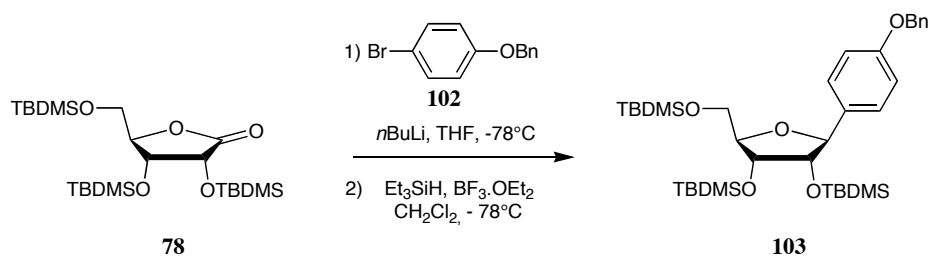
¹H-NMR (400 MHz, CDCl₃ δ/ppm):

7.42-7.31 (m, 7H, H_{ar}); 6.85 (d, *J* = 9.2 Hz, 2H, H_{ar}); 5.28 (s, 2H, CH₂Bn).

¹³C-NMR (101 MHz, CDCl₃, δ/ppm):

159.2, 137.8, 114.2 (C_q, 3 C_{ar}); 133.5, 129.8, 129.3, 128.6, 117.8 (C_t, 9 C_{ar}); 71.1 (C_s, CH₂Bn).

4-*O*-(Benzyl)-1-[3',4',5'-tris-*O*-(*tert*-butyldimethylsilyl)- β -D-ribofuranosyl] phenol (103)



Reaction 1

1-*O*-Benzyl-4-bromophenol **102** (429 mg, 1.63 mmol) was dissolved in THF abs. (10 ml) and the temperature was cooled down to -78°C . *n*-Butyllithium (1 ml, 1.96 mmol) was added and the reaction mixture was stirred for 30 min at -78°C . To the previously prepared solution of aryllithium compound **78** (490 mg, 1 mmol) in THF (10 ml) was added and the reaction mixture was stirred for 1 h at -78°C . The reaction was quenched at -78°C with aqueous saturated NH_4Cl solution (10 ml). The organic layer was diluted with diethylether (50 ml) and washed with saturated NH_4Cl solution (100 ml), then water (100 ml) and brine (100 ml). The organic phase was dried over MgSO_4 , filtered and the solvent removed.

Reaction 2

The thus obtained residue was dissolved in dichloromethane (15 ml), the solution was cooled to -78°C and Et_3SiH (0.48 ml, 3 mmol) as well as $\text{BF}_3\cdot\text{OEt}_2$ (0.39 ml, 3 mmol) were added. The reaction mixture was stirred for 6 h at -78°C . A saturated solution of NaHCO_3 in water was added (10 ml) and the solution was warmed up to RT. The reaction mixture was diluted with diethylether (50 ml) and washed with aqueous saturated NaHCO_3 solution (20 ml), then water (20 ml) and brine (20 ml). The organic phase was dried over MgSO_4 , filtered and the solvent removed. The residue was purified by column chromatography on silica gel (toluene) to give 408 mg (0.62 mmol, 62%) of compound **103** as a colorless oil.

$\text{C}_{36}\text{H}_{62}\text{O}_5\text{Si}_3$: 659.14 g.mol⁻¹

R_f (Toluene) = 0.64

$^1\text{H-NMR}$ (400 MHz, CDCl_3 , δ/ppm):

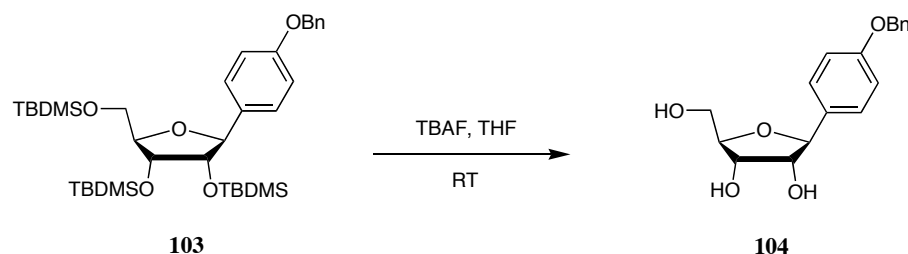
7.44-7.15 (m, 7H, H_{ar}); 6.91 (d, $J = 9.6$ Hz, 2H, H_{ar}); 5.07 (s, 2H, CH_2Bn); 4.71 (d, $J = 7.8$ Hz, 1H, H-1'); 4.12 (dd, $J = 2.0, 4.3$ Hz, 1H, H-3'); 4.00 (m, 1H, H-4'); 3.82 (dd, $J = 4.3, 7.8$ Hz 1H, H-2'); 3.76 (d, $J = 3.8$ Hz, 2H, H-5'); 0.94 (s, 18H, 6Me *t*-BuSi); 1.78 (s, 9H, 3Me *t*-BuSi); 0.11 (m, 12H, 4MeSi); -0.14 (s, 3H, MeSi); -0.44 (s, 3H, MeSi)

$^{13}\text{C-NMR}$ (101 MHz, CDCl_3 , δ/ppm):

158.4, 137.2, 133.1 (C_q , 3 C_{ar}); 128.5, 128.2, 127.8, 127.4 (C_t , 9 C_{ar}); 85.7 (C_i , C-1'); 82.7 (C_i , C-4'); 79.5 (C_i , C-3'); 73.9 (C_i , C-2'); 70 (C_s , CH_2Bn); 63.8 (C_s , C-5'); 25.9 (C_p , 9C, $\text{SiC}(\text{CH}_3)_3$); 18.4, 18.1, 18 (C_q , 3C, $\text{SiC}(\text{CH}_3)_3$); -4.5 (C_p , 6C, SiCH_3)

MS (FAB, KCl): 660 $[\text{M}+\text{H}]^+$; 698 $[\text{M}+\text{K}]^+$

4-*O*-(Benzyl)-1-(β -D-ribofuranosyl)phenol (**104**)



A mixture of **103** (366 mg, 0.55 mmol) and tetrabutylammoniumfluoride (1M in THF, 0.9 ml, 0.9 ml) in THF (15 ml) was stirred at RT for 2 h. A 1N solution of sodiumhydroxide (0.5 ml) was added and the solvent was removed and coevaporated with ethanol. After purification by flash chromatography on silica gel (Dichloromethane/Methanol, gradient to 9/1) 128 mg (0.40 mmol, 74%) pure product **104** was isolated as a white solid.

$\text{C}_{18}\text{H}_{20}\text{O}_5$: 316.35 g.mol⁻¹

R_f (Dichloromethane/Methanol, 95/5) = 0.23

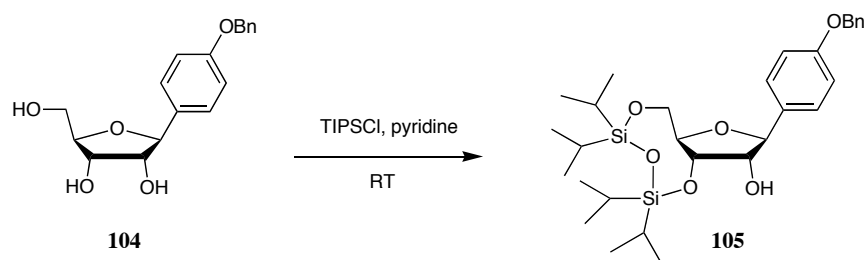
¹H-NMR (400 MHz, CD₃OD δ/ppm):

7.42-7.28 (m, 7H, H_{ar}); 6.95 (d, *J* = 9.6 Hz, 2H, H_{ar}); 5.08 (s, 2H, CH₂Bn); 4.64 (d, *J* = 6.8 Hz, 1H, H-1'); 4.03 (dd, *J* = 4.0, 5.6 Hz, 1H, H-3'); 3.94 (dd, *J* = 4.0, 8.6 Hz 1H, H-4'); 3.85 (dd, *J* = 5.8, 6.8 Hz 1 H, H-2'); 3.73 (m, 2H, H-5').

¹³C-NMR (101 MHz, CD₃OD, δ/ppm):

137.8, 133 (C_q, 2 C_{ar}); 128.5, 127.8, 127.5, 114.8 (C_t, 9 C_{ar}); 85.3 (C_t, C-1'); 84.3 (C_t, C-4'); 77.9 (C_t, C-3'); 72 (C_t, C-2'); 70 (C_s, CH₂Bn); 62.7 (C_s, C-5').

4-*O*-(Benzyl)-1-[3',5'-*O*-(tetraisopropylsilyl)-β-D-ribofuranosyl]phenol (**105**)



Triol **104** (1.55g, 4.90 mmol) was dissolved in dry pyridine (40 ml) and dichloro 1,1',3,3'-tetraisopropyl disiloxane (1.9 ml, 5.88 mmol) was added. The reaction mixture was stirred at RT under argon for 18 h. Methanol was added to quench the reaction and the solvent was co-evaporated with toluene until no more pyridine is detected. The residue was purified by column chromatography on silica gel (Pentane/AcOEt 8/1 + 0.5% Et₃N to afford 2.74 g (4.90 mmol, 100%) of compound **105** as a colorless oil, 2.74 g.

C₃₀H₄₆O₆Si₂: 558.86 g.mol⁻¹

R_f(Pentane/AcOEt 8/1) = 0.28

¹H-NMR (400 MHz, CDCl₃, δ/ppm):

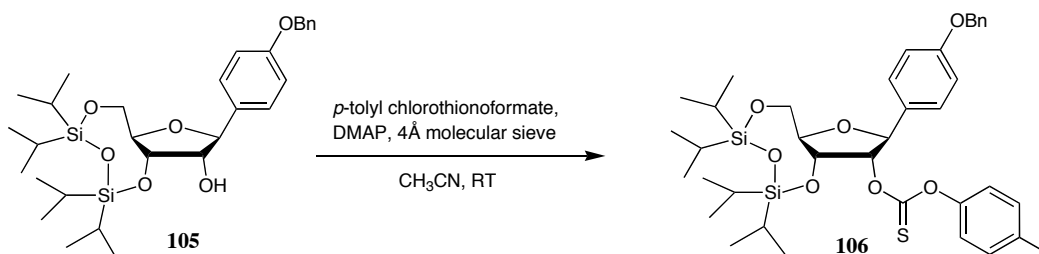
7.34-7.44 (m, 7H, H_{ar}); 6.96 (d, *J* = 8.8 Hz, 2H, H_{ar}); 5.06 (s, 2H, CH₂Bn); 4.80 (d, *J* = 3.8 Hz, 1H, H-1'); 4.39 (dd, *J* = 6.3, 6.6 Hz, 1H, H-3'); 4.00-4.14 (m, 3H, H-2', H-5'); 3.94 (m, 1H, H-4'); 2.99 (d, *J* = 3.8 Hz, 1H, OH); 1.03-1.28 (m, 28 H, 4x(i-Pr)₂Si).

$^{13}\text{C-NMR}$ (101 MHz, CDCl_3 , δ/ppm):

158.3, 137, 132.3 (C_q , 3 C_{ar}); 128.5, 128, 127.4, 127.1, 114.7 (C_t , 9 C_{ar}); 85.6 (C_t , C-1'); 82.8 (C_t , C-4'); 77.6 (C_t , C-3'); 72 (C_t , C-2'); 70.4 (C_s , CH_2Bn); 62.9 (C_s , C-5'); 17.4–16.9 (C_p , 8C, $\text{SiCH}(\underline{\text{C}}\text{H}_3)_2$); 13.3, 13.1, 12.8, 12.6 (C_t , 4C, $\text{SiCH}(\underline{\text{C}}\text{H}_3)_2$).

MS (FAB, KCl): 559 $[\text{M}+\text{H}]^+$; 597 $[\text{M}+\text{K}]^+$

4-O-(Benzyl)-1-[3',5'-O-(tetraisopropylsilyl)-2'-O-(*p*-tolyl thionoformate)- β -D-ribofuranosyl]phenol (106**)**



To a mixture of **105** (2.74 g, 4.90 mmol), 4-dimethylaminopyridine (1.32g, 10.78 mmol) and 4 Å molecular sieve (2 spatules) in acetonitrile (50 ml) was added *p*-tolyl chlorothionoformate (1.185 ml, 7.84 mmol) and the reaction was stirred overnight under argon. The reaction mixture was filtered through celite and the solid was washed with dichloromethane (300 ml). The solvent was evaporated under reduced pressure. The residue was purified by column chromatography on silica gel (Pentane/AcOEt 95/5 + 0.5% Et_3N) to give 2.69 g (3.79 mmol, 77%) of compound **106** as a colorless smelly oil.

$\text{C}_{38}\text{H}_{52}\text{O}_7\text{SSi}_2$: 709.05 $\text{g}\cdot\text{mol}^{-1}$

R_f (Pentane/AcOEt 9:1) = 0,59.

¹H-NMR (400 MHz, CDCl₃, δ/ppm):

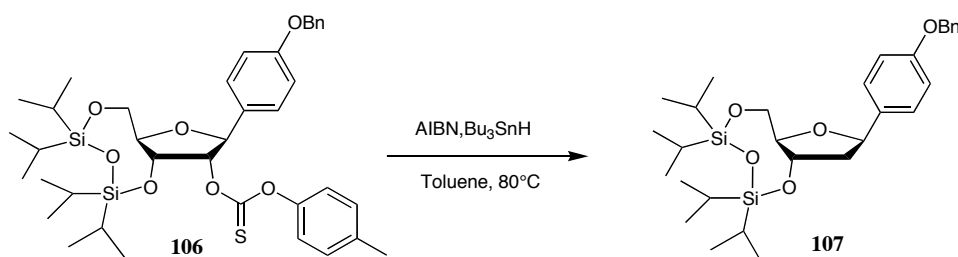
6.87-7.48 (m, 13H, H_{ar}); 5.66 (dd, *J* = 1.6, 4.5 Hz, 1H, H-2'); 5.17 (d, *J* = 1.6 Hz, 1H, H-1'); 5.07 (s, 2H, CH₂Bn); 4.59 (dd, *J* = 4.8, 8.5 Hz, 1H, H-3'); 4.2 (dd, *J* = 3.3, 13.9 Hz, 1H, H-4'); 4.06 (m, 2H, H-5'); 2.37 (s, 3H, CH₃ toluene); 0.82-1.15 (m, 28 H, 2x(i-Pr)₂Si).

¹³C-NMR (101 MHz, CDCl₃, δ/ppm):

194.9 (C_q, C=S); 159.7, 151.6, 136.7, 134.5, 131.5 (C_q, 5 C_{ar}); 130.6, 129.2, 129, 127.7, 127.1, 121.8, 114.2 (C_v, 12 C_{ar}); 88.5 (C_v, C-4'); 83.2 (C_v, C-1'); 82 (C_v, C-2'); 70.9 (C_s, CH₂Bn); 69.5 (C_v, C-3'); 61.2 (C_s, C-5'); 21.4 (C_p, CH₃ toluene); 17.9-17.4 (C_p, 8C, SiCH(CH₃)₂); 13.8-13.1 (C_v, 4C, SiCH(CH₃)₂).

MS (FAB, KCl): 710 [M+H]⁺; 748 [M+K]⁺

4-*O*-(Benzyl)-1-[2'-deoxy-3',5'-*O*-(tetraisopropylsilyl)-β-D-ribofuranosyl] phenol (107)



A solution of **106** (243 mg, 0.342 mmol), Bu₃SnH (134 ml, 0.528 mmol) and AIBN (6 mg, 0.034 mmol) in toluene (5 ml) was degassed and argon was bubbled through the solution for 30 min. The reaction mixture was then stirred at 80°C for 3 h. After the resulting solution was cooled down to RT, ethylacetate was added (30 ml) and the organic layer was washed with 0.1M NaOH solution (30 ml). The aqueous layer was extracted with AcOEt (3 × 30ml). The organic layer was dried over MgSO₄. Removal of solvent followed by column chromatography on silical gel (Pentane/AcOEt 97/3 + 0.5% Et₃N) gave 160 mg (0.295 mmol, 86%) of compound **107** as colorless oil.

$C_{30}H_{46}O_5Si_2$: 542.86 g.mol⁻¹

R_f (Pentane/AcOEt, 9/1)= 0.63

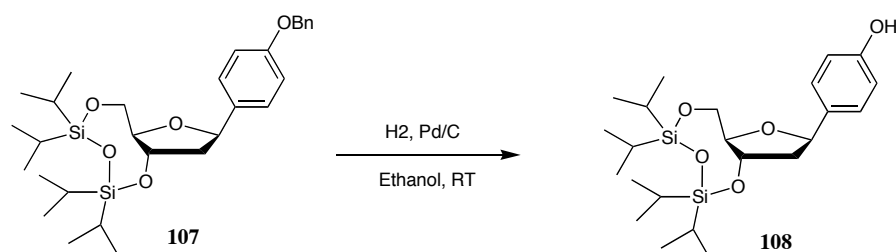
¹H-NMR (400 MHz, CDCl₃, δ/ppm):

7.43-7.27 (m, 7H, H_{ar}); 6.96 (d, $J = 8.8$ Hz, 2H, H_{ar}); 5.06 (s, 2H, CH₂Bn); 5.04 (dd, $J = 7.1$ Hz, 1H, H-1'); 4.56 (m, 1H, H-3'); 4.15 (dd, $J = 2.8, 10.6$ Hz 1H, H-4'); 3.91(m, 2H, H-5'); 2.35 (m, 1H, Ha-2'); 2.08 (m, 1H, Hb-2'); 1.08-1.12 (m, 28 H, 2x(i-Pr)₂Si).

¹³C-NMR (101MHz, CDCl₃, δ/ppm):

158.2, 137, 134.2 (C_q, 3 C_{ar}); 128.5, 128, 127.4, 127.2, 114.7 (C_v, 9 C_{ar}); 86.4 (C_v, C-4'); 78.8 (C_v, C-1'); 73.5 (C_v, C-3'); 69.9(C_s, CH₂Bn); 63.8 (C_s, C-5'); 43.0 (C_s, C-2'); 17.5-17(C_p, 8C, SiCH(CH₃)₂); 13.5, 13.4, 13, 12.5 (C_v, 4C, SiCH(CH₃)₂).

1-[2'-Deoxy-3',5'-O-(tetraisopropylsilyl)-β-D-ribofuranosyl]phenol (108)



To a solution of **107** (160 mg, 0.295 mmol) in ethanol (5 ml) was added palladium on active carbone (catalytic amount) and the reaction mixture was placed under argon. The argon was replaced three times and hydrogen was introduced over the solution. The reaction mixture was stirred for 3 h under hydrogen and then filtered through celite. The solid was washed with AcOEt and the solvent was evaporated. Product **108** was obtained as a colorless oil, 98 mg (0.217 mmol, 74%) and was used without further purification in the next step.

$C_{23}H_{40}O_5Si_2$: 452.74 g.mol⁻¹

R_f (Pentane/AcOEt 80/20) = 0.53

$^1\text{H-NMR}$ (400 MHz, CDCl_3 , δ /ppm):

7.20 (d, $J = 8.6$ Hz, H_{ar}); 6.76 (d, $J = 8.6$ Hz, 2H , H_{ar}); 5.02 (t, $J = 7.3$ Hz, 1 H, H-1'); 4.52 (m, 1H, H-3'); 4.12 (m, 1H, H-4'); 3.87 (m, 2H, H-5'); 2.32 (m, 1H, Ha-2'); 2.07 (m, 1H, Hb-2'); 1.06 (m, 28 H, $2 \times (\text{i-Pr})_2\text{Si}$).

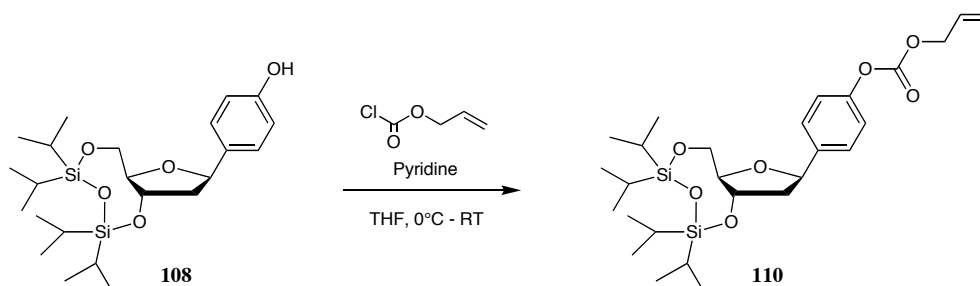
$^{13}\text{C-NMR}$ (101 MHz, CDCl_3 , δ /ppm):

155.1, 133.9 (C_q , 2 C_{ar}); 127.4 (C_t , 2 $\text{C}_{\text{ar-ortho}}$), 115.2 (C_t , 2 $\text{C}_{\text{ar-meta}}$); 86.3 (C_t , C-4'); 78.9 (C_t , C-1'); 73.4 (C_t , C-3'); 63.7 (C_s , C-5'); 43.0 (C_s , C-2'); 17.6-17 (C_p , 8C, $\text{SiCH}(\underline{\text{C}}\text{H}_3)_2$); 13.5, 13.4, 13, 12.5 (C_t , 4C, $\text{SiCH}(\underline{\text{C}}\text{H}_3)_2$).

Elemental analysis: calculated: C 61.02, H 8.91.

found: C 60.72, H 8.87.

4-*O*-(Allyloxycarbonate)-1-[2'-deoxy-3',5'-*O*-(tetraisopropylsilyl)- β -D-ribofuranosyl]phenol (**110**)



To a solution of compound **108** (165 mg, 0.365 mmol) and pyridine (0.5 ml, 0.42 mmol) in THF (4 ml) was added dropwise with vigorous stirring allylchloroformate (46 μl , 0.73 mmol) at 0°C. The temperature was raised up to RT and the reaction mixture was stirred for 2 h and the resulting precipitates were removed by filtration and washed with ether (3 x 15 ml). The filtrate and washings were collected and evaporated. The residue was purified by column chromatography on silica gel (Pentane/AcOEt 9/1) to give 169 mg (0.315 mmol, 86%) of pure product **110** as a colorless oil.

$\text{C}_{27}\text{H}_{44}\text{O}_7\text{Si}_2$: 536.81 $\text{g}\cdot\text{mol}^{-1}$

R_f (Pentane/AcOEt 4/1) = 0.79

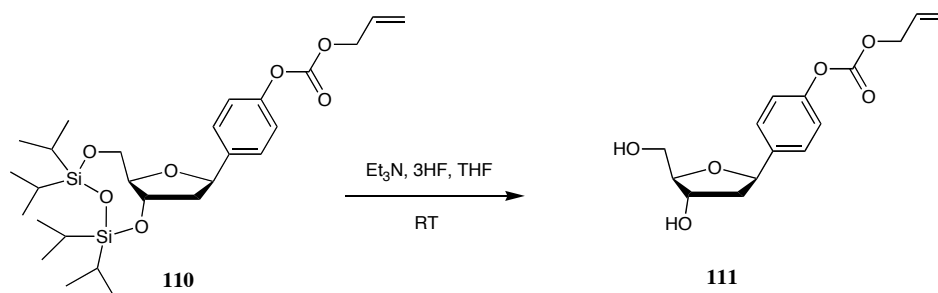
$^1\text{H-NMR}$ (400 MHz, CDCl_3 , δ /ppm):

7.23 (d, $J = 8.56$ Hz, 2H, H_{ar}); 6.82 (d, $J = 8.6$ Hz, 2H, H_{ar}); 6.01 (m, 1H, $\text{H}_{\text{AOC}(2)}$); 5.32 (d, $J = 16.5$ Hz, 1H, $\text{H}_{\text{AOC}(3)}$); 5.25 (d, $J = 11.4$ Hz, 1H, $\text{H}_{\text{AOC}(3')}$); 5.02 (dd, $J = 6$ Hz, 1H, H-1'); 4.68 (d, $J = 5.2$ Hz, 2H, $2\text{H}_{\text{AOC}(1)}$); 4.43 (m, 1H, H-4'); 3.92 (m, 1H, H-3'); 3.73 (m, 2H, H-5'); 2.25 (m, 1H, Ha-2'); 2.02 (m, 1H, Hb-2'); 1.1 (m, 28 H, $2 \times (\text{i-Pr})_2\text{Si}$).

$^{13}\text{C-NMR}$ (101 MHz, CDCl_3 , δ /ppm):

159.1 (C_q , C_{ar}); 154.2 (C_q , C=O); 135.3 (C_q , C_{ar}); 131.4 (C , $\text{C}_{\text{AOC}(2)}$); 128.5 (C_t , 2 $\text{C}_{\text{ar-ortho}}$); 116.9 (C , $\text{C}_{\text{AOC}(3)}$); 115.5 (C_t , 2 $\text{C}_{\text{ar-meta}}$); 88.4 (C_t , C-4'); 80.1 (C_t , C-1'); 74.4 (C_t , C-3'); 69.7 (C_s , $\text{C}_{\text{AOC}(1)}$); 63.8 (C_s , C-5'); 44.2 (C_s , C-2'); 17-17.5 (C_p , 8C, $\text{SiCH}(\underline{\text{C}}\text{H}_3)_2$); 13.6, 13.5, 13, 12.6 (C_p , 4C, $\text{SiCH}(\underline{\text{C}}\text{H}_3)_2$).

4-*O*-(Allyloxycarbonate)-1-(2'-deoxy- β -D-ribofuranosyl)phenol (**111**)



Compound **110** (106 mg, 0.2 mmol) was dissolved in tetrahydrofuran (5 ml) and $\text{Et}_3\text{N} \cdot 3\text{HF}$ (0.33 ml, 2.25 mmol) was added. The solution was stirred at RT, under argon for 16 h. The reaction mixture was cooled down to 0°C and silica gel was added. The solvent was removed under vacuum with water bath at RT. Flash column chromatography on silica gel (Dichloromethane/Methanol, 95/5) gave 50 mg (0.17 mmol, 85 %) of the pure product **111** as colourless oil.

$\text{C}_{15}\text{H}_{18}\text{O}_6$; 294.3 $\text{g} \cdot \text{mol}^{-1}$

R_f (Dichloromethane/Methanol, 95/5) = 0.19

$^1\text{H-NMR}$ (400 MHz, CDCl_3 , δ/ppm):

7.24 (d, $J = 8.6$, 2H, H_{ar}); 6.82 (d, $J = 8.6$ Hz, 2H, H_{ar}); 6.02 (m, 1H, $\text{H}_{\text{AOC}(2)}$); 5.36 (d, $J = 16.6$ Hz, 1 H, $\text{H}_{\text{AOC}(3)}$); 5.25 (d, $J = 11.4$ Hz, 1H, $\text{H}_{\text{AOC}(3')}$); 5.01 (dd, $J = 6$ Hz, 1H, H-1'); 4.68 (d, $J = 5.2$ Hz, 2H, $2\text{H}_{\text{AOC}(1)}$); 4.44 (m, 1H, H-4'); 3.92 (m, 1H, H-3'); 3.73 (m, 2H, H-5'); 2.21 (m, 1H, Ha-2'); 2.02 (m, 1H, Hb-2').

$^{13}\text{C-NMR}$ (101 MHz, CDCl_3 , δ/ppm):

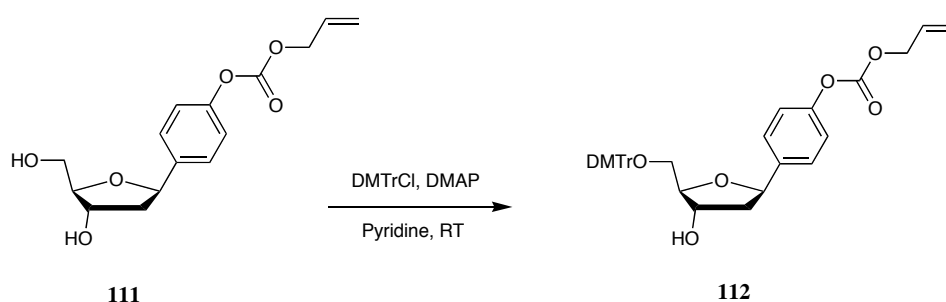
159.5 (C_q , C_{ar}); 153.1 (C_q , C=O); 135.6 (C_q , C_{ar}); 133.2 (C , $\text{C}_{\text{AOC}(2)}$); 128.5 (C_t , 2 $\text{C}_{\text{ar-ortho}}$); 117.1 (C , $\text{C}_{\text{AOC}(3)}$); 115.4 (C_t , 2 $\text{C}_{\text{ar-meta}}$); 88.4 (C_t , C-4'); 80.4 (C_t , C-1'); 74.4 (C_t , C-3'); 69.9 (C_s , $\text{C}_{\text{AOC}(1)}$); 63.9 (C_s C-5'); 44.4 (C_s , C-2').

MS (ESI, MeOH/ CH_2Cl_2 1/1): 317.4 $[\text{M} + \text{Na}]^+$

Elemental analysis: calculated: C 61.22, H 6.16

found: C 61.31, H 6.18

4-*O*-(Allyloxycarbonate)-1-[2'-deoxy-5'-*O*-(dimethoxytrityl)- β -D-ribofuranosyl] phenol (112**)**



Compound **111** (60 mg, 0.2 mmol) was co-evaporated two times with pyridine (3 ml) and then dissolved in pyridine (1.5 ml). 4,4'-Dimethoxytriphenylmethylchloride (98 mg, 0.30 mmol) was added as well as DMAP (5 mg, 0.041 mmol). The mixture was stirred for 2.5 h at RT under argon and methanol (1ml) was added to quench the reaction. Saturated NaHCO₃ solution was added (20 ml) and the aqueous layer was extracted with dichloromethane (3 x 20 ml). The collected organic layer was dried over MgSO₄ and the solvent was removed. The residue was purified by column chromatography on silica gel (Hexane/AcOEt 1/1 + 0.1% Et₃N) to give 79 mg (0.13 mmol, 66%) of pure product **112** as a slightly yellow oil.

C₃₆H₃₆O₈: 596.67 g.mol⁻¹

R_f (Hexane/AcOEt 1/1) = 0.24

¹H-NMR (400 MHz, CDCl₃, δ/ppm):

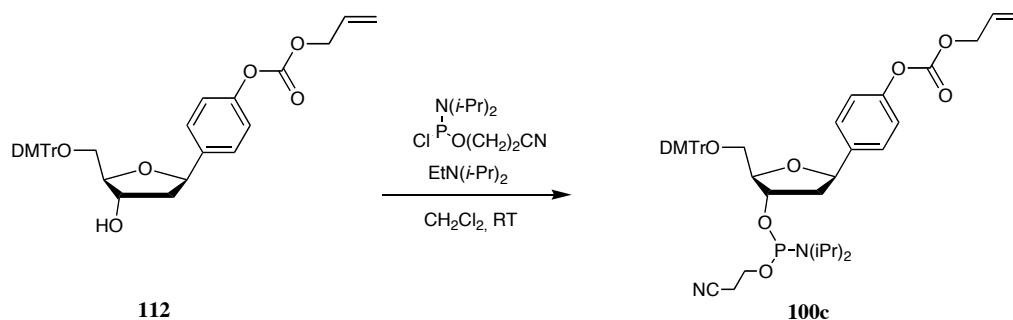
7.16-7.51 (m, 11H, H_{ar}); 7.02 (d, *J* = 8.8 Hz, 2H, H_{ar}); 6.82 (d, *J* = 10.2 Hz, 4H, H_{ar}); 5.93 (m, 1H, H_{AOC(2)}); 5.32 (d, *J* = 16.9 Hz, 1 H, H_{AOC(3)}); 5.24 (d, *J* = 11.5 Hz, 1H, H_{AOC(3')}); 5.08 (dd, *J* = 5.4 Hz, 1 H, H-1'); 4.69 (d, *J* = 5.2 Hz, 2H, 2H_{AOC(1)}); 4.41 (m, 1H, H-4'); 3.96 (m, 1H, H-3'); 3.76 (s, 6H, 2x OCH₃ trityl); 3.71 (m, 2H, H-5'); 2.24 (m, 1 H, Ha-2'); 2.02 (m, 1H, Hb-2'); 1.90 (bs, 1H, OH).

¹³C-NMR (101MHz, CDCl₃, δ/ppm):

159.5 (C_q, C_{ar}); 151.8 (C_q, C=O); 150.8, 146.2, 141.1, 136.1 (C_q, 6C_{ar}); 133.3 (C_t, C_{AOC(2)}); 130.2, 128.6, 128.3, 127.8, 127.3, 121.8, 113.5 (C_t, 17 C_{ar}); 116.4 (C_s, C_{AOC(3)}); 88.8 (C_t, C-4'); 80.7 (C_t, C-1'); 74.3 (C_t, C-3'); 70.1 (C_s, C_{AOC(1)}); 63.9 (C_s, C-5'); 55.5 (C_p, 2x OCH₃ trityl); 44.2 (C_s, C-2').

MS (ESI, MeOH/ CH₂Cl₂ 1/3) : 619.7 [M + Na]⁺

4-*O*-(Allyloxycarbonate)-1-[3'-*O*-(2-cyanoethyl-*N,N*-diisopropyl-phosphoramidite)-2'-deoxy-5'-*O*-(dimethoxytrityl)-β-*D*-ribofuranosyl] phenol (100c**)**



To a solution of **160** (79 mg, 0.13 mmol) and ethyl-diisopropylamine (139 μ l, 0.78 mmol) in CH₂Cl₂ (1.5 ml) under argon was added 2-cyanoethyl-*N,N*-(diisopropyl)chloro-phosphoramidite (104 μ l, 0.46 mmol). The mixture was stirred at RT for 2.5 h. Saturated NaHCO₃ solution was added (10 ml) and the aqueous layer was extracted with dichloromethane (4 x 25 ml). The collected organic layer was dried over MgSO₄ and the solvent was removed. The residue was purified by column chromatography on silica gel (hexane/AcOEt gradient 8/2 to 5/5 + 0.1% Et₃N) to give 70 mg (0.088 mmol, 67%) of the pure phosphoramidite **100c** as a colorless oil.

C₄₅H₅₃N₂O₉P: 796.89 g.mol⁻¹

R_f(Hexane/AcOEt 1/1) = 0.57

¹H-NMR (400 MHz, CDCl₃, δ /ppm):

mixture of both diastereoisomers: 7.18-7.50 (m, 11H, H_{ar}); 7.02 (d, *J* = 8.8 Hz, 2H, H_{ar}); 6.81 (d, *J* = 10.3 Hz, 4H, H_{ar}); 5.94 (m, 1H, H_{AOC(2)}); 5.29 (d, *J* = 16.8 Hz, 1 H, H_{AOC(3)}); 5.22 (d, *J* = 11.5 Hz, 1H, H_{AOC(3')}); 5.11 (dd, *J* = 5.5, 10.4 Hz, 1H, H-1'); 4.69 (d, *J* = 5.2 Hz, 2H, 2H_{AOC(1)}); 4.50 (m, 1H, H-4'); 4.02 (m, 1H, H-3'); 3.76 (s, 6H, 2x OCH₃ trityl); 3.25-3.66 (2m, 4H, H-5', CH₂CN); 2.46-2.62 (m, 2H, N(CH₂(CH₃)₂)); 2.18 (m, 1H, H_a-2'); 1.98 (m, 1H, H_b-2'); 1.16-1.28 (m, 12H, N(CH₃)₂).

^{13}C -NMR (101 MHz, CDCl_3 , δ/ppm):

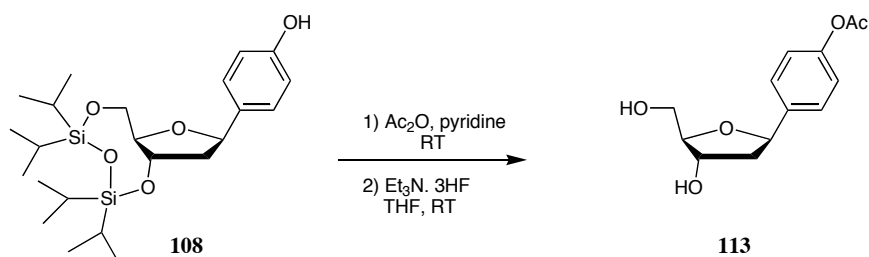
mixture of both diastereoisomers: 159.1 (C_q , C_{ar}); 152.4 (C_q , $\text{C}=\text{O}$); 150.4, 145.8, 140.7, 136.1 (C_q , 6C_{ar}); 133.5 (C_t , $\text{C}_{\text{AOC}(2)}$); 130.4, 128.6, 128.3, 127.5, 127.2, 121.6, 113.5 (C_t , 17C_{ar}); 116.3 (C_s , $\text{C}_{\text{AOC}(3)}$); 88.1 (C_t , $\text{C}-4'$); 80.5 (C_t , $\text{C}-1'$); 74.8 (C_t , $\text{C}-3'$); 70.2 (C_s , $\text{C}_{\text{AOC}(1)}$); 64.7 (C_s , $\text{C}-5'$); 58.9 (C_s , CH_2OP); 55.6 (C_p , $2\times\text{OCH}_3$ trityl); 44.3 (C_s , $\text{C}-2'$); 43.4 (C_t , 2C , $\text{N}(\text{CH}(\text{CH}_3)_2)$); 20.8, 20.6, 20.5, 20.4 (C_p , 4C , $\text{N}(\text{CH}(\text{CH}_3)_2)$); 18.4 (C_s , CH_2CN).

^{31}P -NMR (162MHz, CDCl_3 , δ/ppm):

mixture of both diastereoisomers: 145.3, 147.7

MS (ESI, $\text{MeOH}/\text{CH}_2\text{Cl}_2$ 1/1): 819.6 $[\text{M} + \text{Na}]^+$

4-O-(Acetyl)-1-(2'-deoxy- β -D-ribofuranosyl)phenol (113)



Reaction1

Compound **108** (75 mg, 0,17 mmol) was dissolved in a mixture pyridine/acetic anhydride, 1/1, v/v (2ml) and the reaction mixture was stirred for 2 h. Methanol was added to quench the reaction and the solvent was co-evaporated with toluene until no more pyridine is detected. The thus obtained residue was used without further purification.

Reaction2

The crude residue was dissolved in tetrahydrofuran (5 ml) and $\text{Et}_3\text{N}\cdot 3\text{HF}$ (0.25 ml, 1.7 mmol) was added. The solution was stirred at RT, under argon overnight. The reaction mixture was cooled down to 0°C and silica gel was added. The solvent was removed under reduced pressure.

Flash column chromatography on silica gel (Dichloromethane/Methanol, 95/5) gave 35 mg (0.139 mmol, 97%) of the pure product **113** as white oily solid.

$C_{11}H_{14}O_4$: 210.23 g.mol⁻¹

R_f (Dichloromethane/Methanol 95/5) = 0.23

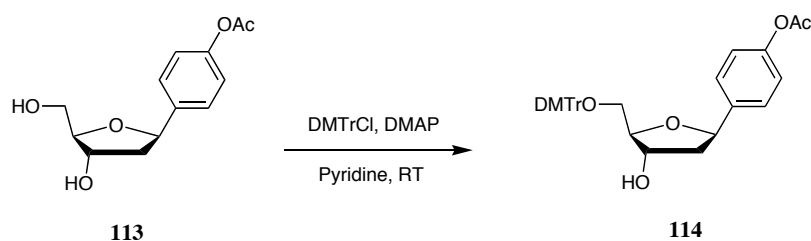
¹H-NMR (400 MHz, CDCl₃, δ/ppm):

7.34 (d, $J = 9$ Hz, 2H, H_{ar}); 7.07 (d, $J = 8.9$ Hz, 2H, H_{ar}); 5.14 (dd, $J = 5.6, 10.1$ Hz, 1 H, H-1'); 4.38 (m, 1H, H-3'); 3.97 (m, 1H, H-4'); 3.79 (m, 2H, H-5'); 2.64 (bs, 1H, OH); 2.42 (bs, 1H, OH); 2.29 (s, 3H, CH₃ acetate); 2.21 (m, 1H, Ha-2'); 1.98 (m, 1H, Hb-2').

¹³C-NMR (101 MHz, CDCl₃, δ/ppm):

170.08 (C_q, C=O); 150.5, 139.3 (C_q, 2 C_{ar}); 127.6 (C_v, 2 C_{ar-ortho}); 122 (C_v, 2 C_{ar-meta}); 87.7 (C_t, C-4'); 80.0 (C_t, C-1'); 74.0 (C_t, C-3'); 63.8 (C_s, C-5'); 44.2 (C_s, C-2'); 21.5 (C_p, CH₃ acetate).

4-*O*-(Acetyl)-1-[2'-deoxy-5'-*O*-(dimethoxytrityl)-β-D-ribofuranosyl]phenol (**114**)



113 (35 mg, 0.167 mmol) was co-evaporated two times with pyridine (2 ml) and then dissolved in pyridine (2 ml). 4,4'-Dimethoxytriphenylmethylchloride (79 mg, 0.23 mmol) was added as well as DMAP (4 mg, 0.033 mmol). The mixture was stirred for 2.5 h at RT under argon. The reaction was quenched by addition of methanol (1 ml). Saturated NaHCO₃ solution was added (2 ml) and the aqueous layer was extracted with dichloromethane (3x10 ml). The collected organic layer was dried over MgSO₄ and the solvent was removed. The residue was purified by column chromatography on silica gel (Pentane/AcOEt 7/3 + 0.1% Et₃N to 5/5 + 0.1% Et₃N) to give 59 mg (0.11 mmol, 66%) of pure product **114** as a white oily residue.

$C_{34}H_{34}O_7$: 554.64 g.mol⁻¹

R_f (Pentane/AcOEt 2/1) = 0.13

¹H-NMR (400 MHz, CDCl₃, δ/ppm):

7.18-7.49 (m, 11H, H_a); 7.04 (d, J = 8.9 Hz, 2H, H_{ar}); 6.81 (d, J = 10.3 Hz, 4H, H_{ar}); 5.16 (dd, J = 5.6, 10.1 Hz, 1H, H-1'); 4.41 (m, 1H, H-3'); 4.06 (m, 1H, H-4'); 3.78 (s, 6H, 2x OCH₃ trityl); 3.35 (dd, J = 4.5, 9.9 Hz, 1H, H-5'a); 3.26 (dd, J = 5.3, 9.8 Hz, 1H, H-5'b); 2.27 (s, 3H, CH₃ acetate); 2.21 (m, 1H, Ha-2'); 2.01 (m, 1H, Hb-2'); 1.92 (bs, 1H, OH).

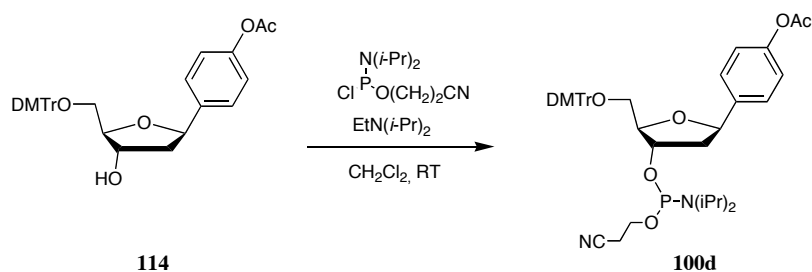
¹³C-NMR (101MHz, CDCl₃, δ/ppm):

170 (C_q, C=O); 158.9; 150.3, 145.2, 139.8, 136.4 (C_q, 7C_{ar}); 130.5, 128.6, 128.3, 127.5, 127.3, 121.8, 113.5 (C_i, 17 C_{ar}); 86.7 (C_i, C-4'); 79.9 (C_i, C-1'); 75.0 (C_i, C-3'); 64.8 (C_s, C-5'); 55.6 (C_p, 2x OCH₃ trityl); 44.3 (C_s, C-2'); 21.6 (C_p, CH₃ acetate).

MS (ESI, MeOH/ CH₂Cl₂ 1/3): 577.3 [M + Na]⁺

Elemental analysis: calculated: C 73.63, H 6.18
found: C 73.36, H 6.37

4-O-(Acetyl)-1-[3'-O-(2-cyanoethyl-*N,N*-diisopropylphosphoramidite)-2'-deoxy-5'-O-(dimethoxytrityl)-β-D-ribofuranosyl]phenol (100d)



To a solution of **161** (59 mg, 0.106 mmol) and ethyl-diisopropylamine (75 μl, 0.425 mmol) in CH₂Cl₂ (2 ml) under argon was added 2-cyanoethyl-*N,N*-(diisopropyl)chloro-phosphoramidite (60

μl , 0.265 mmol). The mixture was stirred at RT for 1.5 h. The reaction mixture was then added directly to a silica gel chromatography column (Pentane/AcOEt 2/1) to give 60 mg (0.080 mol, 75%) of the pure phosphoramidite **100d** as a white foam.

$\text{C}_{43}\text{H}_{51}\text{N}_2\text{O}_8\text{P}$: 754.86 g.mol⁻¹

R_f (Pentane/AcOEt 2/1) = 0.4

¹H-NMR (400 MHz, CDCl₃, δ /ppm):

mixture of both diastereomer: 7.18-7.50 (m, 11H, H_{ar}); 7.02 (d, $J = 8.9$ Hz, 2H, H_{ar}); 6.81 (d, $J = 10.3$ Hz, 4H, H_{ar}); 5.18 (dd, $J = 5.5, 10.2$ Hz, 1 H, H-1'); 4.52 (m, 1H, H-3'); 4.11 (m, 1H, H-4'); 3.78 (s, 6H, 2x OCH₃, trityl); 3.22-3.58 (2m, 4H, H-5', CH₂CN); 2.48-2.63 (m, 2H N(CH(CH₃)₂)); 2.28 (s, 3H, CH₃ acetate); 2.20 (m, 1H, Ha-2'); 2.00 (m, 1H, Hb-2'); 1.17-1.28 (m, 12H N(CH(CH₃)₂)).

¹³C-NMR (101MHz, CDCl₃, δ /ppm):

mixture of both diastereoisomers: 170.1 (C_q, C=O); 158.9, 150.4, 145.3, 139.8, 136.4 (C_q, 7C_{ar}); 130.4, 128.7, 128.3, 127.5, 127.3, 121.8, 113.4 (C_t, 17 C_{ar}); 119.9 (C_q, CN); 86.7 (C_t, C-4'); 80.0 (C_t, C-1'); 75.1 (C_t, C-3'); 64.8 (C_s, C-5'); 58.8 (C_s, CH₂OP); 55.6 (C_p, 2x OCH₃, trityl); 44.3 (C_s, C-2'); 43.8 (C_t, 2C, N(CH(CH₃)₂)); 21.6 (C_p, CH₃ acetate); 20.8, 20.7, 20.6, 20.5 (C_p, 4C, N(CH(CH₃)₂)); 18.2 (C_s, CH₂CN).

³¹P NMR (162, CDCl₃, δ /ppm):

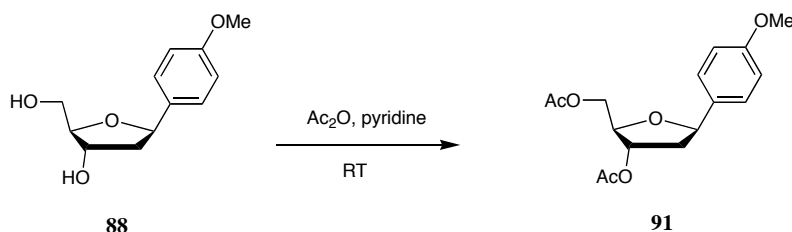
mixture of both diastereoisomers: 147.9, 149.9

MS (ESI, MeOH/ CH₂Cl₂ 1/1): 777.5 [M + Na]⁺

9.2 The methoxy approach

The synthesis of compound **88** was already described in the literature¹⁴³

1-[2'-Deoxy-3', 5'-O-(diacetyl)- β -D-ribofuranosyl]anisole (**91**)



Compound **88** (172 mg, 0.8 mmol) was dissolved in a mixture of pyridine/acetic anhydride, 1/1 (4 ml) and the solution was stirred for 4 hrs at RT under argon. The reaction mixture was then cooled down to 0°C and methanol was added. The solvent was evaporated and co-evaporated with toluene (3 x 5 ml) until no more pyridine is detected to give 236 mg (0.77 mmol, 96 %) of **91** a colorless oil was used without further purification.

$C_{16}H_{20}O_6$; 308.33 g.mol⁻¹

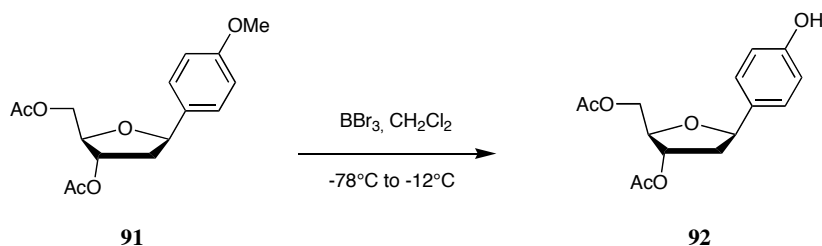
R_f (Hexane/AcOEt 7/3) = 0.46

¹H-NMR (400 MHz, CDCl₃, δ /ppm):

7.27 (d, J = 8.5 Hz, 2H, H_{ar}); 6.88 (d, J = 8.5 Hz, 2H, H_{ar}); 5.21 (d, J = 6.3 Hz, 1 H, H-1'); 5.04 (dd, J = 5.1, 10.8 Hz, 1H, H-3'); 4.36 (dd, J = 3.76, 11 Hz, 1H, H-4'); 4.25 (m, 2H, H-5'); 3.8 (s, 3H, CH₃, OMe); 2.38 (dd, J = 5.1, 6.4 Hz, 1H, Ha-2'); 2.11 (s, 3H, CH₃ acetate); 2.08 (s, 3H, CH₃ acetate); 2.04 (m, 1H, Hb-2').

¹³C-NMR (101MHz, CDCl₃, δ /ppm):

171.0, 170.8 (C_q, 2 x C=O); 159.2, 132.6 (C_q, 2 C_{ar}); 128.1 (C_t, 2 C_{ar}-ortho); 114.3 (C_t, 2 C_{ar}-meta); 82.9 (C_t, C-1'); 80.8 (C_t, C-4'); 76.8 (C_t, C-3'); 65.0 (C_s, C-5'); 55.9 (C_p, OCH₃); 41.7 (C_s, C-2'); 21.8, 21.4 (C_p, 2 x CH₃ acetate).

1-[2'-Deoxy-3', 5'-O-(diacetyl)- β -D-ribofuranosyl]phenol (92)

Compound **91** (530 mg, 1.72 mmol) was dissolved in anhydrous dichloromethane (30 ml) and the temperature was cooled down to -78°C . A 1M solution of BBr_3 in dichloromethane (17.2 ml, 17.2 mmol) was added slowly and the reaction mixture was stirred for 30 min at -78°C under argon. The temperature was raised up to -12°C and the reaction mixture was stirred again for 6 h. Diethylether (10 ml) was added very slowly at -12°C and then water (50 ml) also at -12°C . The mixture was stirred for 30 min and allowed to come back to RT. The aqueous layer was extracted with dichloromethane (3 x 30 ml). The collected organic phase was dried over MgSO_4 , filtered and the solvent removed. The residue was purified by column chromatography on silica gel (Pentane/AcOEt 1/1) to give 430 mg (1.462 mmol, 85 %) of compound **92** as a colorless oil.

$\text{C}_{15}\text{H}_{18}\text{O}_6$; 294.30 g.mol $^{-1}$

R_f (Pentane/AcOEt 1/1) = 0.25

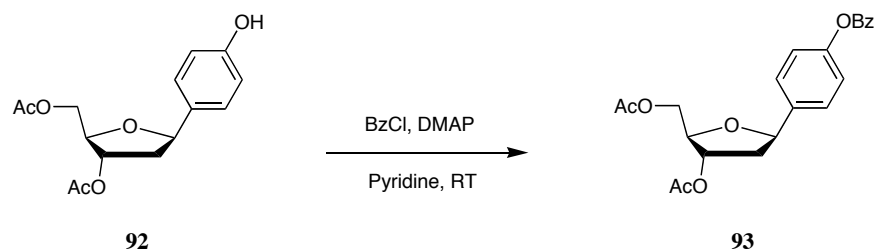
$^1\text{H-NMR}$ (400 MHz, CDCl_3 , δ /ppm):

7.17 (d, $J = 8.5$ Hz, 2H, H_{ar}); 7.07 (d, $J = 8.5$ Hz, 2H, H_{ar}); 6.47 (bs, 1H, OH); 5.20 (d, $J = 6.3$ Hz, 1H, H-1'); 5.02 (dd, $J = 5.0, 10.9$ Hz, 1H, H-3'); 4.37 (dd, $J = 3.8, 11$ Hz, 1H, H-4'); 4.22 (m, 2H, H-5'); 2.38 (dd, $J = 5.1, 6.4$ Hz, 1H, $\text{H}_{\text{a-2'}}$); 2.13 (s, 3H, CH_3 acetate); 2.10 (s, 3H, CH_3 acetate); 2.02 (m, 1H, $\text{H}_{\text{b-2'}}$).

$^{13}\text{C-NMR}$ (101MHz, CDCl_3 , δ /ppm):

171.1, 170.8 (C_{q} , 2 x C=O); 155.9, 131.6 (C_{q} , 2 C_{ar}); 127.4 (C_{t} , 2 $\text{C}_{\text{ar-ortho}}$); 115.3 (C_{t} , 2 $\text{C}_{\text{ar-meta}}$); 82.3 (C_{t} , C-1'); 80.5 (C_{t} , C-4'); 75.6 (C_{t} , C-3'); 64.3 (C_{s} , C-5'); 40.9 (C_{s} , C-2'); 21, 20.9 (C_{p} , 2 x CH_3 acetate).

MS (ESI, MeOH/ CH_2Cl_2 1/1): 317.2 $[\text{M} + \text{Na}]^+$

4-(*O*-Benzoyl)-1-[2'-deoxy-3', 5'-*O*-(diacetyl)- β -D-ribofuranosyl]phenol (93**)**

Compound **92** (49 mg, 0.17 mmol) was dissolved in pyridine (2 ml) and DMAP (catalytic amount) was added as well as benzoylchloride (25 μ l, 0.20 mmol). The reaction mixture was stirred for 18 h at RT under argon and methanol (2 ml) was added. The solvents were evaporated and co-evaporated with toluene (4 x 5 ml) and dichloromethane (5 ml). The residue was purified by preparative Thin Layer Chromatography (TLC) (Hexane/AcOEt 7/3) to give 51 mg (0.128 mmol, 77%) of compound **93** as a colorless oil.

$C_{22}H_{22}O_7$; 398.41g.mol⁻¹

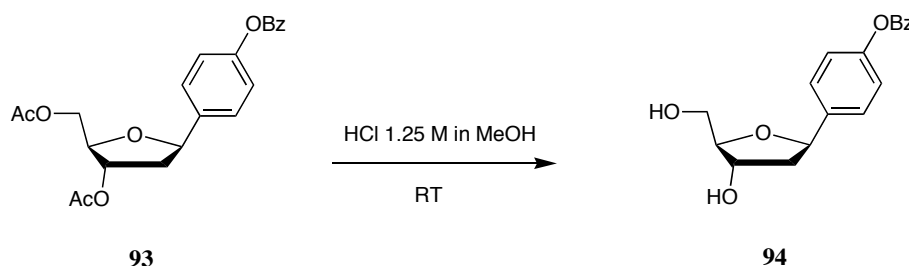
R_f (Hexane/AcOEt 7/3) = 0.33

¹H-NMR (400 MHz, CDCl₃, δ /ppm):

7.38 – 8.15 (m, 5H, H_{ar} benzoyl); 7.21 (d, $J = 8.6$ Hz, 2H, H_{ar}); 7.06 (d, $J = 8.6$ Hz, 2H, H_{ar}); 5.18 (d, $J = 6.8$ Hz, 1H, H-1'); 5.02 (dd, $J = 5, 10.7$ Hz, 1H, H-3'); 4.39 (dd, $J = 4.4, 10.2$ Hz, 1H, H-4'); 4.25 (m, 2H, H-5'); 2.39 (dd, $J = 5.0, 6.6$ Hz, 1H, Ha-2'); 2.13 (s, 3H, CH₃ acetate); 2.11 (s, 3H, CH₃ acetate); 2.06 (m, 1H, Hb-2').

¹³C-NMR (101MHz, CDCl₃, δ /ppm):

171.2, 170.8 (C_q, 2 x C=O acetate); 166.1 (C_q, 2 x C=O benzoyl); 155.8, 131.5, 130.4 (C_q, 3C_{ar}); 134.8 (C_t, C_{ar}); 131 (C_t, 2C_{ar}); 129.1 (C_t, 2C_{ar}); 127.4 (C_t, 2 C_{ar}-ortho); 115.2 (C_t, 2 C_{ar}-meta); 82.2 (C_t, C-1'); 80.5 (C_t, C-4'); 75.7 (C_t, C-3'); 63.9 (C_s C-5'); 40.6 (C_s, C-2'); 21, 20.7 (C_p, 2 x CH₃ acetate).

4-(*O*-Benzoyl)-1-(2'-deoxy- β -D-ribofuranosyl)phenol (94**)**

Compound **93** (85 mg, 0.21 mmol) was dissolved in a solution of 1.25 M HCl in methanol (1 ml) and the reaction mixture was stirred for 4 h under argon at RT. The solvent was evaporated and the residue was purified by column chromatography on silica gel (Dichloromethane/Methanol 95/5) to give 57 mg (0.18 mmol, 85 %) of compound **94** as a colorless oil.

$C_{18}H_{18}O_5$: 314.34 g.mol⁻¹

R_f (Dichloromethane/Methanol 95/5) = 0.28

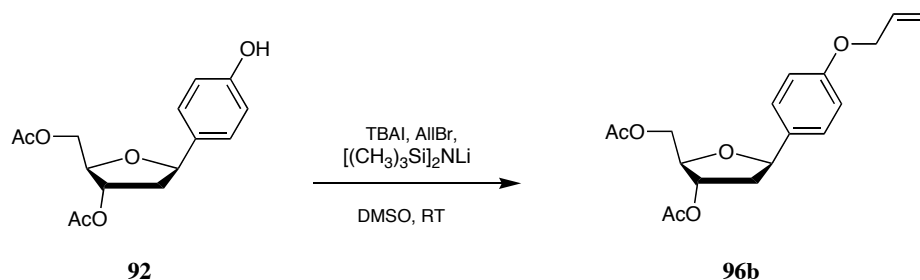
¹H-NMR (400 MHz, CDCl₃, δ/ppm):

7.40 – 8.15 (m, 5H, H_{ar} benzoyl); 7.19 (d, $J = 8.6$ Hz, 2H, H_{ar}); 7.08 (d, $J = 8.6$ Hz, 2H, H_{ar}); 5.16 (d, $J = 6.8$ Hz, 1 H, H-1'); 5.02 (dd, $J = 5.2, 11$ Hz, 1H, H-3'); 4.38 (dd, $J = 4.4, 10.3$ Hz, 1H, H-4'); 4.22 (m, 2H, H-5'); 2.38 (dd, $J = 5.1, 6.6$ Hz, 1H, Ha-2'); 2.06 (m, 1H, Hb-2'); 2.0 (2bs, 2H, 2 x OH).

¹³C-NMR (101 MHz, CDCl₃, δ/ppm):

166 (C_q, 2 x C=O benzoyl); 155.8, 131.4, 130.2 (C_q, 3C_{ar}); 134.6 (C_t, C_{ar}); 131 (C_t, 2C_{ar}); 129.1 (C_t, 2C_{ar}); 127.5 (C_t, 2C_{ar}-ortho); 115.4 (C_t, 2 C_{ar}-meta); 82.6 (C_t, C-1'); 80.5 (C_t, C-4'); 74.9 (C_t, C-3'); 62.8 (C_s, C-5'); 40.6 (C_s, C-2').

MS (ESI, MeOH/ CH₂Cl₂ 1/1): 337.8 [M + Na]⁺

4-(*O*-Allyl)-1-[2'-deoxy-3', 5'-*O*-(diacetyl)- β -D-ribofuranosyl]phenol (96b**)**

To a solution of **92** (94 mg, 0.32 mmol) and tetrabutyl ammonium iodide (130 mg, 0.35 mmol) in DMSO (2 ml) was added allyl bromide (34 μ l, 0.41 mmol). The reaction mixture was stirred for 5 min under argon at RT. While the solution was vigorously stirred, lithium bis(trimethylsilyl)amide (320 μ l, 1.7 mmol) was added at once. The reaction was complete within 45 min. The yellow reaction mixture was then diluted with AcOEt (30 ml) and washed with 1N HCl (2 x 20 ml), saturated NaHCO₃ (2 x 20 ml), water (2 x 20 ml) and saturated brine (20 ml). The organic phase was then dried over MgSO₄ and filtered. The filtrate was evaporated under reduced pressure containing a mixture of the α -anomer **96a** and the β -anomer **96b**. These anomers were separated by column chromatography on silica gel (Pentane/AcOEt 3/1). The desired β -compound **96b** was isolated as a colorless oil, 70 mg (0.21 mmol, 65 %).

C₁₈H₂₂O₆; 334.36 g.mol⁻¹

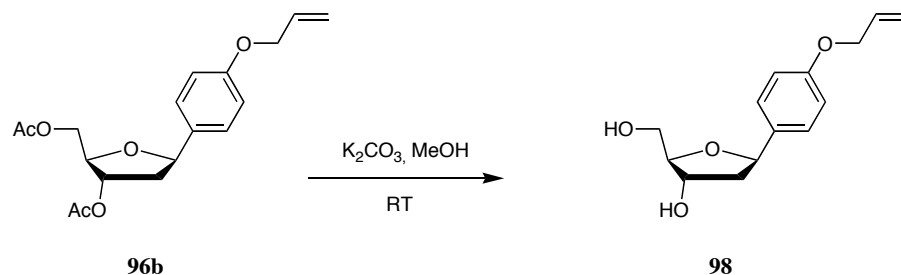
R_f (Pentane/AcOEt 3/1) = 0.22

¹H-NMR (400 MHz, CDCl₃, δ /ppm):

7.27 (d, *J* = 8.5 Hz, 2H, H_{ar}); 6.89 (d, *J* = 8.6 Hz, 2H, H_{ar}); 6.06 (m, 1H, H_{all(2)}); 5.42 (d, *J* = 16.8 Hz, 1 H, H_{all(3)}); 5.26 (d, *J* = 10.4 Hz, 1H, H_{all(3')}); 5.20 (m, 1 H, H-1'); 5.05 (dd, *J* = 5.0, 10.8 Hz, 1H, H-3'); 4.53 (d, *J* = 5.3 Hz, 2H, 2H_{all(1)}); 4.37 (m, 1H, H-4'); 4.22 (m, 2H, H-5'); 2.27 (m, 1H, Ha-2'); 2.11 (s, 3H, CH₃ acetate); 2.10 (m, 1H, Hb-2'); 2.09 (s, 3H, CH₃ acetate).

¹³C-NMR (101 MHz, CDCl₃, δ /ppm):

170.7, 170.5 (C_q, 2 x C=O); 158.4, 133.2 (C_q, 2 C_{ar}); 132.6 (C, C_{all(2)}); 127.2 (C_t, 2 C_{ar}-ortho); 117.6 (C, C_{all(3)}); 114.7 (C_t, 2 C_{ar}-meta); 82.5 (C_t, C-1'); 80.4 (C_t, C-4'); 75.6 (C_t, C-3'); 68.8 (C_s, C_{all(1)}); 64.5 (C_s C-5'); 41.1 (C_s, C-2'); 21, 20.8 (C_p, 2 x CH₃ acetate).

4-(*O*-Allyl)-1-(2'-deoxy- β -D-ribofuranosyl)phenol (98)

To a solution of **96b** (55 mg, 0.16 mmol) in methanol (2 ml) was added K_2CO_3 (catalytic amount). The reaction mixture was stirred for 4 h at RT and the solvent was removed under reduced pressure. The residue was purified by preparative TLC (Hexane/AcOEt 1/1) to give 31 mg (0.125 mmol, 78 %) of the desired product **98** as a white foam.

$\text{C}_{14}\text{H}_{18}\text{O}_4$: 250.24 g.mol⁻¹

R_f (Hexane/AcOEt 1/1) = 0.26

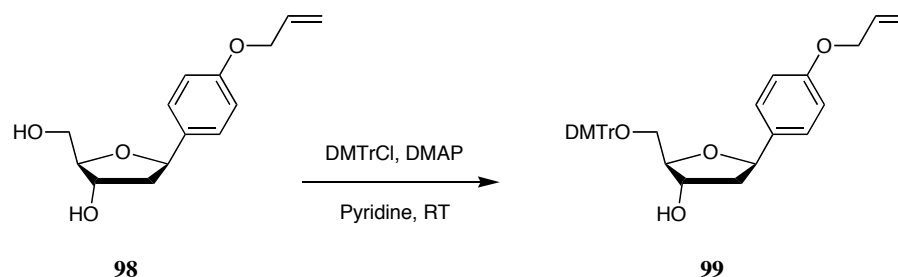
¹H-NMR (400 MHz, CDCl_3 , δ /ppm):

7.30 (d, $J = 8.6$ Hz, 2H, H_{ar}); 6.88 (d, $J = 8.6$ Hz, 2H, H_{ar}); 6.04 (m, 1H, $\text{H}_{\text{all}(2)}$); 5.40 (d, $J = 17.2$ Hz, 1 H, $\text{H}_{\text{all}(3)}$); 5.23 (d, $J = 10.4$ Hz, 1H, $\text{H}_{\text{all}(3')}$); 5.05 (dd, $J = 5.3, 10.8$ Hz, 1 H, H-1'); 4.52 (d, $J = 5.3$ Hz, 2H, 2 $\text{H}_{\text{all}(1)}$); 4.31 (m, 1H, H-4'); 3.92 (m, 1H, H-3'); 3.65 (m, 2H, H-5'); 2.12 (m, 1H, Ha-2'); 1.93 (m, 1 H, Hb-2').

¹³C-NMR (101 MHz, CDCl_3 , δ /ppm):

159.6, 136.0 ($\text{C}_{\text{q}}, 2 \text{C}_{\text{ar}}$); 134.9 (C, $\text{C}_{\text{all}(2)}$); 128.5 ($\text{C}_{\text{t}}, 2 \text{C}_{\text{ar-ortho}}$); 117.4 (C, $\text{C}_{\text{all}(3)}$); 115.5 ($\text{C}_{\text{t}}, 2 \text{C}_{\text{ar-meta}}$); 89.0 ($\text{C}_{\text{t}}, \text{C-4}'$); 81.4 ($\text{C}_{\text{t}}, \text{C-1}'$); 74.4 ($\text{C}_{\text{t}}, \text{C-3}'$); 69.7 ($\text{C}_{\text{s}}, \text{C}_{\text{all}(1)}$); 64.0 ($\text{C}_{\text{s}}, \text{C-5}'$); 44.7 ($\text{C}_{\text{s}}, \text{C-2}'$).

MS (ESI, MeOH/ CH_2Cl_2 1/1): 273.4 [$\text{M} + \text{Na}$]⁺

4-O-(Allyl)-1-[2'-deoxy-5'-O-(dimethoxytrityl)- β -D-ribofuranosyl]phenol (99)

Diol **98** (95 mg, 0.38 mmol) was co-evaporated with pyridine (2 x 3 ml) and then dissolved in pyridine (5 ml). 4,4'-Dimethoxytriphenylmethylchloride (193 mg, 0.57 mmol) was added as well as DMAP (9 mg, 0.076 mmol). The mixture was stirred for 3 h at RT under argon. Methanol (5ml) was added to quench the reaction and the solution was evaporated and co-evaporated with toluene. The residue was purified by column chromatography on silica gel (Pentane/AcOEt, 2/1+ 1% Et₃N) to give 138 mg (0.25 mmol, 65%) of pure product **99** as a colorless oil.

C₃₅**H**₃₆**O**₆: 552.66 g.mol⁻¹

R_f (Pentane/AcOEt 2/1) = 0.23

¹H-NMR (400 MHz, CD₃OD, δ /ppm):

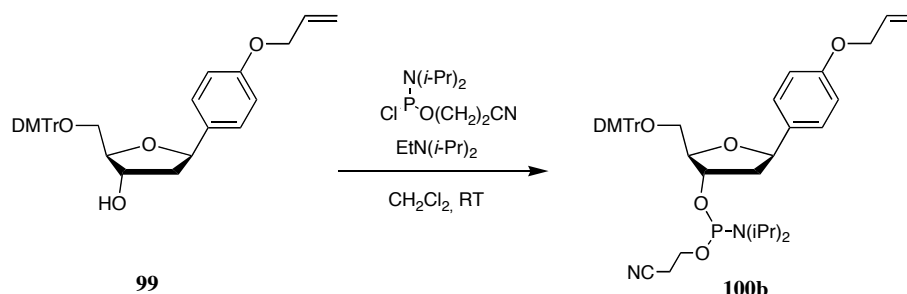
7.16-7.47 (m, 13H, H_{ar}); 6.85 (d, *J* = 8.6 Hz, 2H, H_{ar}); 6.81 (d, *J* = 8.6 Hz, 2H, H_{ar}); 6.02 (m, 1H, H_{all(2)}); 5.35 (d, *J* = 17.1 Hz, 1 H, H_{all(3)}); 5.20 (d, *J* = 10.6 Hz, 1H, H_{all(3')}); 5.08 (dd, *J* = 5.2, 10.7 Hz, 1 H, H-1'); 4.48 (d, *J* = 5.04 Hz, 2H, 2H_{all(1)}); 4.31 (m, 1H, H-4'); 4.03 (m, 1H, H-3'); 3.72 (s, 6H, 2 x OCH₃); 2.14 (m, 1H, H_a-2'); 1.97 (m, 1 H, H_b-2').

¹³C-NMR (101 MHz, CD₃OD, δ /ppm):

173.8, 160.9, 160.5, 147.3, 138.2, 135.8 (C_q, 7 C_{ar}); 134.0 (C, C_{all(2)}); 130.4, 128.4, 127.8, 127.7, 127.6, 126.8 (C_t, 13 C_{ar}); 116.5 (C_s, C_{all(3)}); 114.6, 113.1 (C_t, 4 C_{ar}); 86.9 (C_t, C-4'); 80.5 (C_t, C-1'); 73.9 (C_t, C-3'); 68.8 (C_s, C_{all(1)}); 64.8 (C_s, C-5'); 54.7 (C_p, 2 x OCH₃); 43.9 (C_s, C-2').

MS (ESI, MeOH/ CH₂Cl₂ 1/1): 575.2 [M + Na]⁺

4-*O*-(Allyl)-1-[3'-*O*-(2-cyanoethyl-*N,N*-diisopropylphosphoramidite)-2'-deoxy-5'-*O*-(dimethoxytrityl)- β -D-ribofuranosyl]phenol (100b**)**



To a solution of **99** (65 mg, 117 μ mol) and ethyl-diisopropylamine (82 μ l, 470 μ mol) in dichloromethane (2 ml) 2-cyanoethyl-*N,N*-(diisopropyl)chlorophosphoramidite (52 μ l, 234 μ mol) was added. The mixture was stirred at RT under argon for 3 h. Saturated NaHCO₃ (10 ml) was added and the mixture was diluted with dichloromethane (10 ml). The aqueous layer was extracted with dichloromethane (3 x 20 ml). The organic phase was dried over MgSO₄, filtered and the solvent removed. The residue was purified by column chromatography on silica gel (Pentane/AcOEt 2/1 + 1% Et₃N) to give 72 mg (95 μ mol, 85 %) of compound **100b** as a colorless oil.

C₄₄H₅₂N₂O₇P: 751.88 g.mol⁻¹

R_f (Pentane/AcOEt 2/1) = 0.35

¹H-NMR (400 MHz, CDCl₃, δ /ppm):

mixture of both diastereoisomers: 7.19-7.50 (m, 13H, H_{ar}); 6.79-6.88 (m, 4H, H_{ar}); 6.04 (m, 1H, H_{all(2)}); 5.40 (d, *J* = 17.1 Hz, 1 H, H_{all(3)}); 5.28 (d, *J* = 10.4 Hz, 1H, H_{all(3')}); 5.10 (m, 1 H, H-1'); 4.52 (m, 1H, H-3'); 4.10 (m, 1H, H-4'); 3.76 (s, 6H, 2 x OCH₃); 3.23-3.45 (2m, 4H, H-5', CH₂CN); 2.43-2.58 (m, 2H N(CH(CH₃)₂)); 2.18 (m, 1H, Ha-2'); 2.05 (m, 1H, Hb-2'); 1.13-1.26 (m, 12H N(CH(CH₃)₂)).

¹³C-NMR (101MHz, CDCl₃, δ /ppm):

mixture of both diastereoisomers: 160.0, 159.7, 146.3, 137.3 (C_q, 7C_{ar}); 133.9, 130.4, 128.4, 127.7, 126.8 (C_t, 13 C_{ar}); 119.9 (C_q, CN); 117.4 (C_s, C_{all(3)}); 115.6, 114.0 (C_t, 4 C_{ar}); 87.4 (C_t, C-4'); 81.6

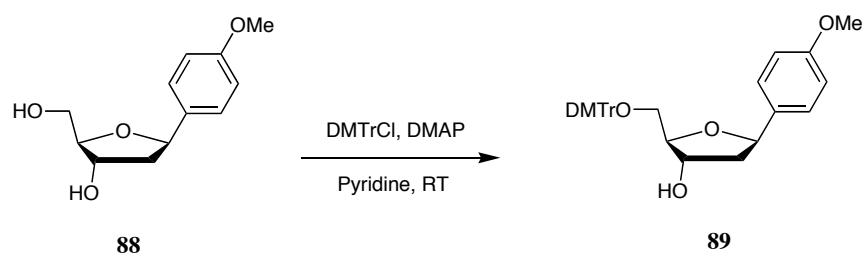
(C_t, C-1'); 78.8 (C_t, C-3'); 69.7 (C_s, C_{all(1)}); 65.4 (C_s, C-5'); 61.5 (C_s, CH₂OP); 55.7 (C_p, 2 x OCH₃); 44.4 (C_s, C-2'); 44.2 (C_t, 2C, N(CH(CH₃)₂)); 25.1, 24.9, 20.9 (C_p, 4C, N(CH(CH₃)₂)); 14.4 (C_s, CH₂CN).

³¹P-NMR (162 MHz, CDCl₃, δ/ppm):

mixture of both diastereoisomers: 137.3, 145.9

MS (ESI, MeOH/ CH₂Cl₂ 1/1): 752.4 [M]⁺

1-[2'-Deoxy-5'-O-(dimethoxytrityl)-β-D-ribofuranosyl]anisole (**89**)



Diol **88** (102 mg, 0.45 mmol) was co-evaporated two times with pyridine (4 ml) and then dissolved in pyridine (4 ml). 4,4'-Dimethoxytriphenylmethylchloride (156 mg, 0.455 mmol) was added as well as DMAP (8 mg, 0.065 mmol). The mixture was stirred for 16 h at RT under argon. Methanol (1ml) was added to quench the reaction and the solution was evaporated and co-evaporated with toluene. The residue was purified by column chromatography on silica gel (Hexane/AcOEt, gradient to 6/4 + 1% Et₃N) to give 197 mg (0.37 mmol, 82%) of pure product **89** as a colorless oil.

C₃₃H₃₄O₆: 526.62 g.mol⁻¹

R_f (Hexane/AcOEt 7/3) = 0.26

$^1\text{H-NMR}$ (400 MHz, CDCl_3 , δ/ppm):

7.21-7.51 (m, 11H, H_{ar}); 6.84 (d, $J = 9.5$ Hz, 2H, H_{ar}); 6.81 (d, $J = 10.3$ Hz, 4H, H_{ar}); 5.12 (dd, $J = 5.3, 10.8$ Hz, 1 H, $\text{H-1}'$); 4.42 (bs, 1H, $\text{H-3}'$); 4.04 (m, 1H, $\text{H-4}'$); 3.78 (s, 9H, 3x OCH_3); 3.42 (m, 2H, $\text{H-5}'$); 2.18 (m, 1H, $\text{H}_{\text{a-2}'}$); 2.05 (m, 1H, $\text{H}_{\text{b-2}'}$); 1.82 (bs, 1H, OH).

$^{13}\text{C-NMR}$ (101 MHz, CDCl_3 , δ/ppm):

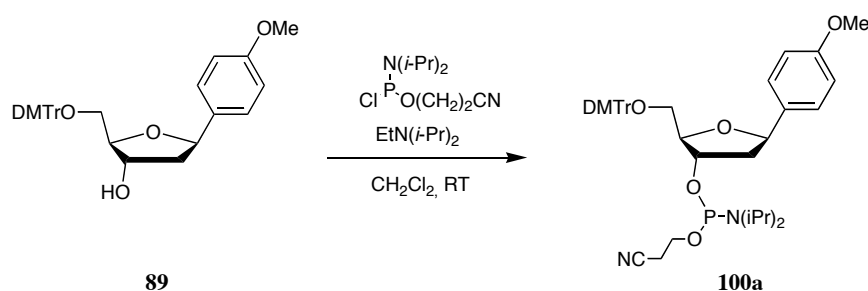
159.5, 158.9, 145.3, 136.5, 134 ($\text{C}_{\text{q}}, 7\text{C}_{\text{ar}}$); 130.5, 128.6, 128.2, 127.8, 127.2, 114.1, 113.5 ($\text{C}_{\text{t}}, 17\text{C}_{\text{ar}}$); 85.6 ($\text{C}_{\text{s}}, \text{C-4}'$); 80.2 ($\text{C}_{\text{t}}, \text{C-1}'$); 75.2 ($\text{C}_{\text{t}}, \text{C-3}'$); 65 ($\text{C}_{\text{s}}, \text{C-5}'$); 55.6 ($\text{C}_{\text{p}}, 3 \times \text{OCH}_3$); 44.2 ($\text{C}_{\text{s}}, \text{C-2}'$)

MS (FAB, KCl): 527 [$\text{M}+\text{H}$] $^+$; 565 [$\text{M}+\text{K}$] $^+$

Elemental analysis: calculated: C 75.26, H 6.51

found: C 75.33, H 6.47

1-[3'-O-(2-Cyanoethyl-*N,N*-diisopropylphosphoramidite)-2'-deoxy-5'-O-(dimethoxytrityl)- β -D-ribofuranosyl]anisole (100a**)**



To a solution of **89** (100 mg, 0.19 mmol) and ethyl-diisopropylamine (75 μl , 1.14 mmol) in dichloromethane (2 ml) under argon was added 2-cyanoethyl-*N,N*-(diisopropyl)chlorophosphoramidite (148 μl , 0.65 mmol). The mixture was stirred at RT for 2.5 h. The reaction was quenched with saturated solution of NaHCO_3 in water (10 ml) and diluted with dichloromethane (10 ml). The aqueous layer was extracted with dichloromethane (3 x 20 ml). The organic phase was dried over MgSO_4 , filtered and the solvent removed. The residue was purified by column chromatography on silica gel (Hexane/ AcOEt 4/1 + 1% Et_3N) to give 111 mg (0.153 mmol, 80%) of compound **100a** as a colorless oil.

C₄₂H₅₁N₂O₇P: 726.85 g.mol⁻¹

R_f(Pentane/AcOEt 7/3) = 0.31

¹H-NMR (400 MHz, CDCl₃, δ/ppm):

mixture of both diastereoisomers: 7.18-7.50 (m, 11H, H_a); 6.92 (d, *J* = 9.4 Hz, 2H, H_{ar}); 6.81 (d, *J* = 10.3 Hz, 4H, H_{ar}); 5.18 (dd, *J* = 5.28, 10.2 Hz, 1 H, H-1'); 4.48 (m, 1H, H-3'); 4.10 (m, 1H, H-4'); 3.78 (s, 9H, 3 x OCH₃); 3.2-3.55 (2m, 4H, H-5', CH₂CN); 2.44-2.62 (m, 2H N(CH(CH₃)₂)); 2.22 (m, 1H, Ha-2'); 2.00 (m, 1H, Hb-2'); 1.17-1.28 (m, 12H N(CH(CH₃)₂)).

¹³C NMR (101 MHz, CDCl₃, δ/ppm):

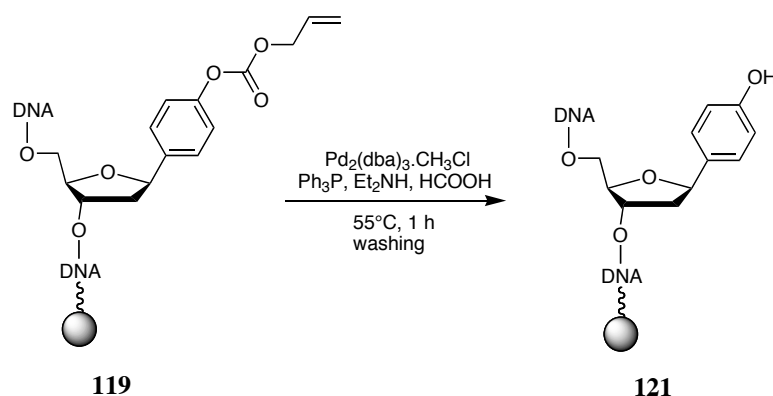
mixture of both diastereoisomers: 159.9, 158.4, 145.3, 137.2, 134.3 (C_q, 7C_{ar}); 130.4, 128.8, 128.3, 127.7, 127.2, 114.4, 113.2 (C_t, 17 C_{ar}); 119.7 (C_q, CN); 85.8 (C_t, C-4'); 80.1 (C_t, C-1'); 75.3 (C_t, C-3'); 64.9 (C_s, C-5'); 58.8 (C_s, CH₂OP); 55.5 (C_p, 3 x OCH₃); 44.3 (C_s, C-2'); 43.6 (C_t, 2C, N(CH(CH₃)₂)); 20.5, 20.6, 20.7, 20.8 (C_p, 4C, N(CH(CH₃)₂)); 18.2 (C_s, CH₂CN).

³¹P-NMR (162 MHz, CDCl₃, δ/ppm):

mixture of both diastereoisomers: 147.6, 148.7

MS (ESI, MeOH/ CH₂Cl₂ 1/1): 749.5 [M + Na]⁺

10. Deprotection of the allyloxycarbonate protected oligonucleotide (**119**)



The CPG supports binding the protected oligomer **119** were washed with THF (1 ml) and dried in vacuo. To the resulting polymer were added triphenylphosphine (360 mg, 1.37 mmol), $\text{Pd}_2(\text{dba})\cdot\text{CHCl}_3$ (140 mg, 0.135 mmol) and a 1.2 M solution of $\text{Et}_2\text{NH}/\text{HCOOH}$ 1/1 in THF (6.7 ml, 8.04 mmol). After being vigorously shaken with a mixer, the mixture was heated at 50°C for 0.5-1 h. The supernatant fluid was decanted and the resulting CPG supports were washed successively with THF (2 x 1 ml), acetone (2 x 1 ml), a 0.1 M sodium N,N-diethyldithiocarbamate (ddtc) aqueous solution (pH 9.7, 1 ml, 15 min), acetone (3 x 1 ml), and water (1 ml). The ddtc washing was repeated once more. The cleaned CPG supports were then treated with concentrated ammonium hydroxide (1.5 ml) at 25°C to afford the fully deprotected oligonucleotide **121**.

11. Oligonucleotide sequences

Sequences	[M-H] ⁻ Calculated (m/z)	[M-H] ⁻ Found (m/z)	ϵ_{260} (M ⁻¹ .cm ⁻¹)
121: 5'-TATATATATATA(PhOH)ATATATATTTT-3'	7905.14	7906.01	256245
122a: 5'-GCCTTATAP hOHT *ATAAATCGT-3'	5829.67	5826.98	178845
122b: 5'-GCCTTATAP hOHTT *ATAAATCGT-3'	6133.87	6136.48	186675
122c: 5'-GCCTTATAP hOHTTT *ATAAATCGT-3'	6438.07	6441.14	194505
122d: 5'-GCCTTATAP hOHTTTT *ATAAATCGT-3'	6742.27	6751.37	202335
132: 5'-TTTTTATA(PhOH)TT*ATAAATAAT-3'	6146.90	6147.84	197205
133: 5'-TTATATATATATA(PhOH)AT*ATATATTTT-3'	7990.14	7991.07	256245
134: 5'-ACGATTTATAAATATAAGGC-3'	6148.24	6152.82	216090
134: 5'-ACGATTTATAACTATAAGGC-3'	6124.21	6127.33	208890
134: 5'-ACGATTTATAATTATAAGGC-3'	6139.22	6138.74	210060
134: 5'-ACGATTTATAAA b TATAAGGC-3'	6015.12	6012.01	201940
137: 3'-AAATATATATATAT*ATATATATAAAA-5'	8076.54	8075.87	300060

12. Literature

- (1) Stryer, L. *Biochemistry*, III.ed; Freeman W.H. and Company, New York, 1995
- (2) Blackburn, G.M. (editor: Gait, M.J.) *Nucleic Acids in Chemistry and Biology*, 2nd ed, Oxford University Press, Oxford 1996.
- (3) Watson, J.D.; Crick, F.H. *Nature* **1953**, 171,737 and 964.
- (4) Saenger, W. *Principles of Nucleic Acid Structure*, Springer, New York 1984.
- (5) Benevides, J.M.; Thomas, G.J. *Nucleic Acids Res.* **1983**, 11, 5747.
- (6) Well, R.D.; Harvey, S.C. *J. Biol.Chem.* **1988**, 263, 1095.
- (7) Herber, A.; Rich, A. *J. Biol.Chem.* **1996**, 271, 11595.
- (8) Guéron, M.; D., J.-Ph.; Filoche, M. *Biophys. J.* **2000**, 78, 1080.
- (9) Watson, J.D.; Crick, F.H. *Nature* **1961** 192,1227.
- (10) Finkel, T.; Holbrook, H. *Nature* **2000**, 408, 239.
- (11) Özben, T. *Free Radicals, Oxidative Stress and Antioxidants*, NATO ASI Series, Plenum Press, New York , London 1998.
- (12) Sies, H.; Schulz, W.A. ; Steenken, S. *Photochem.Photobiol. B* **1996**, 32, 97.
- (13) Ames, B.N.; Shigenaga, M.K.; Hagen, T.M. *Proc. Natl. Acad. Sci. USA* **1993**, 90, 7915.
- (14) Sohal, R.S.; Weindruch, R. *Science* **1996**, 273, 59.
- (15) Halliwell, B.; Gutteridge, J.M.C. *Free Radicals in Biology and Medicine*, Oxford University Press, Oxford 1999.
- (16) (a) Imlay, J.A.; Linn,S. *J. Bacteriol.* **1986**, 166, 519-527. (b) Imlay, J.A.; Linn,S. *J.Bacteriol*, **1988**, 240,1302.
- (17) (a) Steenken, S. *Chem. Rev.* **1989**, 89, 503. (b) Steenken, S. ; Jovanovic, S.V. *J. Am. Chem. Soc.* **1997**, 119, 617.
- (18) Bruner, S.D.; Norman, D.P.G.; Verdine, G.L. *Nature* **2000**, 403, 859.
- (19) Kaplan, H.S. *Nature* **1978**, 272, 379.
- (20) Croteau, D.L.; Bohr, V.A. *J. Biol. Chem.* **1997**, 272, 25409.
- (21) Bohr, V.A.; Anson, R.M. *Mutat. Res.* **1995**, 338, 25.
- (22) Heller, A. *Faraday Discuss.* **2000**, 116, 1.

- (23) (a) Sugiyama, H.; Saito, I. *J. Am. Chem. Soc.* **1996**, *118*, 7063. (b) Saito, I.; Nakaruma, T.; Nakatani, K.; Yoshioka, Y.; Yamaguchi, K.; Sugiyama, H.; *J. Am. Chem. Soc.* **1998**, *120*, 12686.
- (24) Cech, T.R. *Angew.Chem.* **2000**, *112*, 34.
- (25) Lowy, D.G.; Willumsen, B.M. *Ann. Rev. Biochem.* **1993**, *62*, 851.
- (26) Hussain, S.P. *Oncogene* **1994**, *9*, 2277.
- (27) Eley, D. D.; Spivey, D. I. *Trans. Faraday Soc.* **1962**, *58*, 411.
- (28) (a) Wilson, E. K. *Chem. Eng. News* **1998**, *76* (30), 51-54. (b) Wilson, E. K. *Chem. Eng. News* **1999**, *77*, 43. (c) Wu, C. *Sci. News* **1999**, *156*, 104. (d) Ratner, M. *Nature* **1999**, *397*, 480.
- (29) (a) Holmlin, R. E.; Dandliker, P. J.; Barton, J. K. *Angew. Chem., Int. Ed. Engl.* **1997**, *36*, 2714. (b) Netzel, T. L. *In Organic and Inorganic Photochemistry Vol 2.*; Ramamurthy, V.; Schanze, K. S.; ed. Dekker New York, 1998, pp. 1-54. (c) Barbara, P. F.; Olson, E. J. C. *Adv. Chem. Phys.* **1999**, *107*, 647.
- (30) Lewis F. D. *Electron transfer in Chemistry*; V. Balzani, Ed.; WILEY-VCH Verlag GmbH: Weinheim, 2001, pp. 105.
- (31) Giese, B. *Acc. Chem. Res.* **2000**, *33*, 631.
- (32) Schuster, G.B. *Acc. Chem. Res.* **2000**, *33*, 253
- (33) Lewis, F.D.; Liu, X.; Liu, J.; Miller, S.E.; Hayes, R.T.; Wasielewski, M.R. *Nature*, **2000**, *406*, 51
- (34) Murphy, C. J.; Arkin, M. R.; Ghatlia, N. D.; Bossmann, S.; Turro, N. J.; Barton, J. K. *Proc. Natl. Acad. Sci. U.S.A.* **1994**, *91*, 5315. (b) Arkin, M. R.; Stemp, E. D. A.; Holmlin, R. E.; Barton, J. K.; Hörmann, A.; Olson, E. J. C.; Barbara, P. F. *Science* **1996**, *273*, 475.
- (35) Kelley, S. O.; Barton, J. K. *Chem. Biol.* **1998**, *5*, 413. (b) Wan, C.; Fiebig, T.; Kelley, S. O.; Treadway, C. R.; Barton, J. K.; Zewail, A. H. *Proc. Natl. Acad. Sci. U.S.A.* **1999**, *96*, 6014.
- (36) Fukui, K.; Tanaka, K. *Angew. Chem., Int. Ed. Engl.* **1998**, *37*, 158. (b) Fukui, K.; Tanaka, K.; Fujitsuka, M.; Watanabe, A.; Ito, O. *J. Photochem. Photobiol., B* **1999**, *50*, 18.
- (37) Henderson, P. T.; Jones, D.; Hampikian, G.; Kan, Y.; Schuster, G. B. *Proc. Natl. Acad. Sci. U.S.A.* **1999**, *96*, 8353. (b) Ly, D.; Sanii, L.; Schuster, G. B. *J. Am. Chem. Soc.* **1999**, JA991753S.

- (38) Kelley, S. O.; Barton, J. K. *Science* **1999**, 283, 375.
- (39) (a) Meggers, E.; Michel-Beyerle, M. E.; Giese, B. *J. Am. Chem. Soc.* **1998**, 120, 12950. (b) Giese, B.; Wessley, S.; Spormann, M.; Lindemann, U.; Meggers, E.; Michel-Beyerle, M. E. *Angew. Chem. Int. Ed.* **1999**, 38, 996.
- (40) Lewis, F.D.; Wu, T.; Liu, X.; Letsinger, R.L.; Greenfield, S.R.; Miller, S.E.; Wasielewski, M.R. *J. Am. Chem. Soc.*, **2000**, 122, 2089.
- (41) Jortner, J.; Bixon, M.; Langenbacher, T.; Michel-Beyerle, M. E. *Proc. Natl. Acad. Sci. U.S.A.* **1998**, 95, 12759.
- (42) Giese, B.; Beyrich-Graf, X.; Erdmann, P.; Giraud, L.; Imwinkelried, P.; Müller, S.N.; Schwitter, U. *J. Am. Chem. Soc.* **1995**, 117, 6146.
- (43) Giese, B.; Dussy, A.; Elie, P.; Erdmann, P.; Schwitter, U. *Angew. Chem.* **1994**, 106, 1941.
- (44) (a) Giese, B.; Beyrich-Graf, X.; Burger, J.; Kesselheim, C.; Senn, M.; Schäfer, T. *Angew. Chem. Int. Ed. Engl.*, **1993**, 32, 1742. (b) Giese, B.; Burger, J.; Kang, T.W.; Wittmer, T. *J. Am. Chem. Soc.*, **1992**, 114, 7322.
- (45) Meggers E., *Zum Elektrontransfer in DNA*, Inauguraldissertation, Philosophisch-Naturwissenschaftliche Fakultät, Universität Basel, 1999.
- (46) Yang, N.C.; Feit, E.D. *J. Am. Chem. Soc.* **1968**, 90, 504.
- (47) Glatthar, R.; Spichty, M.; Gugger, A.; Batra, R.; Damm, W.; Mohr, M.; Zipse, H.; Giese, B. *Tetrahedron*, **2000**, 56, 4117.
- (48) Meggers, E.; Kusch, D.; Spichty, M.; Wille, U.; Giese, B. *Angew. Chem. Int. Ed. Engl.*, **1998**, 37, 460.
- (49) Meggers, E.; Dussy, A.; Schäfer, T.; Giese, B. *Chem. Euro. J.* **2000**, 6, 485.
- (50) Kasai, H.; Yamaizumi, Z.; Berger, M.; Cadet, J. *J. Am. Chem. Soc.* **1992**, 114, 96924.
- (51) Chung, M.H.; Kiyosawa, H.; Ohtsuka, E.; Nishimura, S.; Kasai, H. *Biochem. Biophys. Res. Commun.* **1992**, 188, 1.
- (52) Muller, J. G.; Duarte, V.; Hickerson, R. P.; Burrows, C. J. *Nucleic Acids Res.* **1998**, 26, 2247.
- (53) Schuster, B.; Kann, Y. *J. Am. Chem. Soc.* **1999**, 121, 11607.
- (54) (a) Winkler, J. R.; Gray, H. B. *Chem. Rev.* **1992**, 92, 369. (b) Wasielewski, M. R. *Chem. Rev.* **1992**, 92, 435. (c) Paulson, B.; Pramod, K.; Eaton, P.; Closs, G.; Miller, J. R. *J. Phys. Chem.* **1993**, 97, 13042.

- (55) Davis, W. B.; Svec, W. A.; Ratner, M. A.; Wasielewski, M. R. *Nature* **1998**, 396, 60.
- (56) Chang, I.J.; Gray, H. B.; Winkler, J. R. *J. Am. Chem. Soc.* **1991**, 113, 7056.
- (57) Fukuzumi, S.; Mochizuki, S.; Tanaka, T. *Inorg. Chem.* **1989**, 28, 2459.
- (58) (a) Prins, R.; Korswagen, A.R.; Kortbeek, A.G.T.G. *J. Organometal. Chem.*, **1972**, 39, 335. (b) 13 Prins, R. *Chem. Commun.*, **1970**, 280.
- (59) (a) Bent, D.V.; Hayon, E. *J. Am. Chem. Soc.* **1975**, 97, 2599. (b) Creed, D. *Photochem. Photobiol.* **1984**, 39, 563.
- (60) (a) Meade, T. J.; Kayyem, J. F. *Angew. Chem., Int. Engl.* **1995**, 34, 352.
(b) Krider, E. S.; Meade, T. J. *J. Bio. Inorg. Chem.* **1998**, 3, 222.
- (61) Hurley, D. J.; Tor, Y. *J. Am. Chem. Soc.* **1998**, 120, 2194.
- (62) Murphy, C. J.; Arkin, M. R.; Jenkins, Y.; Ghatlia, N. D.; Bossmann, S. H.; Turro, N. J.; Barton, J. K. *Science* **1993**, 262, 1025.
- (63) (a) Meggers, E.; Kusch, D.; Giese, B. *Helv. Chim. Acta* **1997**, 80, 640.
(b) Hortholary, C.; Minc, F.; Coudret, C.; Bonvoisin, J. *Chem. Commun.*, **2002**, 1932.
- (64) Holmlin, R. E.; Yao, J. A.; Barton, J. K. *Inorg. Chem.* **1999**, 38, 174-189.
- (65) (a) Hall, D. B.; Barton, J. K. *J. Am. Chem. Soc.* **1997**, 119, 5045-5046. (b) Hall, D. B.; Holmin, R. E.; Barton, J. K. *Nature* **1996**, 382, 731-735.
- (66) Bashkin, J. K.; Frolova, E. I.; Sampath, U. *J. Am. Chem. Soc.* **1994**, 116, 5981.
- (67) Ihara, T.; Nakayama, M.; Murata, M.; Nakano, K.; Maeda, M. *Chem. Commun.* **1997**, 1609.
- (68) Ihara, T.; Maruo, Y.; Takenaka, S.; Takagi, M. *Nucleic Acids Res.* **1996**, 24, 4273.
- (69) Mucic, R. C.; Herrlein, M. K.; Mirkin, C. A.; Letsinger, R. L. *Chem. Commun.* **1996**, 555.
- (70) (a) Yu, C. J.; Wan, Y.; Yowanto, H.; Li, J.; Tao, C.; James, M.D.; Tan, C.L.; Blackburn, G.F.; Meade, T.J. *J. Am. Chem. Soc.* **2001**, 123, 11155. (b) Yu, C. J.; Wang, H.; Wan, Y.; Yowanto, H.; Kim, J.C.; Donilon, L.H.; Tao, C.; Strong, M.; Chong, Y. *J. Org. Chem.* **2001**, 66, 2937.
- (71) Sumner, J.J.; Weber, K.S.; Hockett L.A.; Creager, S.E. *J. Phys. Chem. B* **2000**, 104, 7449.
- (72) (a) Creager, S. E.; Yu, C. J.; Bamdad, C.; O'Connor, S. D.; Maclean, T.; Lam, E.; Chong, Y.; Olsen, G. T.; Luo, J. Y.; Gozin, M.; Kayyem, J. F. *J. Am. Chem. Soc.*

- 1999**, 121, 1059. (b) Yu, C. J.; Chong, Y.; Kayyem, J. F.; Gozin, M. *J. Org. Chem.* **1999**, 64, 2070.
- (73) Wilson, E. K. *Chem. Eng. News* **1998**, May 25, 47.
- (74) Engtrakul, C.; Sita, L.R. *Nano Lett.* **2001**, 1, 541.
- (75) Kealy, J.; Pauson, P.L.; *Nature* **1951**, 168, 1039.
- (76) Gorton, J.E.; Lentzner, H.L.; Watts, W.E. *Tetrahedron* **1971**, 27, 4353.
- (77) Bucci, E.; De Napoli, L.; Di Fabio, G.; Messere, A.; Montesarchio, D.; Romanelli, A.; Piccialli, G.; Varra, M. *Tetrahedron* **1999**, 55, 14435.
- (78) Yu, C. J.; Yowanto, H.; Wan, Y.; Meade, T.J.; Chong, Y.; Strong, M.; Donilon, L.H.; Kayyem, J. F.; Gozin, M.; Blackburn, G.F. *J. Am. Chem. Soc.* **2000**, 122, 6767.
- (79) Wiessler et al. US 6,211,356 B1, Apr.3, 2001.
- (80) Takenaka, S.; Uto, Y.; Kondo, H.; Ihara, T.; Takagi, M. *Anal. Biochem.* **1994**, 218, 436.
- (81) (a) Gait, M.J. Ed., *Oligonucleotide synthesis: a practical approach*, IRL Press, Washington, DC, 1990, pp 35-81 (Atkinson, T., Smith, M.); (b) Eckstein, F. Ed., *Oligonucleotides and analogues: a practical approach*, IRL Press, Oxford, U.K., pp. 1-23, 1991.
- (82) Gugger, A.; Batra, R.; Rzadek, P.; Rist, G.; Giese, B. *J. Am. Chem. Soc.* **1997**, 119, 8740.
- (83) Bernhard, K.; Geimer, J.; Canle-Lopez, M.; Reynisson, J.; Beckert, D.; Gleiter, R.; Steenken, S. *Chem. Eur. J.* **2001**, 7, 4640.
- (84) Bhattacharyya S. *Synlett*, **1998**, 8, 837.
- (85) Glatthar, R. *Der Radikalbeschleunigte β -Bindungsbruch*, Inauguraldissertation, Philosophisch-Naturwissenschaftliche Fakultät, Universität Basel, 2000.
- (86) Glatthar, R.; Giese, B. *Organic Letters* **2000**, 2, 2315.
- (87) Bernady, K.F.; Floyd, M.B.; Poletto, J.F.; Weiss, M.J. *J. Org. Chem.* **1979**, 44, 1438.
- (88) Corey, E.J.; Czekely, I.; Shiner, C.S. *Tetrahedron Lett.* **1977**, 18, 3529.
- (89) Brill, W.K.-D.; DesMesmaeker, A.; Wendeborn, S. *Synlett* **1998**, 1085.
- (90) Neises, B.; Steglich, W.; *Angew. Chem. Int. Ed.* **1978**, 17, 522.
- (91) Dauzonne, D.; Royer, R. *Synthesis* **1987**, 399.
- (92) Uchiyama, M.; Aso, M.; Noyori, R.; Hayama, Y. *J. Org. Chem.* **1993**, 58, 373.

-
- (93) Hammes, G.G. *Techniques of chemistry, Vol. VI*, John Wiley & Sons, New York, 1974.
- (94) Mahalaxmi, R. G.; Hermann, R.; Naumov, S.; Brede, O. *Phys. Chem. Chem. Phys.* **2000**, 2, 4947.
- (95) Brede, O.; Wojnarovis, L. *Radiat. Phys. Chem.* **1991**, 37, 537.
- (96) Geto, N.; Solar, S. *Radiat. Phys. Chem.* **1988**, 31, 121.
- (97) Steenken, S.; Neta, N. *J. Phys. Chem.* **1982**, 86, 3661.
- (98) Brede, O.; Orthner, H.; Hermann, R. *Chem. Phys. Lett.* **1994**, 229, 571.
- (99) Land, E.J.; Porter, G.; Strachan, E. *Trans. Faraday Soc.* **1961**, 57, 1885.
- (100) Bansal, K.M.; Fessenden, R.W. *Radiat. Res.*, **1976**, 67, 69.
- (101) Brede, O.; Hermann, R.; Mehnert, R. *J. Chem. Soc. Faraday Trans. 1* **1987**, 83, 2365.
- (102) Stubbe, J.; Nocera, D.G.; Yee, C.S.; Chang, M.C.Y. *Chem. Rev.* **2003**, 103, 2167.
- (103) Stubbe, J.; van der Donk, W.A. *Chem. Rev.* **1998**, 98, 705.
- (104) Napp, M. *Elektronentransfer durch Oligopeptide : Synthese und kinetische Untersuchung von Polyprolin-Modellsystemen*, Inauguraldissertation, Philosophisch-Naturwissenschaftliche Fakultät, Universität Basel, 2004.
- (105) Giese, B.; Napp, M.; Jacques, O.; Boudebous, H.; Taylor, A. M.; Wirz, J. *Angew. Chem., Int. Engl.* **2005**, in press.
- (106) Sjödin, M.; Stenbjörn, S.; Akermark, B.; Sun, L.; Hammarström, L. *Phil. Trans. R. Soc. Lond. B* **2002**, 357, 1471.
- (107) Sjödin, M.; Styring, S.; Akermark, B.; Sun, L.; Hammarström, L. *J. Am. Chem. Soc.* **2000**, 122, 3932.
- (108) Matray, T.J.; Kool, E.T. *J. Am. Chem. Soc.* **1998**, 120, 6191.
- (109) Guckian, K.M.; Schweitzer, B.A.; Ren, R.X.-F.; Sheils, C.J.; Paris, P.L.; Tahmassebi, D.C.; Kool, E.T. *J. Am. Chem. Soc.* **1996**, 118, 8182.
- (110) Wichai, U.; Woski, S.A. *Bioorg. Med. Chem. Lett.* **1998**, 8, 3465.
- (111) Hoffer, M. *Chem. Ber.* **1960**, 93, 2777.
- (112) (a) Ren, R.X.-F.; Chaudhuri, N.C.; Paris, P.L.; Rumney, S.; Kool, E.T. *J. Am. Chem. Soc.* **1996**, 118, 7671. (b) Chaudhuri, N.C.; Ren, R.X.-F.; Kool, E.T. *Synlett* **1997**, 341.
- (113) Kraus, G. A.; Molina, M. T. *J. Org. Chem.* **1988**, 53, 752.
- (114) Krohn, K.; Heins, H.; Wielckens, K. *J. Med. Chem.* **1992**, 35, 511.

- (115) (a) Matulic-Adamic, J.; Beigelman, L.; Portmann, S.; Egli, M.; Usman, N.; *J. Org. Chem.* **1996**, *61*, 3909. (b) Matulic-Adamic, J.; Beigelman, L. *Tetrahedron Lett.* **1997**, *38*, 203. (c) Matulic-Adamic, J.; Beigelman, L. *Tetrahedron Lett.* **1997**, *38*, 1669.
- (116) Wichai, U.; Woski, S. *Org. Lett.* **1999**, *8*, 1173.
- (117) Hildbrand, S.; Blaser, A.; Parel, S.P.; Leumann, C.J. *J. Am. Chem. Soc.* **1997**, *119*, 5499.
- (118) (a) Robins, M.J.; Wilson, J.S.; *J. Am. Chem. Soc.* **1981**, *103*, 932. (b) Robins, M. J.; Wilson, J. S.; Hansske, F. *J. Am. Chem. Soc.* **1983**, *105*, 4059. (c) Zou, R.; Robins, M. J. *Can. J. Chem.* **1987**, *65*, 1436.
- (119) (a) Markiewicz, W. T.; Wiewiórowski, M. *Nucleic Acids Res., Spec. Publ.* **1978**, *4*, 185. (b) Markiewicz, W. T. *J. Chem. Res., Synop.* **1979**, *24*; *J. Chem. Res., Miniprint* 1979, 181.
- (120) (a) Sinha, N.D.; Biern, J.; McManus, J.; Köster, H. *Nucl. Acids Res.* **1984**, *12*, 4539. (b) Svendsen, M.L.; Wengel, J.; Dahl, O.; Kirpekar, F.; Roepstorff, P. *Tetrahedron* **1993**, *49*, 11341.
- (121) Grieco, P.A.; Nishizawa, M.; Oguri, T.; Burke, S.D.; Marinovic, N. *J. Am. Chem. Soc.* **1977**, *99*, 5773.
- (122) Guibé, F. *Tetrahedron* **1997**, vol.53, No. 40 pp.13509-13556.
- (123) Park, W.K.C.; Auer, M.; Jaksche, H.; Wong, C.H. *J. Am. Chem. Soc.* **1996**, *118*, 10150.
- (124) Damha, M.; Giannaris, P.; Zabarylo, S. *Nucl. Acids Res.* **1990**, *18*, 3818.
- (125) Price, C. C.; Snyder, W.H. *J. Am. Chem. Soc.* **1961**, *83*, 1701.
- (126) Smith III, A.B.; Rivero, R.A.; Hale, K.J.; Vaccaro, H.A. *J. Am. Chem. Soc.* **1991**, *113*, 2092.
- (127) (a) Hayakawa, Y.; Wakabayashi, S.; Kato, H.; Noyori, R. *J. Am. Chem. Soc.* **1990**, *112*, 1691. (b) Hayakawa, Y.; Hirose, M.; Hayakawa, M.; Noyori, R. *J. Org. Chem.* **1995**, *60*, 925.
- (128) (a) Biland-Thommen, A.S. *Elektrontransfer in der DNS : Der Einfluss des Donors und der Brücke*, Inauguraldissertation, Philosophisch-Naturwissenschaftliche Fakultät, Universität Basel, 2002. (b) Giese, B.; Biland, A. *Chem. Com.* **2002**, *7*, 667.

- (129) Lewis, F.D.; Kalgutkar, F.S.; Wu, T.; Liu, X.; Hayes, R.T.; Miller, S.E. Wasielewski, M.R. *J. Am. Chem. Soc.*, **2000**, 122, 12346.
- (130) Marcus, R.A.; Sutin, N. *Biochim. Biophys. Acta* **1985**, 811, 265.
- (131) Jortner, J.; Bixon, M.; Langenbacher, T.; Michel-Beyerle, M.E. *Charge Transfer and Transport in DNA, Proc. Natl. Acad. Sci. U.S.A.* **1998**, 95, 12759.
- (132) (a) Closs, G.L.; Miller, J.R. *Science* **1988**, 240, 440. (b) Moser, C.C.; Keske, J.M.; Warncke, K.; Farid, R.S.; Dutton, P.L. *Nature* **1992**, 355, 796. c) Beratan, D.N.; Onuchic, J.N.; Winkler, J.R.; Gray, H.B. *Science* **1992**, 258, 740.
- (133) Zweig, A.; Hodgson W. G.; Jura, W. H. *J. Am. Chem. Soc.* **1964**, 86, 4124.
- (134) Bernhard, K.; Geimer, J.; Canle-Lopez, M.; Reynisson, J.; Beckert, D.; Gleiter, R.; Steenken, S. *Chem. Eur. J.* **2001**, 7, 4640.
- (135) a) E. Babini, I. Bertini, M. Borsari, F. Capozzi, C. Luchinat, X. Zhang, G. L. C. Moura, I. V. Kurnikova, D. N. Beratan, A. Ponce, A. J. Di Bilio, J. R. Winkler, H. B. Gray, *J. Am. Chem. Soc.* **2000**, 122, 4532. b) C. C. Moser, J. M. Keske, K. Warncke, R. S. Farid, P. L. Dutton, *Nature* **1992**, 355, 796.
- (136) Calculated by Stanislav Ivan in the Giese group.
- (137) Von Ahsen, N.; Oellerich, M.; Armstrong, V.W.; Schütz, E. *Clin. Chem.* **1999**, 45, 2094.
- (138) Lipsky, R.H.; Mazzanti, C.M.; Rudolph, J.G.; Xu, K.; Vyas, G.; Bozak, D.; Radcliff, M.Q.; Goldman, D. *Clin. Chem.* **2001**, 47, 635.
- (139) Yi, M.; Scheiner, S. *Chem. Phys. Lett.* **1996**, 262, 567.
- (140) Dixon, W.T.; Murphy, D.J. *J. Chem. Soc., Faraday Trans. 2* **1976**, 72, 1221.
- (141) Harriman, A. *J. Phys. Chem.* **1987**, 91, 6102.
- (142) Canonica, S.; Hellrung, B.; Wirz, J. *J. Phys. Chem. A* **2000**, 104, 1226.
- (143) Chaudhuri, N. C.; Kool, E. T. *Tetrahedron Lett.* **1995**, 36, 1795.
- (144) Pascaly, M.; Yoo, J.; Barton, J.K. *J. Am. Chem. Soc.* **2002**, 124, 9083.
- (145) Fukuzumi, S.; Okamoto, K.; Imahori, H. *Angew. Chem. Int. Ed.* **2002**, 41, 620.
- (146) Furrer, E. *On the Distance-Independent Hole Transfer over Long (AT)_n- Sequences in DNA*, Inauguraldissertation, Philosophisch-Naturwissenschaft-liche Fakultät, Universität Basel, 2004.
- (147) Furrer, E.; Giese, B. *Helv. Chim. Acta* **2003**, 86, 3623.
- (148) Cannon, R. D. *Electron Transfer Reactions*, Butterworth, London, Boston, **1980**.
- (149) Amiot, N.; Giese, B., unpublished data

13. Abbreviations and Acronyms

A	adenine
Å	angstrom
ab	abasic site
Ac	acetyl, acetate
AcOH	acetic acid
AIBN	2,2'-Azo-bis-isobutyronitrile
All	allyl
AOC	allyloxycarbonate
APT	attached proton test (NMR)
ar	aromatic
Ar	argon
Bn	benzyl
bs	broad singlet
^t Bu	tert-butyl
BuLi	Butyllithium
Bz	benzoyl
C	cytosine
C°	degre centigrade
COSY	correlation spectroscopy (NMR)
CPG	controlled pore glass
d	doublet
D	deuterium
δ	chemical shift (ppm, NMR)
dba	dibenzylideneacetone
DMAP	4- <i>N,N'</i> -dimethylaminopyridine
DMF	<i>N,N'</i> -dimethylformamide
DMSO	dimethylsulfoxide
DMTr	4,4'-dimethoxytrityl
DMTrCl	4,4'-dimethoxytrityl chloride
DNA	deoxyribonucleic acid

EDC	1-ethyl-3-[3-(dimethylamino)propyl]carbodiimide hydrochloride
e.g.	for example
EPR	electron paramagnetic resonance
E°_{ox}	oxidation potential
ESI	electrospray ionization
Et	ethyl
ET	electron transfer
EtOAc	ethyl acetate
FAB	fast atom bombardment
Fc	ferrocene
G	guanine
GGG	triple G unit
G^{Br}	8-Bromoguanine
G^{oxo}	8-Oxoguanine
G^{Z}	7-Deazaguanine
h	hour(s)
HPLC	high performance liquid chromatography
Hz	hertz
hv	light
<i>i</i> -Pr	isopropyl
J	coupling constant (Hertz, NMR)
$k_{ET,rel}$	relative electron transfer rate constant
k_{H_2O}	water addition rate constant
KI	kalium iodide
m	multiplet
MALDI-TOF	matrix assisted laser desorption ionisation time-of-flight
max	maximal
Me	methyl
m/z	mass unit per charge
MHz	Megahertz
min	minute(s)
MS	mass spectroscopy
nm	nanometer

NMI	<i>N</i> -methylimidazole
NMR	nuclear magnetic resonance
NOE	nuclear overhauser effect
NOESY	nuclear overhauser and exchange spectroscopy (NMR)
Pent	pentane
Ph	phenyl
PhOH	phenol
PhOMe	anisole
ppm	part(s) per million
PPTS	pyridinium paratoluene sulfonate
R_f	retention factor (TLC)
RI	redox-indicator
ROS	reactive oxugen species
RP	reversed phase
rt	retention time (HPLC)
RT	room temperature
s	singulet
SCE	saturated calomel electrode
t	triplet
T	thymine
T*	C4'-pivaloylthymidine
TBAF	tetrabutylammonium fluoride
TBDMS	tert-butyldimethylsilyl
TEAA	triethylammoniumacetate
THF	tetrahydrofurane
TIPS	1,1',3,3'-teraisopropyl disiloxane
TIPSCI	dichloro-1,1',3,3'-teraisopropyl disiloxane
TLC	thin layer chromatography
T_m	DNA melting temperature
UV/Vis	ultraviolet/visible spectroscopy
V	volt
vs	versus
λ	wavelength

Eidesstattliche Erklärung

Ich erkläre, dass ich die Dissertation "Towards a new assay to investigate electron transfer in DNA" selbständig nur mit der darin angegebenen Hilfe verfasst und bei keiner anderen Fakultät eingereicht habe.

Basel, den 9. Juni 2005

Stéphanie Saigne

Curriculum Vitae

Stéphanie Saigne

*August 08, 1974 in Colmar, France

Nationality : french, married (borne Schunck), one child

Academic Education

- 2000 – 2004 **University of Basel, Switzerland**
PhD Organic Chemistry in the research group of Prof. Dr. Bernd Giese :
„ Towards a new assay to investigate electron transfer in DNA “.
- 1998 – 1999 **University Louis Pasteur (ULP) of Strasbourg, France**
Diploma work in Organic Chemistry in the research group of Prof. Dr. D. Uguen.
A „ DEA de Chimie Organique Moléculaire et Supramoléculaire“ was obtained.
- 92 – 98 **University Louis Pasteur of Strasbourg**
Major studies in Chemistry, minor studies in Pharmacy. A master’s degree in
Chemistry (B) was obtained.
- 89 – 92 **Lycée Bartholdi of Colmar, France**
Matura (Type C: Mathematics and Physics)

Experience

- 01 – 03 **University of Basel**
Assistant in the inorganic-chemical practical training for students with major
studies biology
- 97 (6 months) **University Louis Pasteur of Strasbourg**
Training period in electrochemistry laboratory under the supervision of
Prof.R.Louis
- Industry** **Novartis Pharma A.G. Basel:**
- 98 (6 months) Training period in Research and Development under the supervision of Prof.
Dr. Sedelmeier

The following lecturers contributed to my education:

University of Strasbourg:

D. Uguen, G. Solladié, J.M. Lehn, J. Suffert, J. Osborn, M.W. Hosseini, P. Pale, G. Wipff,
R. Weiss, J.P. Lepoittevin, D. Heissler, M. Rohmer, R. Louis.

University of Basel:

B. Giese, H. Wennemers, G. Gescheidt, W.D. Woggon